PERSPECTIVE

From lab to market: the future of zinc–air batteries powered by MOF/MXene hybrids

Tholkappiyan Ramachandran, [ID] *[a] Ramesh Kumar Raji [ID] [bc] and Moh'd Rezeq*[ad]

Zinc–air batteries (ZABs) stand at the forefront of future energy storage technologies, lauded for their exceptional energy density, cost-efficiency, and eco-compatibility. This review meticulously explores the cutting-edge advancements in the engineering of Metal–Organic Framework (MOF) and MXene hybrid materials, specifically designed to elevate the performance of ZABs. This review begins by elucidating the fundamental architecture and operational mechanisms of ZABs, delving into the roles of critical components such as the current collector, catalytic layer, and gas diffusion film in enhancing the batteries electrochemical efficacy. A detailed discourse is provided on the intricacies of the electrochemical reactions underpinning ZAB functionality, with a focus on the Oxygen Reduction Reaction (ORR) and Oxygen Evolution Reaction (OER). The review offers an in-depth examination of ORR mechanisms, encompassing both the four-electron and two-electron pathways, alongside a rigorous analysis of OER mechanisms, which include the direct combination and metal–OOH intermediate routes. The kinetic challenges inherent to these reactions are scrutinized, underscoring the pivotal role of catalyst design in mitigating these barriers. MOF/MXene hybrids emerge as transformative materials in this context, attributed to their synergistic structural and electronic properties. We explore the synthesis methodologies for these hybrids, emphasizing both *in situ* and *ex situ* tactics, and evaluate their profound impact on ORR and OER activities. The discussion extends to the performance metrics of ZABs—such as energy efficiency, power density, and cycling durability—while highlighting the critical influence of the electrolyte in determining overall system performance. Design considerations for rechargeable ZABs are presented, with a particular emphasis on optimizing the air electrode and addressing challenges related to bifunctional catalyst stability and gas diffusion layer efficiency. The review meticulously examines the formidable challenges that ZAB technology faces, particularly the kinetic constraints of ORR and OER, material robustness, and the complexities of system integration. In conclusion, the review offers forward-looking perspectives on the future expansion of advanced MOF/MXene hybrid materials and innovative design strategies for ZABs. These insights aim to push the boundaries of performance, efficiency, and durability in ZAB technology, thereby paving the way for their widespread commercial adoption. The summary synthesizes the critical findings and accentuates the transformative potential of MOF/MXene hybrids in advancing ZAB technology, suggesting strategic directions to overcome existing limitations and accelerate the deployment of sustainable energy storage solutions.

1. Introduction

Sustainable development has become an imperative in today's world, driven by the pressing need to address the intertwined crises of energy scarcity and environmental degradation. The modern era is characterized by an unprecedented demand for energy, fueled by rapid industrialization, urbanization, and the increasing prevalence of technology in daily life.[1] At the same time, the environmental consequences of traditional fossil fuel-based energy generation, such as climate change, air pollution, and the depletion of natural resources, have reached alarming levels.[2] These challenges have galvanized global efforts to transition toward cleaner, more sustainable energy systems. Renewable energy sources including wind, hydropower, and solar energy have emerged as key components of this transition.

[a]Department of Physics, Khalifa University of Science and Technology, Abu Dhabi, P. O. Box 127788, United Arab Emirates. E-mail: tholkappiyan.ramachandran@ku.ac. ae; mohd.rezeq@ku.ac.ae

[b]Department of Physics, College of Science, United Arab Emirates University, P. O. Box 15551, Al-Ain, Abu Dhabi, United Arab Emirates

[c]Department of Condensed Matter Physics, Saveetha School of Engineering, Saveetha Institute of Medical and Technical Sciences, Saveetha University, Chennai 602105, Tamil Nadu, India

[d]System on Chip Lab, Khalifa University of Science and Technology, Abu Dhabi, P. O. Box 127788, United Arab Emirates

This journal is © The Royal Society of Chemistry 2025

J. Mater. Chem. A, 2025, **13**, 12855–12890 | **12855**

They offer the promise of abundant, clean energy that can limit our dependence on fossil fuels and alleviate the environmental impacts of energy production.[3] However, the inherent variability and intermittency of these renewable energy sources pose substantial encounters. Solar and wind energy, for example, are highly dependent on weather atmospheric conditions and geographic location, leading to fluctuations in energy generation that can disrupt the stability of power grids and limit their effectiveness in meeting continuous energy demands. To overcome these challenges, the improvement of advanced energy storage systems has become a critical area of research and innovation. Energy storage technologies, particularly high-performance batteries, are essential for bridging the gap between energy production and utilization. They allow for the collection and preservation of surplus power generated when there is an abundance of renewable energy, which can then be utilized when there is a shortage of production or an increase in demand.[4] This capability is especially crucial for off-grid electricity usage, where consistent and reliable energy access is paramount, and for powering electric vehicles, which are central to the global push for sustainable transportation. The pursuit of novel battery systems has led to meaningful advancements in energy storage technology.[5] Researchers and engineers are exploring a wide range of battery chemistries and configurations, each offering distinct advantages in terms of energy density, power output, charging speed, lifecycle, and environmental impact. Innovations in lithium-ion batteries (LIB), solid-state batteries (SSB), flow batteries (FB), and beyond have opened new possibilities for efficient energy storage, enabling support of widespread adoption of renewable energy on a global scale.[6] Table 1 provides the performance and cost metrics for various battery technologies, highlighting the trade-offs between energy densities and costs.

Rechargeable batteries have become one of the backbones of modern energy infrastructure. Their ability to store and discharge energy efficiently has positioned them as key enablers of the renewable energy revolution.[15] In this way, rechargeable batteries can offset the intermittency of renewable energy sources and ensure a more stable and reliable supply of energy, which is one of the central requirements for continued growth and sustainability of renewable energy systems. Further, advancements in battery technology have the potential to lower

Tholkappiyan Ramachandran

Dr Tholkappiyan Ramachandran is a distinguished Research Scientist in the Department of Physics at Khalifa University of Science and Technology, Abu Dhabi, UAE. He earned his PhD in Materials Science from the College of Engineering, Guindy, Anna University. He is also an adjunct faculty member at PSG Institute of Technology and Applied Research, Coimbatore, India. His postdoctoral research at the United Arab Emirates University (UAEU) and the Dubai Electricity & Water Authority (DEWA) involved projects on high-performance electrode materials for supercapacitors, solid-state batteries, and solar energy applications. His contributions include the development of MXene-based 2D materials, COFs, MOFs, and various nanostructures aimed at enhancing energy storage and conversion efficiencies. Ranked among the top 2% of scientists in the world for the year 2024, recognized by the Elsevier/Stanford University, USA World Top 2% Scientists List, Dr Ramachandran has further solidified his standing in the global scientific community. In addition to his research, Dr Ramachandran serves as an Academic Editor for multiple prestigious journals, including Wiley International Journal of Energy Research, MDPI's Energies, and Hindawi Advances in Condensed Matter Physics. His prolific publication record boasts over 100 peer-reviewed articles with a citation count exceeding 3000+, an h-index of 30, and an i10-index of 75, reflecting his significant impact on the field. Dr Ramachandran has been recognized with numerous awards at international conferences and is a member of several professional societies.

Ramesh Kumar Raji

Dr Ramesh Kumar Raji is a Postdoctoral Fellow in the Department of Physics at United Arab Emirates University, Al Ain, UAE. He earned his PhD from the College of Engineering Guindy, Anna University, Chennai, and previously worked as an Assistant Professor at Surana College, Bengaluru. With over seven years of research experience, he specializes in synthesizing and characterizing advanced materials like MXenes, perovskites, and rare-earth-doped ferrites for energy storage, supercapacitors, hydrogen storage, and gas sensing applications. His work on high-power-density $Ti_3C_2T_x$ MXene electrodes and hybrid nanostructures has led to 30+ publications and collaborations with leading institutions worldwide. Beyond research, Dr Ramesh actively contributes to the scientific community as an editorial board member and reviewer for prestigious journals, including Journal of Industrial and Engineering Chemistry and Applied Surface Science. He mentors young researchers, organizes international webinars, and engages in interdisciplinary projects. Recognized with multiple awards for his research presentations, he is proficient in advanced characterization techniques like XRD, XPS, SEM, Raman spectroscopy, and electrochemical analysis, driving innovation in sustainable energy materials.

12856 | *J. Mater. Chem. A*, 2025, **13**, 12855–12890

This journal is © The Royal Society of Chemistry 2025

the environmental footprint of energy storage, helping pave the way toward a more sustainable and circular economy. As the world continues to grapple with the challenges of energy security and environmental sustainability, the role of advanced energy storage systems, particularly rechargeable batteries, will only become more significant. The ongoing research and improvement in this era are not only crucial for achieving the global energy transition but also for shaping a future where energy is accessible, affordable, and environmentally responsible. This pursuit of sustainable energy solutions is at the heart of the global effort to build a more resilient and sustainable world, ensuring that future generations can thrive in harmony with the planet.[16]

From this perspective, zinc–air batteries (ZABs) hold unparalleled significance due to their many promising characteristics, making them a highly attractive option in the landscape of energy storage technologies.[17] ZABs stand out for their environmentally friendly nature, utilizing abundant and non-toxic resources, which contributes to their relatively low cost and high safety profile. With an estimated cost of around $100 per kW per h, ZABs are both economically viable and accessible, offering a suitable working voltage of 1.66 V that is well-suited for practical applications.[18] This voltage range is particularly advantageous as it avoids the decomposition of water in aqueous electrolytes, enhancing the batteries stability and longevity. Before delving further into the potential of ZABs, it is important to compare them with other metal–air batteries to contextualize their role in the current energy storage scenario. Several metals, including aluminum (Al), iron (Fe), lithium (Li), and manganese (Mn), have been explored as candidates for metal–air batteries, with lithium and zinc receiving the most attention due to their favorable electrochemical properties.

Dr Moh'd Rezeq is an Associate Professor at the Department of Physics. He has a long experience in nanotechnology fields, with more than 75 peer-reviewed journal and conference papers, and 4 patents. He has established a nanofabrication and nanoprobe lab at Khalifa University (KU) with the capability of fabricating and characterizing nanomaterials at sub-1 nm scale. His research is dedicated to low-power and energy-efficient nano-

Moh'd Rezeq

devices and nanomaterials. He is a PI for several internally and externally funded research projects. He is a founding member of the System on Chip research lab. He has supervised several graduate and senior undergraduate students, in addition to 6 postdoctoral research fellows. He is a recipient of "Excellence in Research Award" from KU. Prior to joining KU, Dr Rezeq worked in several world-class research institutes such as the National Institute of Nanotechnology (NINT)/Canada, and the Institute of Materials Research and Engineering (IMRE)/Singapore.

Among these, lithium–air batteries (LABs) have garnered significant interest due to lithium high reactivity with oxygen, which theoretically allows for a very high energy density. However, the experimental application of LABs is severely embarrassed by the high reactivity of lithium towards oxygen, which can lead to safety concerns, and the necessity of using organic electrolytes, which complicates the system and introduces additional challenges, such as electrolyte decomposition and dendrite formation.[19] In contrast, ZABs offer a more practical and safer alternative. The use of zinc as the anode material in ZABs presents several advantages over lithium, including lower reactivity, which enhances safety, and the ability to operate in aqueous electrolytes, which simplifies the system and reduces costs (Fig. 1). The abundant availability of zinc further enhances the sustainability and economic feasibility of ZABs, making them a more scalable and environmentally benign option for large-scale energy storage. Given these considerations, ZABs emerge as a superior choice in the realm of metal–air batteries, particularly when safety, cost, and environmental impact are prioritized. Their combination of high energy density, stability, and practicality positions them as a strong contender for meeting the growing demands of renewable energy storage and off-grid power applications. As research and enhancement continue to advance, ZABs are likely to play an increasingly pivotal role in the transition concerning a more sustainable and resilient energy future.[20]

Metal–organic frameworks (MOFs) represent a rapidly emerging class of hybrid organic–inorganic porous crystalline materials, composed of metal ions coordinated to organic linkers. These materials have garnered huge consideration in the scientific community because of their unique and advantageous characteristics, such as well-defined crystal structures, redox-active metal sites, exceptionally high surface areas, tunable porosity, and customizable physicochemical characteristics.[22] The capacity to modify their structural and chemical makeup has ignited extensive research interest, rendering MOFs a highly prized category of materials for a range of uses, especially in energy storage technologies, like ZABs. The outstanding characteristics of MOFs, including their extensive surface area and organized structure, provide a considerable number of exposed catalytic sites, which improve the efficiency of transport routes and boost electrocatalytic performance. These attributes make MOFs particularly suitable for use in ZABs, where efficient catalysis and effective electron transport are crucial for high performance.[23] Moreover, the electronic structure of MOFs can be fine-tuned through the introduction of various heteroatoms like nitrogen (N), sulfur (S), oxygen (O), and phosphorus (P). This modification alters the adsorption energy of reactants, optimizing the catalytic properties of MOFs for specific electrochemical reactions. Researchers have explored the incorporation of conductive additives into the pores of pristine MOFs to leverage their large surface area and porosity. This strategy aims to enhance the overall conductivity of the MOFs, thereby improving their performance in electrochemical applications.[24] However, this approach often leads to the partial blockage of the pores, which can impede ion transport and diminish the electrochemical effectiveness of the

This journal is © The Royal Society of Chemistry 2025

J. Mater. Chem. A, 2025, **13**, 12855–12890 | **12857**

Table 1 Comparison of key parameters for various battery technologies, including gravimetric energy density, volumetric energy density, cost per kW per h, advantages, and challenges

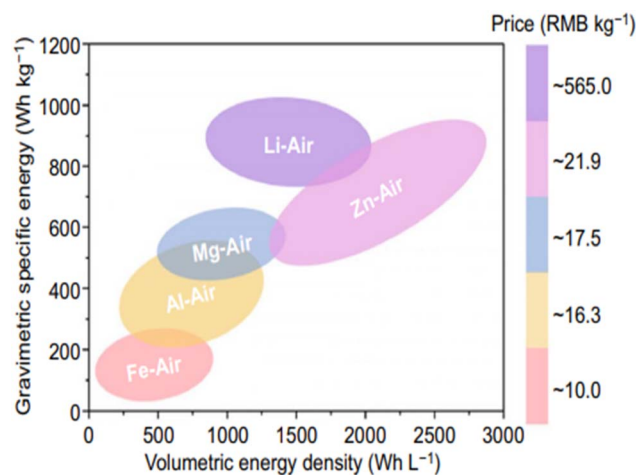| Battery technology	Gravimetric energy density (W h kg^{-1})	Volumetric energy density (W h L^{-1})	Cost per kW per h (USD)	Advantages	Challenges	References
Zn-air	200–400	500–1000	50–100	High energy density, low cost, abundant materials	Limited cycle life, low power density, air electrode issues	7
Li-ion	150–250	250–700	100–200	High energy density, long cycle life, mature technology	High cost, safety concerns (thermal runaway), limited resource availability	8
Na-ion	100–160	200–300	80–150	Low cost, abundant sodium resources, safer than Li-ion	Lower energy density, shorter cycle life, still in early commercialization	9
Solid-state	250–400	500–1000	150–300	High energy density, improved safety, longer cycle life	High manufacturing cost, scalability challenges, interfacial issues	10
Lead-acid	30–50	50–100	50–100	Low cost, mature technology, recyclable	Low energy density, short cycle life, environmental concerns	11
NiMH	60–120	140–300	100–300	Moderate energy density, safer than Li-ion, good cycle life	Lower energy density compared to Li-ion, higher self-discharge rate	12
Li-S	300–500	350–500	100–200	Very high energy density, low cost, lightweight	Poor cycle life, polysulfide shuttle effect, low volumetric energy density	13
Flow batteries	10–50	20–70	150–500	Scalable energy storage, long cycle life, decoupled power/energy capacity	Low energy density, high system complexity, high cost	14

Fig. 1 A comparison of gravimetric specific energy and volumetric energy density across various battery types, along with a typical device diagram of ZABs. Reproduced from ref. 21 with permission from Springer Nature Ltd, copyright © 2021.

MOFs. This challenge has highlighted the need for the development of MOFs that maintain both the integrity of the metal–ligand coordination structure and exhibit enhanced electronic conductivity. In response to this challenge, significant progress has been made in recognizing the fundamental charge transport mechanisms within MOFs. This understanding has paved the way for the synthesis of conductive MOFs (cMOFs), which retain the advantageous properties of traditional MOFs while offering improved electronic conductivity. The development of cMOFs represents a crucial advancement in the field, as these materials hold the potential to overcome the limitations of traditional MOFs and unlock new possibilities for their application in high-performance energy storage devices.[25] By addressing the inherent challenges associated with MOFs, researchers have demonstrated their potential to revolutionize the landscape of energy storage technologies. The continued exploration and development of MOFs are likely to yield materials that not only preserve the desirable characteristics of MOFs but also offer enhanced functionality, paving the route for more competent and sustainable energy storage solutions in the upcoming generation.[26]

MXenes have emerged as a highly valuable class of 2D materials with a wide range of applications, thanks to their remarkable thermal and chemical stability, excellent electrical conductivity, robust mechanical characteristics, superior adsorption capacity, and unique topological landscapes. These attributes have positioned MXenes at the forefront of materials research, particularly in the context of energy storage technologies.[27] The standard formula of MXenes, implied as ($M_{n+1}AX_nT_x$), is versatile, varying according to the transition metal (M), elements from group A, C/N layers (X), and surface-terminating groups (T, such as –Cl, –F, –O, –OH, *etc.*), all of which can be adjusted based on the synthesis methods employed. This versatility in composition and structure has opened numerous possibilities for customizing MXenes to meet specific application needs. Concentrating on MXenes for Zn-based energy systems is a deliberate decision based on

12858 | *J. Mater. Chem. A*, 2025, **13**, 12855–12890

This journal is © The Royal Society of Chemistry 2025

multiple convincing factors that set MXenes apart from other substances in the realm of energy storage. One of the most significant advantages of MXenes is their exceptional electrical conductivity, which sets them apart from other semiconductors that typically require doping or additional modifications to achieve comparable conductivity levels. This inherent conductivity makes MXenes particularly well-suited for electrochemical applications, where efficient electron transport is crucial for performance. In addition to their electrical properties, MXenes offer a high surface area, which provides ample space for electrochemical reactions and enhances the materials overall capacity.[28] The tunable surface chemistry of MXenes is another key feature, allowing for precise control over surface functionalization to optimize the materials interaction with electrolytes and other components in energy storage devices. This adaptability is particularly important in Zn-based energy systems, where surface characteristics can significantly influence the devices efficiency, stability, and overall performance. MXenes have demonstrated impressive electrochemical performance in various applications, characterized by high charge–discharge rates, excellent cycling stability, and the ability to maintain their structural integrity over prolonged use. These substances can also be effortlessly nano-engineered and altered to improve their characteristics, providing a degree of adaptability essential for progressing in the field of energy storage technologies.[29] The two-dimensional nature of MXenes permits accurate manipulation of both the surface properties and the structural makeup, facilitating the creation of customized solutions designed to fulfill energy storage needs. In summary, the distinct blend of attributes provided by MXenes, such as their conductivity, surface area, and adjustable chemistry, positions them as an extremely attractive material for zinc-based energy devices and various other energy storage purposes. As research into MXenes continues to advance, these materials are poised to play a pivotal role in the next generation of high-performance, sustainable energy storage systems.[30]

Recently, MOF/MXene hybrid materials offer several key advantages that enhance the overall performance of ZABs, addressing critical challenges such as low conductivity, sluggish reaction kinetics, and durability issues. MOFs provide a highly tunable porosity, large surface area, and customizable chemical composition, which facilitate the design of efficient electrocatalysts and electrode materials. Their structural versatility enables the incorporation of various metal ions and organic linkers, optimizing catalytic activity and stability.[31] However, pristine MOFs often suffer from limited electronic conductivity, which can hinder their full potential in ZAB applications. This limitation is effectively overcome by integrating MXenes—2D transition metal carbides, nitrides, and carbonitrides—known for their superior electrical conductivity, mechanical robustness, and rapid charge transfer capabilities.[32] MXenes naturally conductive nature, combined with their large surface area and tunable surface chemistry, enhances electrochemical performance, making them ideal for energy storage applications. By leveraging the synergistic effects of MOFs and MXenes, researchers have successfully engineered hybrid materials with improved oxygen evolution reaction (OER) and oxygen
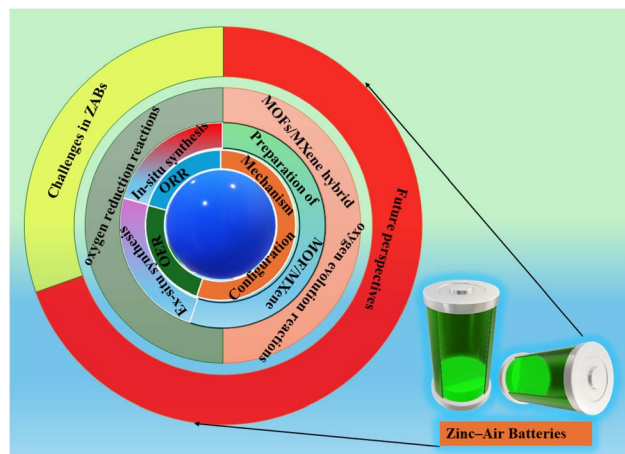

Fig. 2   Outline of the review on the MOFs/MXene hybrid for ZABs.

reduction reaction (ORR) kinetics, higher efficiency, and prolonged cycle life, paving the way for next-generation ZABs with superior energy storage potential.

This review will delve into the potential synergies between MOFs and MXenes when integrated into ZABs, underscoring how their complementary properties can drive substantial enhancements in overall battery performance. The integration of the large surface area and catalytic activity of MOFs with the superior conductivity and structural stability of MXenes presents an opportunity to develop hybrid materials with enhanced catalytic efficiency, improved ion transport, and greater durability under operational conditions.[33] By examining recent research where MOF–MXene hybrids have been successfully applied in ZABs, the review will illustrate the tangible benefits of these innovative materials. Moreover, the review will critically assess the current challenges associated with synthesizing and deploying MOF–MXene hybrids in ZABs, including issues related to material compatibility, stability, and scalability.[34] Key areas for future research will be identified, such as the improvement of novel production techniques, advanced material characterization techniques, and *in situ* analysis of electrochemical processes. These insights will be essential for overcoming existing challenges and advancing the practical application of these hybrids.[35] In summary, this review will highlight the transformative potential of MOF–MXene hybrids to revolutionize ZAB technology, influencing the broader goal of developing more sustainable and efficient energy storage systems. By integrating the unique properties of MOFs and MXenes, the review aims to provide a comprehensive overview of how these materials can foster innovation in ZABs, offering valuable insights for researchers, engineers, and industry professionals in the domain of energy storage.[36] Fig. 2 shows the outline of the review on the MOFs/MXene hybrid for ZABs.

2.   Configuration and mechanism in ZABs

ZABs depend on the reaction between the zinc anode and the air cathode during both the discharging and charging phases,
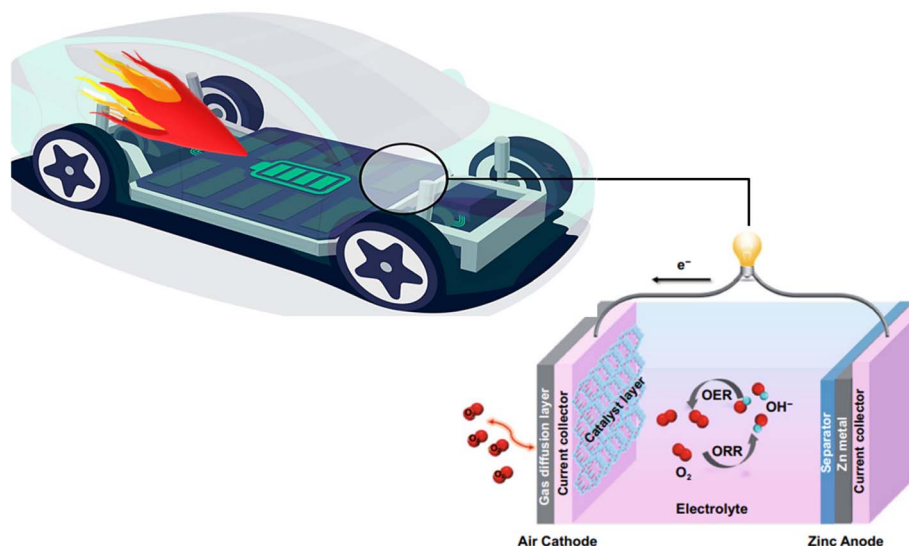
Fig. 3 A typical device diagram of ZABs. Reproduced from ref. 21 with permission from Springer Nature Ltd, copyright © 2021.

highlighting the importance of the arrangement of these elements for the batteries overall efficiency.[37] Fig. 3 shows the typical device diagram of ZABs. Usually, the anode in ZABs is made of a gel solution mixed with granulated zinc powder or a single zinc plate. On the other hand, the air cathode is the most critical part of ZABs, as it employs oxygen from the atmosphere, a renewable and active substance, for the chemical reaction. This utilization of oxygen in the air cathode results in a battery that is much more energy-efficient than those with oxide cathodes found in conventional batteries.[38]

2.1. Configuration of ZABs

The traditional air electrode in ZABs is typically composed of three main components arranged in a sandwich structure: the diffusion gas layer, the current collector, and the catalyst layer. Every part of this setup has a unique function in how the air electrode operates:[39]

(a) Charge collector:

This part is typically constructed from nickel mesh, nickel foam, or a more affordable metal mesh that has been coated with nickel. It acts as the route for the movement of electrons from the outside circuit to the catalytic layer.
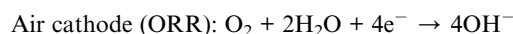
(b) Catalytic layer:

This component serves as the location for the Oxygen Reduction Reaction (ORR) in the main ZABs, as well as for the Oxygen Reduction Reaction (OER) in rechargeable ZABs. The effectiveness of ZABs is mainly determined by the performance of the catalytic layer, as it plays a crucial role in affecting the electrochemical processes taking place at the air electrode.
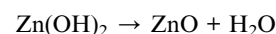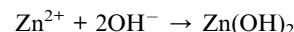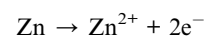
(c) Gas diffusion layer:

The primary function of the gas diffusion layer is to ensure the smooth passage of reaction gases to the catalytic layer while preventing the electrolyte from flooding the gas channels. This layer often contains polytetrafluoroethylene (PTFE) as a key component and may be doped with other carbon materials to enhance its performance.

2.2. Mechanism of ZABs

ZABs operate by utilizing redox reactions involving the zinc anode and the air cathode. In the discharge phase, oxygen moves towards the air electrode, undergoing reduction to hydroxyl ions (OH^-) with the aid of a working catalyst present.[40] These hydroxyl ions then migrate to the zinc anode through the separator, where they combine with zinc ions (Zn^{2+}) to form soluble zincate ions $[Zn(OH)_4^{2-}]$. As the zincate ion concentration increases, it eventually precipitates as zinc oxide (ZnO). The overall reaction during discharge can be described as:
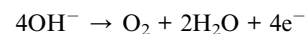
$$\text{Air cathode (ORR): } O_2 + 2H_2O + 4e^- \rightarrow 4OH^-$$

Zinc anode:

$$Zn \rightarrow Zn^{2+} + 2e^-$$

$$Zn^{2+} + 2OH^- \rightarrow Zn(OH)_2$$

$$Zn(OH)_2 \rightarrow ZnO + H_2O$$

During the charging process, the reverse reactions occur. The OER takes place at the air cathode, leading to the decomposition of ZnO back into zinc and oxygen. The OER can be expressed by the following equation:[41]

Air cathode (OER):

$$4OH^- \rightarrow O_2 + 2H_2O + 4e^-$$

2.3. Performance and challenges of the air electrode

The success of ZABs largely depends on the catalysts utilized for the air electrode. For ORR, the success is gauged with the reduction peak potential, onset potential, half-wave potential, and stability.[42] In terms of OER, the overpotential needed to

12860 | *J. Mater. Chem. A*, 2025, **13**, 12855–12890

This journal is © The Royal Society of Chemistry 2025

achieve a current density of 10 mA cm^{-2}, along with the durability of the catalyst, are the important factors. A significant challenge in the operation of ZABs is the different overpotentials required for ORR and OER. The OER typically requires a higher overpotential (around 2.0 V or more), which can deactivate the ORR catalyst during high-voltage charging. This creates a need for the development of bifunctional catalysts that can efficiently catalyze both ORR and OER processes within the same electrode.[43] The three-electrode system in some ZAB configurations allows for the use of separate catalysts for ORR and OER, but this increases the batteries size and weight, reducing its overall energy density. Therefore, the focus has shifted toward developing non-precious metal materials with dual ORR and OER catalytic characteristics, which is crucial for enhancing the working of rechargeable ZABs.[44]

2.4. Electrolyte and performance metrics

The electrolyte is essential for the functioning of ZABs. In standard batteries, 6 M KOH is frequently utilized, whereas in ZABs designed for recharging, zinc acetate (Zn(Ac)$_2$) is frequently incorporated into the 6 M KOH electrolyte to boost their efficiency. The main performance metrics for ZABs are open-circuit voltage (OCV), charging voltage (V_C), discharging voltage (V_D), peak power density (PPD), specific capacitance, and stability. By comprehending the relationship between the catalysts structure and its activity and by refining their design, the efficiency of ZABs can be greatly enhanced.[45] In summary, the configuration and mechanism of ZABs are intricately linked to the design and performance of the air electrode and its components. Advances in catalyst development and a deeper understanding of the electrochemical processes involved are essential for the continued improvement and commercialization of high-performance ZABs.

2.5. Design considerations

The design of ZABs must ensure efficient electron flow and ion transport, minimal polarization losses, and stable long-term operation. The air cathode is typically a layered structure that includes a catalyst layer, a gas diffusion layer, and a current collector. The gas diffusion layer ensures that oxygen from the air is evenly distributed across the catalyst layer, where the ORR takes place. The electrolyte must remain in contact with both the zinc anode and the air cathode, facilitating the movement of ions while minimizing water loss or leakage.[46]

2.6. Rechargeable ZABs

For rechargeable ZABs, the mechanism becomes more complex as the system must also support the reverse reactions during the charging process. During charging, the zinc is re-deposited on the anode, and oxygen has evolved at the cathode. This reversibility poses challenges related to the steadiness of the raw materials, especially the air cathode, which must endure repeated cycles of oxygen reduction and evolution. In conclusion, the design and functioning of ZABs concentrate on efficiently converting chemical energy into electrical energy through the process of oxidation of zinc and reduction of oxygen. The configuration of the anode, cathode, and electrolyte is essential for the batteries performance, with research efforts focused on enhancing these components for better efficiency, longevity, and the capacity for recharging.[47]

3. Oxygen reduction reaction (ORR) in rechargeable ZABs

ORR is a crucial electrochemical process in ZABs, as it is the key reaction responsible for converting oxygen into electrical energy. The ORR mechanism in ZABs is complex due to its multi-electron transfer process, typically encompassing either a 4-electron or 2-electron reaction pathway. The 4-electron pathway is generally associated with the most efficient precious metal catalysts and is the preferred mechanism owing to its higher energy conversion efficiency.[48]

3.1. ORR mechanism in ZABs

Four-electron reaction mechanism. In the four-electron ORR mechanism, oxygen (O$_2$) is reduced directly to water (H$_2$O) in acidic electrolytes or hydroxide ions (OH$^-$) in alkaline electrolytes. The reactions can be summarized as:

• Acidic electrolyte: $O_2 + 4H^+ + 4e^- \rightarrow 2H_2O$

• Alkaline electrolyte: $O_2 + 2H_2O + 4e^- \rightarrow 4OH^-$

This pathway is favored for its ability to produce water directly, leading to more efficient energy conversion and fewer side reactions.

Two-electron reaction mechanism. The two-electron ORR mechanism involves the partial reduction of oxygen to hydrogen peroxide (H$_2$O$_2$) in acidic conditions or the hydroperoxide ion (HO$_2^-$) in alkaline conditions, followed by further reduction:

• Acidic electrolyte (step 1): $O_2 + 2H^+ + 2e^- \rightarrow H_2O_2$

• Acidic electrolyte (step 2): $H_2O_2 + 2H^+ + 2e^- \rightarrow 2H_2O$

• Alkaline electrolyte (step 1): $O_2 + 2H_2O + 2e^- \rightarrow HO_2^- + OH^-$

• Alkaline electrolyte (step 2): $HO_2^- + H_2O + 2e^- \rightarrow 3OH^-$

This mechanism is less efficient than the four-electron pathway and can result in the accumulation of reactive peroxide species, which may degrade the batteries performance over time.

4. Oxygen evolution reaction (OER) in rechargeable ZABs

In rechargeable ZABs, the oxygen electrocatalyst plays a dual role by facilitating the reverse reaction of ORR during charging, known as the Oxygen Evolution Reaction (OER). The OER is essential for regenerating the zinc anode by evolving oxygen at the air cathode. Like the ORR, the OER also involves a multi-electron transfer process, typically following a four-electron mechanism.[49] However, the OER is inherently slower and requires a higher overpotential, which can lead to significant energy losses.

The two primary views on the OER mechanism in ZABs are:

• Direct combination mechanism:

This journal is © The Royal Society of Chemistry 2025

J. Mater. Chem. A, 2025, **13**, 12855–12890 | **12861**

This mechanism involves the direct sequence of two metal–oxygen (M–O) bonds to form oxygen gas (O_2).

● M–OOH intermediate mechanism:

In this pathway, an M–OOH intermediate is first formed, which then decomposes to release O_2. Here, "M" refers to the active site on the catalyst surface.

4.1. Kinetics and challenges

The OER kinetics in ZABs are much slower compared to the ORR, often requiring a charging voltage of around 2.0 V or higher, while the discharge process typically has an open-circuit voltage of about 1.2 V. The high overpotential during charging can lead to the rust of the air electrode and oxidation of the electrocatalyst, which are significant challenges in the design of rechargeable ZABs.[50]

4.2. Catalyst design for rechargeable ZABs

Given the complexity of both ORR and OER, the design of electrocatalysts in rechargeable ZABs is critical. Traditional approaches involve using separate catalysts for ORR and OER, leading to a three-electrode system. However, this configuration increases the batteries volume and weight, reducing its overall energy density. As a result, there is a growing emphasis on developing bifunctional catalysts that can efficiently catalyze both ORR and OER within a two-electrode system. This approach not only simplifies the battery design but also enhances its energy efficiency and stability. In summary, the ORR and OER are fundamental to the operation of ZABs, with the ORR driving the discharge procedure and the OER facilitating recharging.[51] The complexity of these reactions, particularly the multi-electron transfer processes, underscores the need for advanced catalyst development to enhance the performance and longevity of ZABs.

5. Formulation of MOF/MXene hybrid

5.1. *In situ* preparation of MOF/MXene hybrids

The process of creating MOF/MXene hybrid materials involves combining the distinct characteristics of metal–organic frameworks (MOFs) and MXenes to form sophisticated composite materials with improved capabilities.[52] This method seeks to merge MOFs, recognized for their extensive surface areas, adjustable pore structures, and varied functionalities, with MXenes, which provide greater electrical conductivity, expansive surface areas, and affinity for water. Through this combination, the resulting hybrids display cooperative effects that enhance their performance in various fields, including catalysis, energy storage, and sensing.[53]

Various approaches are used to create MOF/MXene hybrids on-site, such as ultrasonication, hydrothermal, mixing, and solvothermal methods. Pan Tian *et al.*[54] reported an innovative approach for synthesizing $Ti_3C_2T_x$ MXene-based composites. Initially, $Ti_3C_2T_x$ MXenes were annealed in a nitrogen atmosphere to convert them into TiO_2 layers, a process resulting in the material implied as TCA. Admiring this, UiO-66-NH$_2$, a type of metal–organic framework (MOF), was coated onto the

surfaces of the annealed $Ti_3C_2T_x$ *via* electrostatic adsorption. This coating was achieved through a one-step hydrothermal technique, as illustrated in Fig. 4. The resulting composite material, combining TiO_2 with UiO-66-NH$_2$, benefits from the enhanced properties of both components, potentially leading to improved performance in various applications.

You Wu *et al.*[55] reported the successful synthesis of Ti_3C_2-modulated MIL-125-NH$_2$-based nanohybrids featuring dual heterojunctions—both type-II heterojunctions and Schottky junctions—using a one-step solvothermal strategy. The process involves the straightforward preparation of these MOF-based nanohybrids, which vary in constituent and morphology. This is depicted in Fig. 5, demonstrating the efficiency and versatility of the one-step solvothermal method in producing complex hybrid structures with enhanced properties.

Hossein Shahriyari Far *et al.*[56] reported the construction of a heterogeneous MXOF by heterojunctioning zeolite imidazole framework-8 (ZIF-8) with titanium carbide ($Ti_3C_2T_x$) MXene nanosheets. This was achieved through the *in situ* synthesis of the MOF in the existence of MXene nanosheets. The resulting MXOF structure exhibited a tunable bandgap energy, which contributed to its enhanced photocatalytic activity. The synergy between ZIF-8 and $Ti_3C_2T_x$ MXene not only improved the materials photocatalytic performance but also offered the potential for fine-tuning its electronic properties for various applications.

Renhao Li and colleagues[57] developed a novel approach for synthesizing MOF-801@MXene materials at room temperature, which were subsequently utilized to create laminar membranes designed for efficient H_2/CO_2 separation as shown in Fig. 6. In their approach was based on the MXenenanosheets, which, being negatively charged, would retain the Zr^{4+} ions from the solution through electrostatic interactions. These Zr^{4+} ions would then coordinate with the organic ligands to give the MOF-801 crystals, which were finally dispersed uniformly over the surface of the MXene nanosheets. This careful and uniform deposition of MOF-801 crystals ensures that the hybrid material exhibits a well-structured and highly porous architecture. The creation method takes advantage of the distinct characteristics
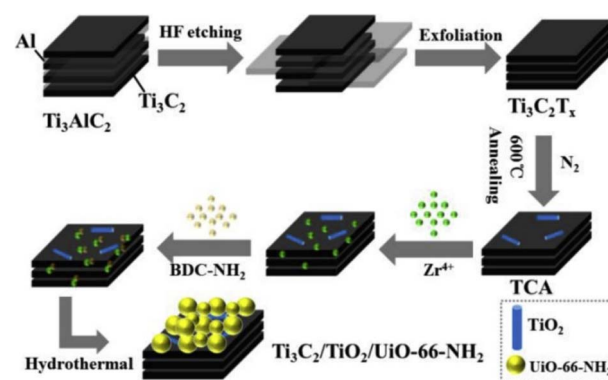

Fig. 4 Schematic of the reaction route for forming $Ti_3C_2/TiO_2/UiO$-66-NH_2.[54] Reproduced from ref. 54 with permission from Elsevier Ltd, copyright © 2019.

12862 | *J. Mater. Chem. A*, 2025, **13**, 12855–12890

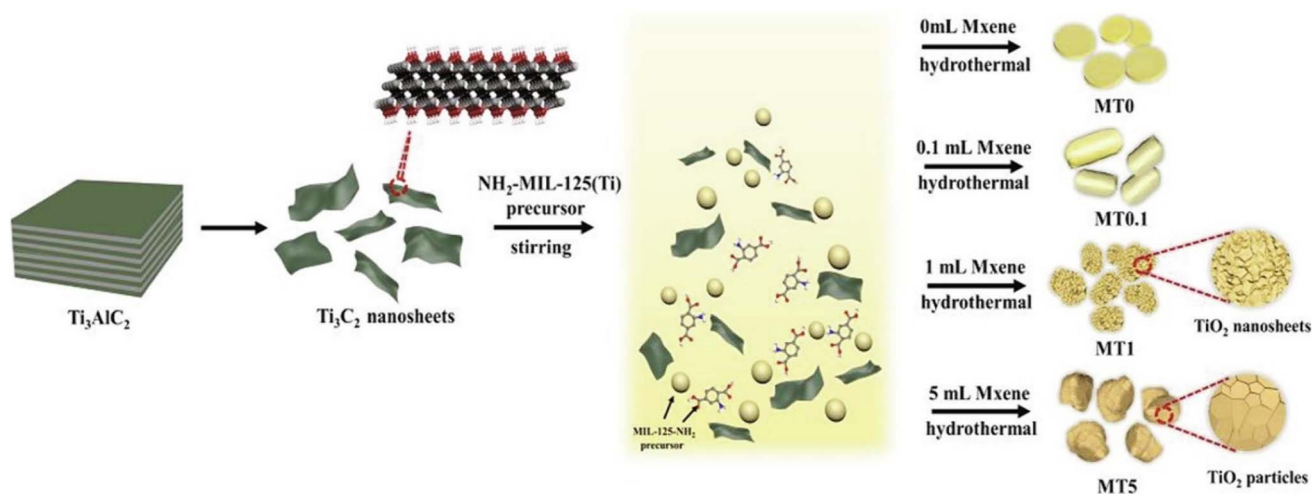This journal is © The Royal Society of Chemistry 2025

Fig. 5 Schematic of preparing Ti_3C_2 nanosheets and MOFs–based heterostructure. Reproduced from ref. 55 with permission from Elsevier Ltd, copyright © 2020.

of MOF-801 and MXene, merging the network of tetrahedral and octahedral cages from the former with the superior conductivity and structural strength of the latter. MOF-801 substance has a framework of porous cages linked by triangular openings, acting as access points for molecular filtering. This interconnected cage structure is ideal for selective gas separation, as it allows for the efficient passage of smaller hydrogen molecules while restricting larger carbon dioxide molecules. To assemble the final laminar membranes, the MOF-801@MXene nanosheets were stacked together using vacuum filtration. This stacking process not only creates a dense and uniform membrane but also enhances the structural integrity and stability of the material under operational conditions.[58] The integration of MOF-801 crystals within the MXene framework significantly expands the nanochannels within the membrane, providing additional pathways for molecular sieving. As a result, the membrane demonstrates superior performance in H_2/CO_2 separation, characterized by increased hydrogen permeance and improved selectivity for hydrogen over carbon dioxide. This innovative synthesis strategy showcases the potential of combining MOF and MXene materials to create advanced membranes for gas separation applications.[59] The intercalation of MOF-801 within the MXene framework effectively optimizes the membranes nano-architecture, leading to enhanced separation efficiency and broader applicability in industrial gas processing.
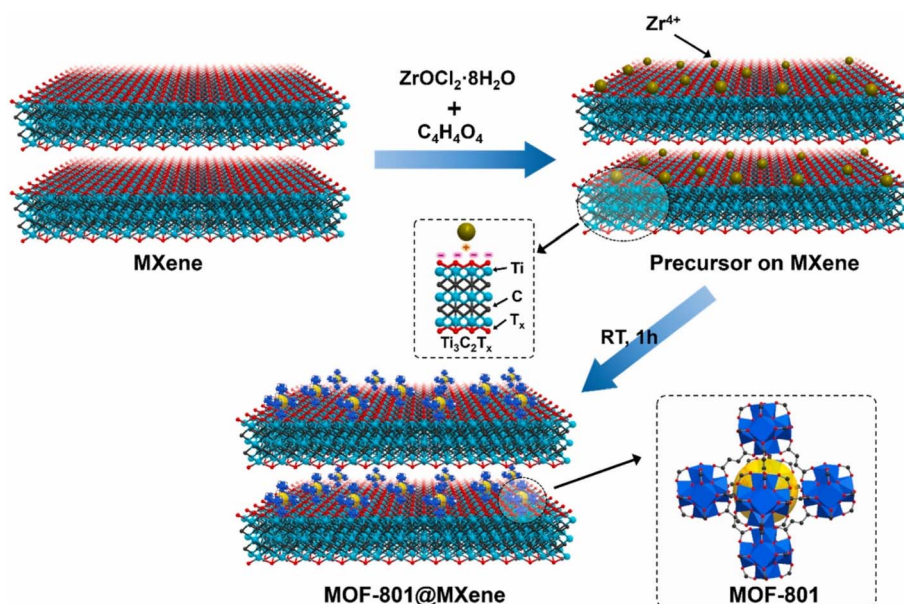

Fig. 6 Diagram of room-temperature *in situ* synthesis of MXene@MOF-801 nanosheets. Reproduced from ref. 57 with permission from Elsevier Ltd, copyright © 2022.

This journal is © The Royal Society of Chemistry 2025

J. Mater. Chem. A, 2025, **13**, 12855–12890 | **12863**

In conclusion, the *in situ* preparation of MOF/MXene hybrids offers a highly effective strategy for developing advanced composite materials with enhanced functionalities. By integrating the high surface area, tunable porosity, and structural versatility of MOFs with the excellent electrical conductivity and mechanical strength of MXenes, these hybrids exhibit significant improvements in performance across various applications. Different synthesis techniques, such as hydrothermal, solvothermal, ultrasonication, and electrostatic adsorption, have been successfully employed to achieve well-structured MOF/MXene composites with tailored properties. However, challenges such as optimizing synthesis conditions, ensuring structural stability, and achieving scalable production remain key areas for future research. The promising outcomes of these studies pave the way for further advancements in MOF/MXene hybrid materials, opening new opportunities for their application in next-generation energy and environmental technologies.

5.2. *Ex situ* synthesis of MOF/MXene hybrids

The *ex situ* manufacturer of MOF/MXene hybrids combines the unique properties of both materials, making them highly effective for diverse applications such as energy storage, catalysis, and sensing. *Ex situ* synthesis refers to the process where the MOF and MXene components are synthesized separately before being combined.[60] This approach allows for better control over the properties of each material and enables the fine-tuning of the final hybrid structure. One of the key contests in the *ex situ* synthesis of MOF/MXene hybrids is ensuring the stability of the hybrid structure under operational conditions, especially in harsh environments where the materials might be exposed to extreme temperatures, pressures, or chemical interactions.[61] Additionally, scalability remains a significant hurdle, as scaling up the *ex situ* synthesis process to industrial levels while maintaining uniformity and consistent performance across large batches is difficult. These challenges must be focused to fully realize the potential of MOF/MXene hybrids in practical applications.[62]

The direct mixing method involves combining pre-synthesized MXene and MOF in a solution to create the MOF/MXene composite. In this process, the prepared MXene nanosheets and MOF particles are mixed directly in a solvent, typically under stirring or sonication, to promote uniform distribution and interaction between the two components.[63] This straightforward approach allows for the integration of MXene and MOF, forming a composite material where the MOF is attached or anchored onto the MXene surface. The resulting MOF/MXene composite benefits from the synergistic properties of both materials, offering potential advantages for several applications such as catalysis, energy storage, and sensing.[64] Yue Chen *et al.*[65] reported the composite material made from a three-dimensional straw-sheaf-like Ce-MOF (cerium-based metal–organic framework) and $Ti_3C_2T_x$ MXene nanosheets as shown in Fig. 7. The integration of Ce-MOF with $Ti_3C_2T_x$ MXene offers significant advantages. The Ce-MOF provides a highly porous structure that enhances the surface area available for interaction with L-Trp, while the $Ti_3C_2T_x$ MXene nanosheets

contribute to increased electrical conductivity. This combination not only improves the overall conductivity of the MOF but also blocks the $Ti_3C_2T_x$ MXene nanosheets from stacking, which can hinder their electrochemical performance. The resulting Ce-MOF/$Ti_3C_2T_x$ MXene composite demonstrates excellent sensitivity and selectivity as an electrochemical sensor, making it a promising tool for the precise detection of L-tryptophan in various advanced electrochemical applications.

Dan Cheng and coworkers[66] developed a novel electrochemical sensor for the detection of hydrogen peroxide (H_2O_2) by combining a three-dimensional flower-like copper-metal–organic framework (Cu-MOF) with very thin MXene nanosheets. The Cu-MOF was synthesized in a simple one-step procedure using copper nitrate and 2-aminoterephthalic acid as starting materials. The Cu-MOF exhibits numerous active sites and large surface areas, which is well suited for applications in electrochemical processes. The integration with MXene nanosheets further enhances the sensors performance by providing high conductivity and stability. This composite material, as depicted in Fig. 8, offers an indicating attempt for the subtle and efficient detection of H_2O_2, demonstrating the synergy between Cu-MOF and MXene in electrochemical sensing.

The self-assembly synthesis of MOF@MXene composites involves the spontaneous organization of pre-synthesized MOF and MXene components into well-ordered structures. This process is guided by several types of noncovalent forces that encompass π–π stacking, electrostatic attraction, and H bonding. It facilitates aligned insertion and assembly of MOF and MXene into a composite bearing highly ordered architectures. In this method, the individual MOF and MXene components are typically dispersed in a solution where they naturally interact and self-organize owing to their complementary chemical and physical properties.[67] The self-assembly process does not require external templating agents or complex procedures, relying instead on the inherent tendencies of the materials to associate and form stable composites. The resulting MOF@MXene composite exhibits a synergistic combination of the characteristics of both materials, such as the large surface
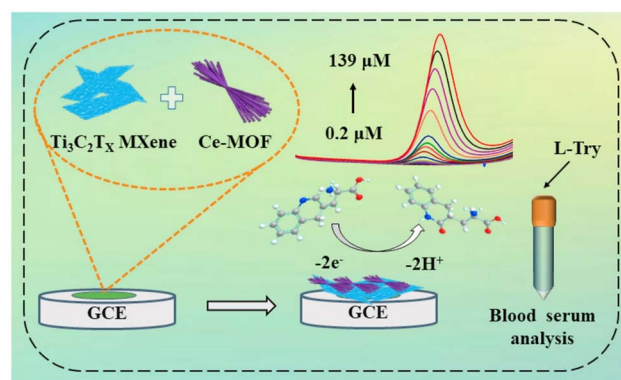

Fig. 7 Schematic illustrating the fast production method for a three-dimensional Ce-MOF/$Ti_3C_2T_x$ MXene blend aimed at achieving superior electrochemical sensing of L-tryptophan. Reproduced from ref. 65 with permission from Elsevier Ltd, copyright © 2022.
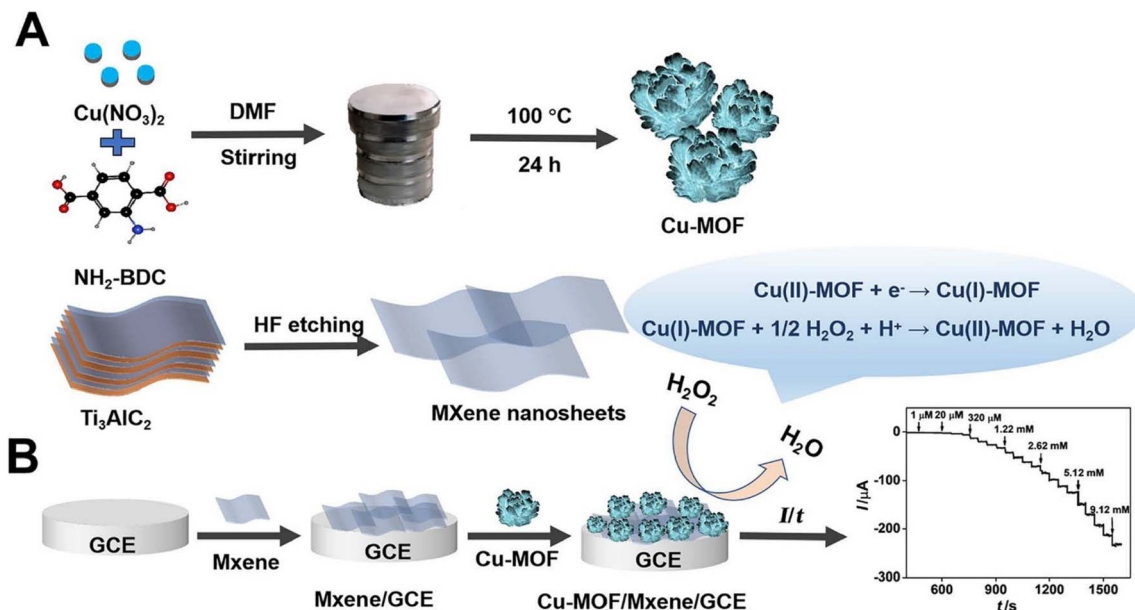
12864 | *J. Mater. Chem. A*, 2025, **13**, 12855–12890

This journal is © The Royal Society of Chemistry 2025

Fig. 8 (A) Synthesis of 3D flower-like Cu-MOF and ultra-thin MXene nanosheets. (B) Construction of an electrochemical sensor for H_2O_2 detection. Reproduced from ref. 66 with permission from Wiley, copyright © 2021.

area and tunable porosity of MOFs and the excellent electrical conductivity and mechanical strength of MXenes.[68] This makes the self-assembled MOF@MXene composites highly suggesting for applications in energy storage, catalysis, sensing, and other advanced technologies. Yitong Sun *et al.*[69] developed a Co-ZIF-9/Ti_3C_2 composite using a straightforward electrostatic self-assembly strategy as shown in Fig. 9. This method facilitates the integration of Co-ZIF-9 with Ti_3C_2, leveraging the unique characteristics of both materials. The Co-ZIF-9 component, known for its robust catalytic activity and large surface area, is combined with Ti_3C_2, which provides enhanced electrical conductivity and structural stability. This composite is designed to optimize performance in various electrochemical applications, showcasing the effectiveness of the self-assembly approach in creating high-performance materials.[70]

The electrochemical preparation technique for synthesizing MOF@MXene composites involves using electrochemical methods to integrate MOF and MXene materials into a composite structure. The process begins with the preparation of an electrolyte solution containing metal salts, organic ligands for MOF synthesis, and MXene dispersions. In an electrochemical cell setup, a working electrode coated with MXene, a counter electrode, and a reference electrode are used. Electrochemical deposition techniques, such as constant current or potential electrolysis, facilitate the formation of MOF on the MXene-coated electrode.[71] During this process, metal ions from the electrolyte are reduced, and organic ligands coordinate to form the MOF structure directly on or interact with the MXene surface, creating the MOF@MXene composite. Post-treatment steps, including washing, drying, and annealing, are employed to remove residual impurities and enhance the structural stability of the composite. This method offers precise control over deposition and uniformity, making it scalable and effective for producing high-quality composites with enhanced properties for applications in energy storage, catalysis, and sensing.[72]

Jiaheng Wang *et al.*[73] reported the development of hexagonal M–NC@NCM/NF nanosheets that are notable for their binder-free and conductive-agent-free design. This material was synthesized using a multi-step approach. Initially, nickel cobalt manganese oxide (NCM) was directly grown onto nickel foam (NF) *via* a solution-based method. Fig. 10 shows the schematic
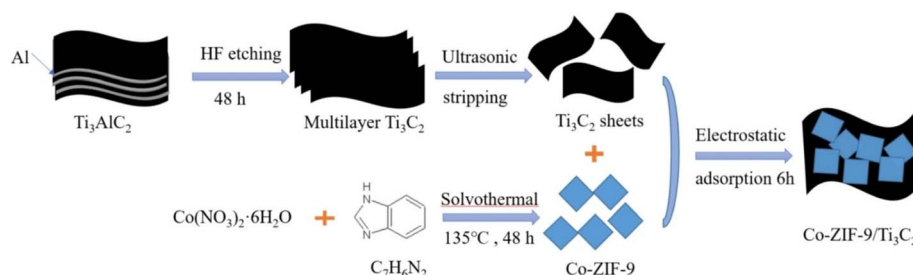

Fig. 9 Preparation process of Co-ZIF-9/Ti_3C_2 composites. Reproduced from ref. 69 with permission from Wiley, copyright © 2022.

This journal is © The Royal Society of Chemistry 2025

J. Mater. Chem. A, 2025, **13**, 12855–12890 | **12865**
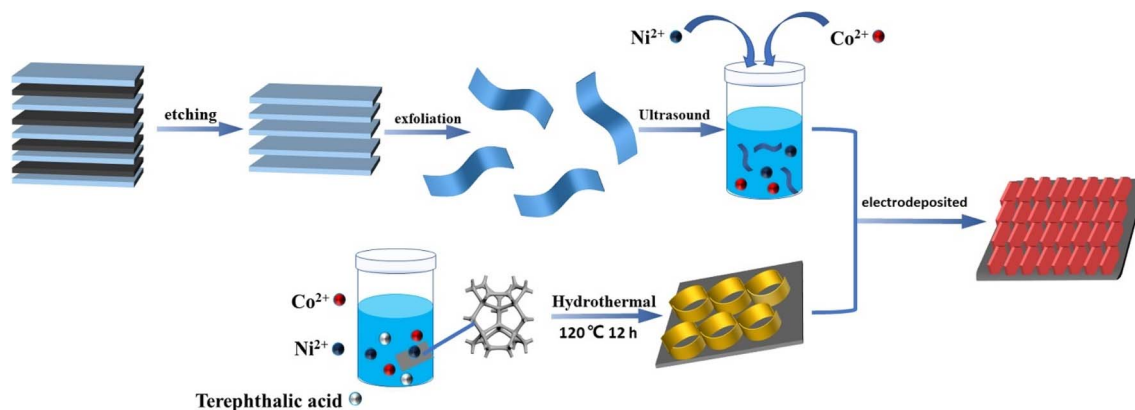
Fig. 10 Schematic of the fabrication process for the M−NC@NCM/NF electrode. Reproduced from ref. 73 with permission from Elsevier, copyright © 2021.
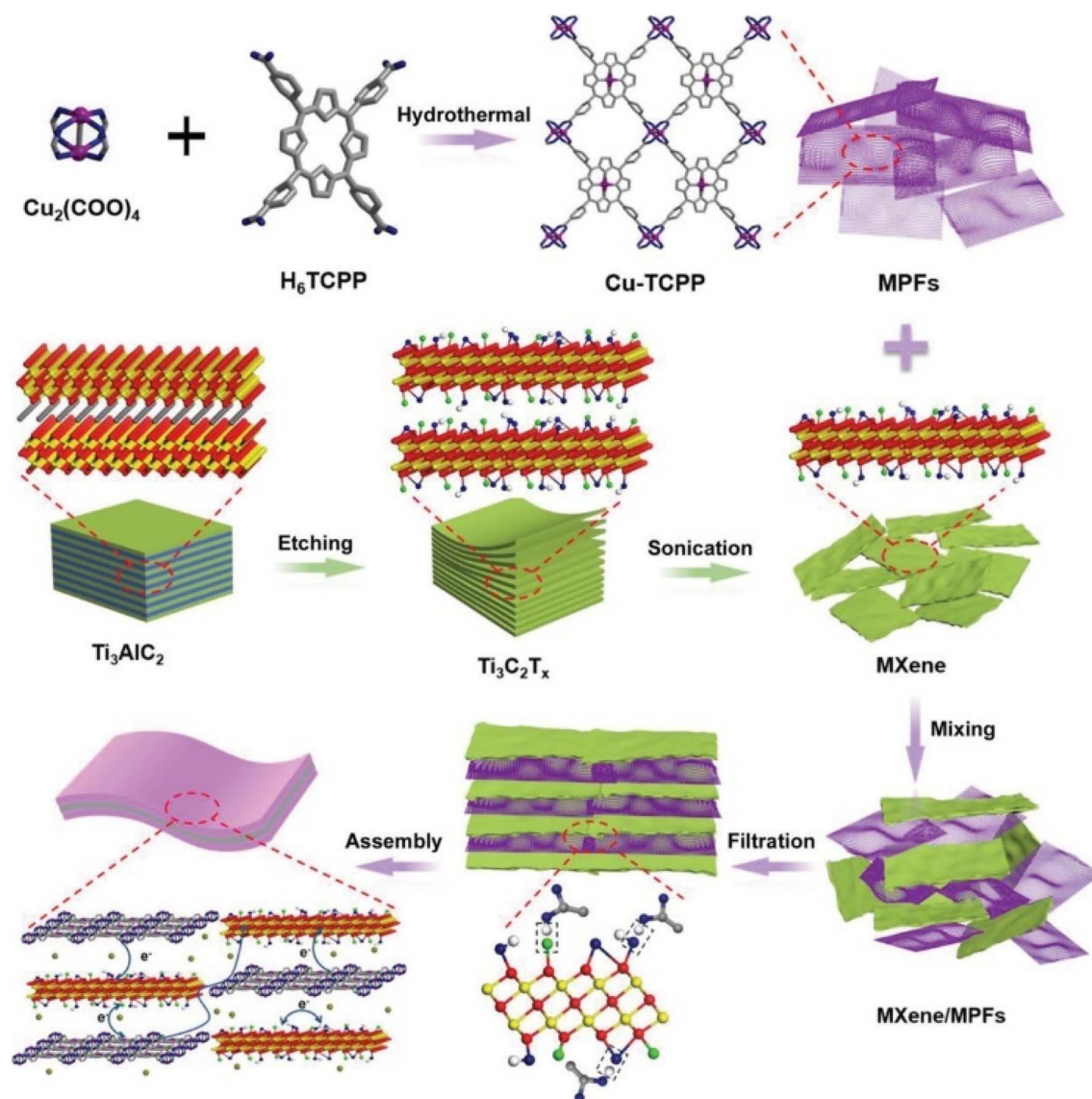
Fig. 11 Schematic of synthesizing and applying interlayer hydrogen-bonded MXene/MPFs films *via* vacuum filtration. Reproduced from ref. 76 with permission from Wiley, copyright © 2019.

12866 | *J. Mater. Chem. A*, 2025, **13**, 12855–12890

This journal is © The Royal Society of Chemistry 2025

of the fabrication process for the M–NC@NCM/NF electrode. In the subsequent step, MXenes interlayer functional groups were employed to adsorb nickel (Ni^{2+}) and cobalt (Co^{2+}) ions. A mixed solution containing MXene, Ni^{2+}, and Co^{2+} was then used as the electrolyte for electrodeposition onto the pre-formed NCM/NF substrate. The resulting M–NC@NCM/NF structure benefits from several key features. The incorporation of MXene enhances electron and ion transmission rates owing to its high conductivity and layered structure. Moreover, the process facilitates the exposure of numerous active sites, which increases the materials electrochemical performance.[74] The design also prevents agglomeration of the nanosheets, thereby significantly extending the materials cycle life. The NC@NCM/NF material demonstrates exceptional electrochemical performance. It achieves improvements in specific capacitance, electrical conductivity, and cycling stability compared to traditional materials. This advanced performance underscores the efficacy of using MXene in combination with NCM to create high-performance energy storage materials.[75]

Weiwei Zhao *et al.*[76] developed an innovative interlayer hydrogen-bonded hybrid film combining MXene and MPFs (metal–organic framework porphyrins). The film was fabricated through a vacuum-assisted filtration process, incorporating two-dimensional (2D) ultrathin MXene nanosheets and Cu-TCPP (5,10,15,20-tetrakis(4-carboxy-phenyl)porphyrin) nanosheets. This method involved dispersing both MXene and Cu-TCPP in a solution and then using vacuum filtration to create a well-structured hybrid film (Fig. 11). In this hybrid system, MXenes surface termination, including –F, –OH, and –O, form hydrogen bonds with the carboxyl groups (–COOH) of the Cu-TCPP nanosheets. This interaction results in a stable and cohesive network where MXene and MPFs are interlinked through hydrogen bonds, forming a three-dimensional interconnected structure. This network, characterized by its porous architecture, promotes efficient ionic and electronic transport by providing a continuous and conductive pathway.[77] The presence of hydrogen bonds within the MXene/MPFs hybrid film plays a crucial role in addressing challenges related to volume changes that predictably occur during rapid charge and discharge cycles. Such volume fluctuations often lead to phase separation and structural collapse in conventional materials. The robust hydrogen bonding in this hybrid film alleviates these issues, thereby enhancing its rate capability and cyclability. Additionally, hybrid film maintains its structural integrity under mechanical stresses such as bending and folding, ensuring long-term stability and performance. This approach not only improves the efficacy of the material in energy storage applications but also extends its operational lifespan, highlighting the potential of such hybrid materials in advanced electrochemical technologies.[78]

In conclusion of this section, the *ex situ* synthesis of MOF/MXene hybrids offers a versatile and effective approach for developing high-performance materials for various applications, including energy storage, catalysis, and sensing. This method allows for precise control over the individual properties of MOFs and MXenes before integration, resulting in composites with enhanced structural stability, electrical conductivity,

and functional performance. However, challenges such as ensuring structural stability under operational conditions and scaling up the synthesis process remain key obstacles that must be addressed. Several synthesis strategies have demonstrated promising results in creating well-structured MOF/MXene composites with improved electrochemical properties.

6. MOFs/MXene hybrid materials for oxygen reduction reactions in ZABs application

Zhongwei Fang *et al.*[79] reported an innovative electrocatalyst for the ORR, composed of CoZn/NC–Ti_3C_2, prepared *via* a one-step pyrolysis of zeolitic imidazolate frameworks (ZIF)-67/ZIF-8 on the Ti_3C_2 surface. This innovative CoZn/NC–Ti_3C_2 catalyst reveals impressive ORR behavior with 0.847 V as the half-wave potential, indicating its substantial catalytic activity. Additionally, the fuel cell incorporating this catalyst achieved a peak power density of 245 mW cm^{-2}, showcasing its effectiveness in practical applications. The stability of the CoZn/NC–Ti_3C_2 catalyst is another key highlight of this study. After 30 000 seconds of continuous testing, the catalyst demonstrated only a 4.83% decrease in relative current, underscoring its durability and long-term performance reliability. This research introduces a major breakthrough in creating highly effective and stable catalysts made from non-precious metals for anion exchange membrane fuel cells (AEMFCs), providing a hopeful substitute for catalysts made from precious metals.[80] The study includes several critical experimental results to substantiate these findings. Fig. 12 presents: (a) voltage *versus* time (*V/T*) plots for CoZn/NC–Ti_3C_2, CoZn/NC, Co/NC–Ti, Zn/NC–Ti, and Pt/C catalysts in an oxygen-rich solution of 0.1 M KOH, showing the relative ORR efficiencies. (b) Voltage *versus* frequency (*V/F*) plots for the same catalysts in the same solution, revealing information about their charge transfer resistances and catalytic effectiveness. (c) Voltage *versus* time (*V/T*) plots for CoZn/NC–Ti_3C_2 (red) and Pt/C (black) catalysts in the same solution, emphasizing their stability and performance over time. (d) Voltage *versus* frequency (*V/F*) plots for CoZn/NC–Ti_3C_2 catalysts employed in H_2/O_2 fuel cells at 60 °C, demonstrating the real-world performance characteristics of the catalyst in fuel cell systems.[81] All the above results together show the potential of this CoZn/NC–Ti_3C_2 catalyst as a highly active and stable non-precious metal alternative to enhance the performance of anion exchange membrane fuel cells, hence making it of great significance in the energy storage and conversion areas.[82]

Recently, Wen-Tao Wang *et al.*[83] introduced a new non-noble metal catalyst, Fe–N–C@$Ti_3C_2T_x$, as a substitute for Pt-based ORR catalysts with high efficiency. The catalyst synthesis is developed using a novel, separated pyrolysis strategy, as explained by the synthesis flow chart. First, carbonization of Fe-doped Zeolitic Imidazolate Framework-8 (ZIF-8) transforms into Fe–N–C. Fig. 13: flow chart of the synthesis process of Fe–N–C@$Ti_3C_2T_x$, highlighting the sequential steps from Fe-doped ZIF-8 to the final composite. This Fe–N–C material is then mixed with few-layered $Ti_3C_2T_x$ and subjected to a subsequent

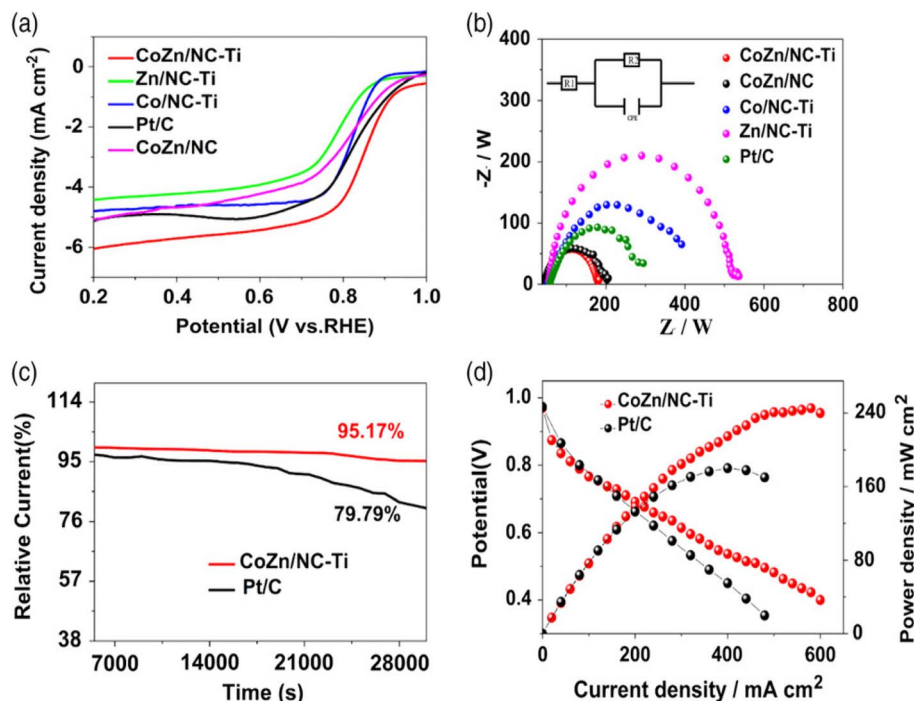This journal is © The Royal Society of Chemistry 2025

J. Mater. Chem. A, 2025, **13**, 12855–12890 | **12867**

Fig. 12 (a) LSV curves of CoZn/NC–Ti$_3$C$_2$, CoZn/NC, Co/NC–Ti, Zn/NC–Ti, and Pt/C in O$_2$-saturated 0.1 M KOH, benchmarking ORR activities. (b) EIS curves of these catalysts in O$_2$-saturated 0.1 M KOH, revealing charge transfer resistances and catalytic efficiencies. (c) Current–time responses of CoZn/NC–Ti$_3$C$_2$ (red) and Pt/C (black) in O$_2$-saturated 0.1 M KOH, comparing stability over time. (d) Polarization and power density curves of CoZn/NC–Ti$_3$C$_2$ in H$_2$/O$_2$ fuel cells at 60 °C, demonstrating practical performance. Reproduced from ref. 79 with permission from Wiley, copyright © 2022.

pyrolysis, resulting in the creation of Fe–N–C@Ti$_3$C$_2$T$_x$ composites. This method is advantageous as it maintains the high carbonization temperatures needed for Fe–N–C, ensuring its large catalytic activity, while simultaneously protecting the Ti$_3$C$_2$T$_x$ from potential damage that could arise from such high temperatures.[84] The Fe–N–C@Ti$_3$C$_2$T$_x$ catalyst exhibits remarkable ORR performance and stability across different conditions. In basic solutions, it exhibits a potential difference of 0.887 V when assessed to the reversible hydrogen electrode (RHE) and a maximum rate of diffusion of 6.3 mA cm^{-2}. Remarkably, it continues to function effectively without any decrease in performance after undergoing 10 000 cycles in a solution of 0.1 M KOH. In acidic conditions, the catalyst demonstrates a potential difference of 0.777 V when compared to RHE and a maximum rate of diffusion of 5.7 mA cm^{-2}, experiencing only a minor decrease of 11 mV after 10 000 cycles in a solution of 0.1 M HClO$_4$. The remarkable and exceptional efficiency exhibited by the Fe–N–C@Ti$_3$C$_2$T$_x$ catalyst can be attributed to the strong and robust interaction that takes place between the Fe–N–C component and the MXene components. This strong interaction is of paramount importance in enhancing the overall efficiency of the catalyst by effectively reducing both the
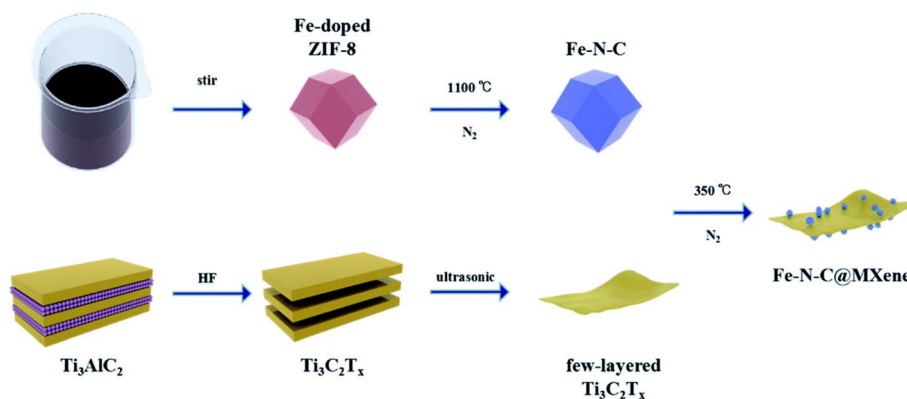

Fig. 13 Synthesis process flow chart for Fe–N–C@MXene. Reproduced from ref. 83 with permission from Royal Society of Chemistry, copyright © 2021.
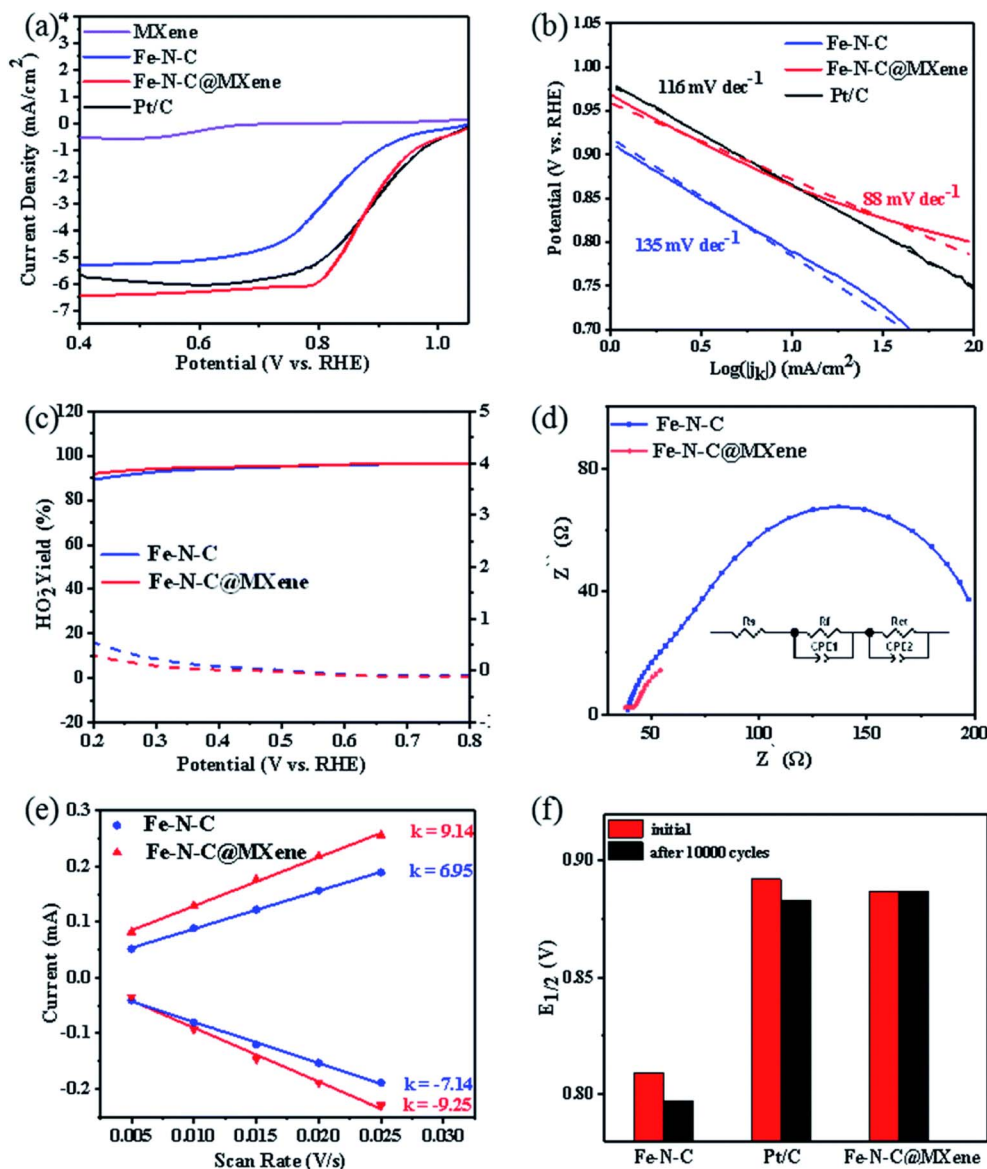
12868 | J. Mater. Chem. A, 2025, 13, 12855–12890

This journal is © The Royal Society of Chemistry 2025

Fig. 14   (a) Linear sweep voltammograms for MXene, Fe−N−C, Fe−N−C@MXene, and Pt/C; (b) linear sweep potentials for Fe−N−C, Fe−N−C@MXene, and Pt/C; (c) ETR and HO_2^- production for Fe−N−C and Fe−N−C@MXene; (d) electrochemical impedance spectroscopy and schematic representation; (e) voltage *vs.* scan rate for Fe−N−C and Fe−N−C@MXene; (f) electrochemical stability of Fe−N−C, Fe−N−C@MXene, and Pt/C. Reproduced from ref. 83 with permission from Royal Society of Chemistry, copyright © 2021.

intrinsic impedances and the charge transfer impedances, while simultaneously increasing the electrochemically active surface area available for reactions. The breakthrough, presented here in this piece of research, is a major, noteworthy stride toward improving the nature of non-noble metal-based catalysts. That it does indeed not merely open a promising but perfectly viable alternative to precious metal platinum for fuel cells and metal-air battery applications in particular is certain.[85] The crucial findings along with the performance metrics pertaining to the Fe−N−C@$Ti_3C_2T_x$ catalyst are comprehensively illustrated across multiple figures. Specifically, in Fig. 14, one can observe a thorough performance analysis conducted in a solution of 0.1 M KOH. This figure includes: (a) linear sweep voltammetry (LSV) curves that present

a comparison between MXene, Fe−N−C, Fe−N−C@$Ti_3C_2T_x$, and Pt/C, thereby showcasing the activity related to the oxygen reduction reaction (ORR). Additionally, (b) Tafel curves for Fe−N−C, Fe−N−C@$Ti_3C_2T_x$, and Pt/C are provided, which offer valuable insights into the kinetics associated with the ORR. (c) The electron transfer number and yield of HO_2^- for the materials Fe−N−C and Fe−N−C@$Ti_3C_2T_x$ have been studied, which would be useful to understand their reaction mechanisms. (d) EIS curves have been obtained along with the simulated circuit diagram, which helps to illustrate and explain the charge transfer properties of these materials.[86] (e) Current–potential plots against the scan rate for both Fe−N−C and Fe−N−C@$Ti_3C_2T_x$ have been analyzed, which shows their electrochemical activity and stability in different conditions. (f)
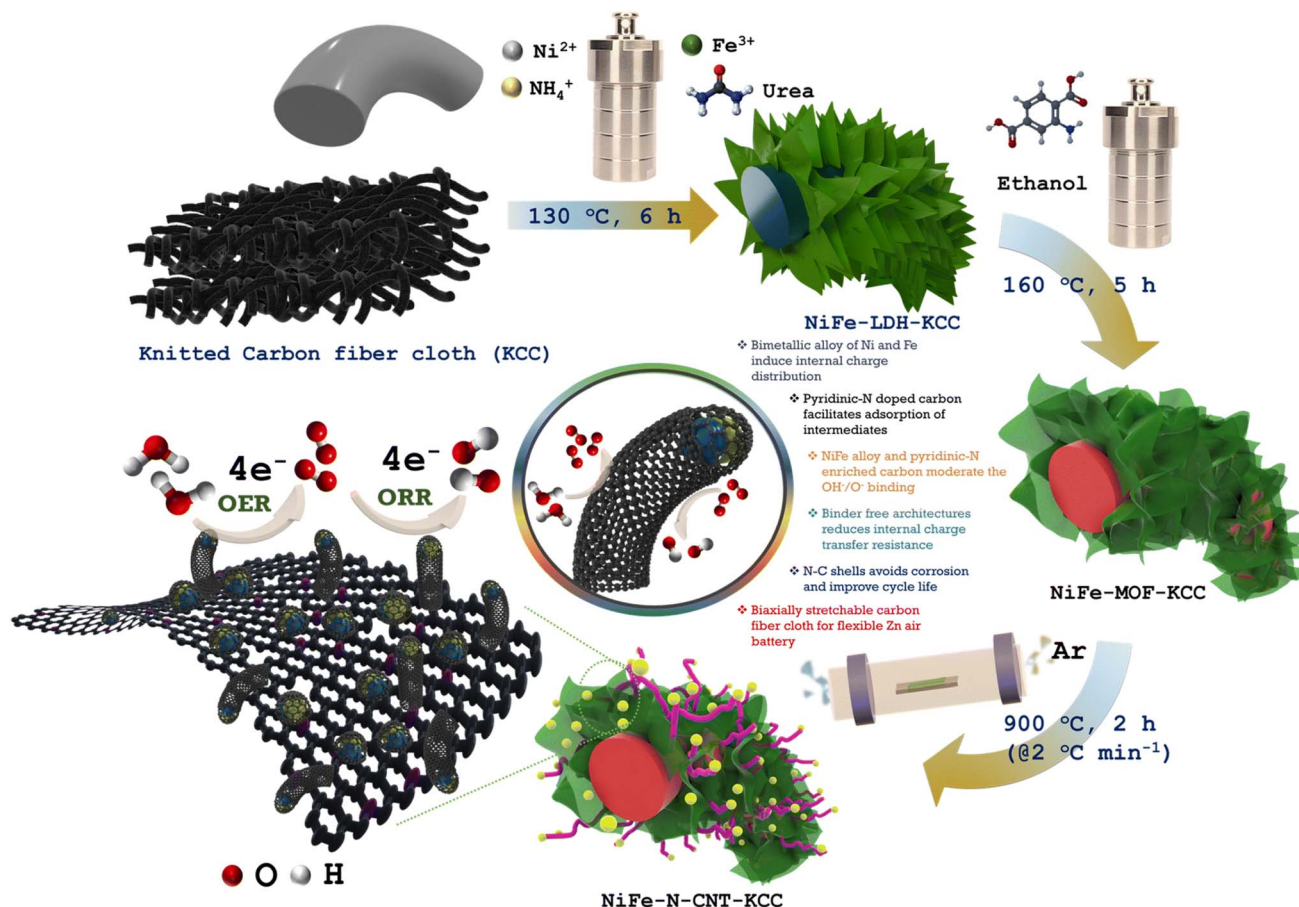
Fig. 15 Fabrication diagram for NiFe−N−CNT−KCC-based catalysts. Reproduced from ref. 88 with permission from Royal Society of Chemistry, copyright © 2024.

Detailed comparison of electrochemical stability properties among three catalysts, namely, Fe−N−C, Fe−N−C@Ti$_3$C$_2$T$_x$, and Pt/C. The noteworthy durability and performance of these catalysts have been highlighted through an extended testing time. These findings not only provide insight into the superior performance of Fe−N−C@Ti$_3$C$_2$T$_x$ as a high-performance catalyst for ORR but also open the doors for developing a new pathway for further increasing the efficiency and stability of non-noble metal catalysts that are very important for many applications in energy technology.[87]

In 2024, Milan Babu Poudel *et al.*[88] introduced an innovative dual-functioning electrocatalyst designed for flexible ZABs, showcasing a unique combination of carbon nanotubes and nickel–iron (NiFe) interfacial alloy nanoparticles decorated inside a pyridinic-N enriched *C*-matrix. The catalyst, referred to as NiFe−N−CNT−KCC, is fabricated utilizing a one-step pyrolysis process applied to zeolitic imidazolate frameworks (ZIFs)—specifically ZIF-67 and ZIF-8—deposited on knitted carbon fiber cloth (KCC). Fig. 15: details the preparation process for the NiFe−N−CNT−KCC electrocatalysts, outlining steps implicated in the manufacture and formation of the final electrocatalyst structure. This approach results in the formation of NiFe nanoparticles that are then encased in carbon nanotube (CNT) tentacles, a structure that is achieved through the catalytic

release of NiFe nanoparticles from the NiFe-metal–organic frameworks (MOFs) during pyrolysis in an inert atmosphere. The NiFe−N−CNT−KCC catalysts are characterized by their dominant presence of pyridinic-N, as exposed by X-ray photoelectron spectroscopy (XPS) and X-ray absorption spectroscopy (XAS). This pyridinic-N plays a crucial role by minimizing electron localization around the NiFe centers and enhancing their interaction with oxygenated species, thereby improving the electrocatalytic performance.[89] As a result, the NiFe−N−CNT−KCC catalysts exhibit exceptional properties with 173 mV as the lowest overpotential (η_{10}) for the OER and $E_{1/2}$ of 0.87 V for the ORR. These performance metrics are higher than those of many conventional electrocatalysts, indicating the effectiveness of NiFe−N−CNT−KCC in catalyzing these critical reactions. It demonstrated outstanding electrochemical characteristics when employed in ZAB as an air cathode. It achieved an OCV of 1.55 V, a supreme power density of 153 mW cm^{-2}, and an impressive specific capacitance of 793.2 mA h g^{-1}.

Additionally, it demonstrated excellent long-term stability, showcasing its reliability and durability in practical applications. A particularly noteworthy aspect of this study is the development of a solid-state flexible ZAB using NiFe−N−CNT−KCC electrode. This battery not only demonstrated exceptional rate performance but also maintained remarkable mechanical
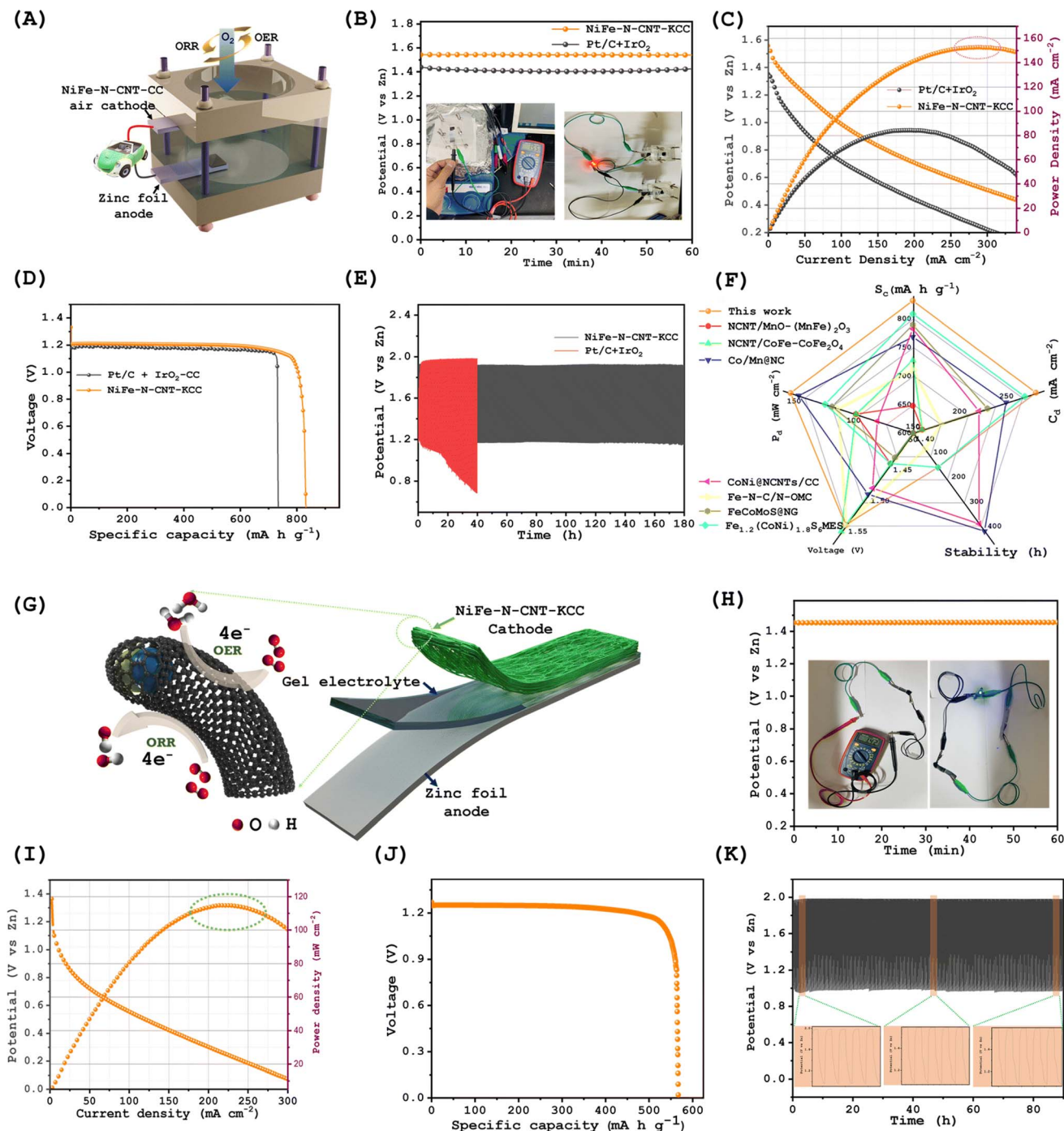
12870 | *J. Mater. Chem. A*, 2025, **13**, 12855–12890

This journal is © The Royal Society of Chemistry 2025

Fig. 16   (A) Typical illustration of aqueous ZAB with NiFe−N−CNT−KCC. (B) Comparison of OCV for NiFe−N−CNT−KCC against standard Pt/C and IrO$_2$ catalysts. (C) Capacity curve comparing NiFe−N−CNT−KCC with standard catalyst. (D) Discharge profiles and power density curves for the constructed ZABs, highlighting their operational efficiency. (E) Prolonged stability of the constructed aqueous ZAB, demonstrating its long-term performance stability. (F) Correlation measurements of NiFe−N−CNT−KCC with previously studied catalysts. (G) Typical sketch of the solid and flexible ZAB using NiFe−N−CNT−KCC catalyst, showing its design and structural features. (H) OCV for the NiFe−N−CNT−KCC in flexible ZABs. (I) Flexible ZABs Discharge and power density plateau, indicating its performance under flexible conditions. (J) Specific capacity curve of flexible ZAB. (K) Long-term stability of solid-state ZAB using NiFe−N−CNT−KCC, reflecting its endurance under various operating conditions. Reproduced from ref. 88 with permission from Royal Society of Chemistry, copyright © 2024.

stability under various twisting and bending situations. Such flexibility and durability are crucial for the practical implementation of batteries in next-generation wearable

applications, where both high power and large energy density are essential.[90] The study is illustrated with several figures that provide comprehensive insights into the performance and
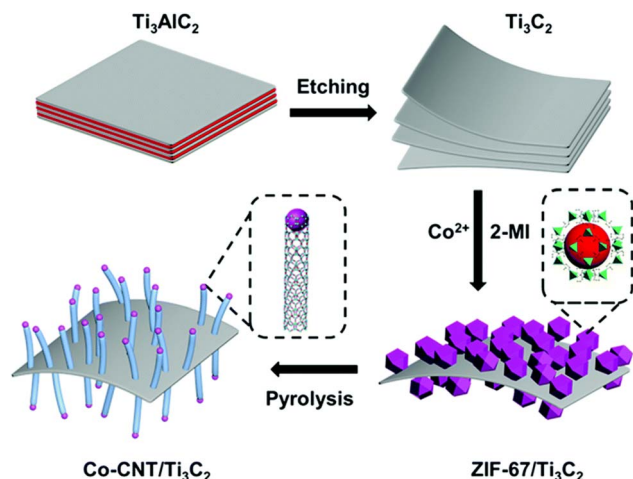
Fig. 17 Schematic illustration of the formation process for Co–CNT/Ti_3C_2 composites. Reproduced from ref. 91 with permission from Royal Society of Chemistry, copyright © 2024.

characteristics of NiFe–N–CNT–KCC catalyst: Fig. 16: displays key performance metrics of the Zn–air battery: (A) typical illustration of aqueous ZAB with NiFe–N–CNT–KCC. (B) Comparison of OCV for NiFe–N–CNT–KCC against standard Pt/C and IrO_2 catalysts. (C) Capacity curve comparing NiFe–N–CNT–KCC with standard catalyst. (D) Discharge profiles and power density

curves for the constructed ZABs, highlighting their operational efficiency. (E) Prolonged stability of the constructed aqueous ZAB, demonstrating its long-term performance stability. (F) Correlation measurements of NiFe–N–CNT–KCC with previously studied catalysts. (G) Typical sketch of the solid and flexible ZAB using NiFe–N–CNT–KCC catalyst, showing its design and structural features. (H) OCV for the NiFe–N–CNT–KCC in flexible ZABs. (I) Flexible ZABs discharge and power density plateau, indicating its performance under flexible conditions. (J) Specific capacity curve of flexible ZAB. (K) Long-term stability of solid-state ZAB using NiFe–N–CNT–KCC, reflecting its endurance under various operating conditions. These comprehensive findings underscore the significant potential of NiFe–N–CNT–KCC catalysts for advancing performance and practical application of ZAB, particularly in flexible and high-energy-density settings.

Jianian Chen *et al.*[91] reported a novel MOF-involved method for fabricating cobalt-tipped carbon nanotube/Ti_3C_2 nanosheet composites (Co–CNT/Ti_3C_2). This method is based on the *in situ* growth of ZIF-67 particles on Ti_3C_2 nanosheets, which are converted into Co-tipped CNTs by pyrolysis. Fig. 17 shows a typical schematic diagram of fabrication process of the composite Co–CNT/Ti_3C_2. This nanosheet will serve a twofold role in the fabrication: help act as a 2D conductive scaffold for the formation of Co–CNTs and assist in balancing the exchange between the graphitization of the carbon and the surface area of
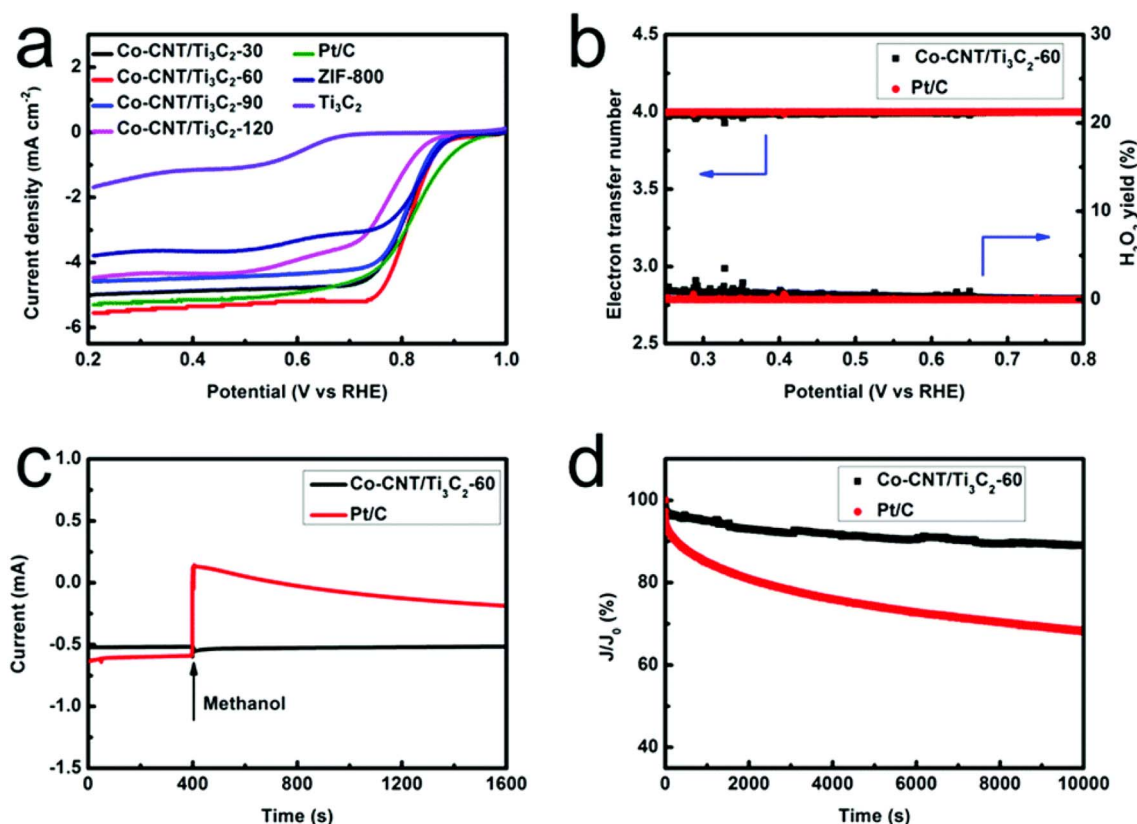

Fig. 18 (a) Load-deformation curves for Co–CNT/Ti_3C_2, Pt/C, ZIF-800, and Ti_3C_2. (b) Yield of H_2O_2 and electron transfer values for Co–CNT/Ti_3C_2-60 and Pt/C. (c) Resistance to methanol crossover for Co–CNT/Ti_3C_2 and Pt/C. (d) Time-dependent current (chronoamperometry) curves for Co–CNT/Ti_3C_2-60. Reproduced from ref. 91 with permission from Royal Society of Chemistry, copyright © 2024.

12872 | *J. Mater. Chem. A*, 2025, **13**, 12855–12890

This journal is © The Royal Society of Chemistry 2025

the material. The resulting Co–CNT/Ti$_3$C$_2$ composite thus shows several distinct features, including abundant Co–N/C active sites, high carbon graphitization, and proper surface areas. These features collectively contribute to the materials excellent electrocatalytic performance, particularly in oxygen reduction reactions (ORR). The enhanced Co–CNT/Ti$_3$C$_2$ material demonstrated ORR activity with a half-wave potential of 0.82 V and a diffusion-limited current density of 5.55 mA cm^{-2}. This performance is comparable to that of commercially available Pt/C catalysts, which also exhibit a half-wave potential of 0.82 V and a diffusion-limited current density of 5.30 mA cm^{-2}. However, the Co–CNT/Ti$_3$C$_2$ material is distinguished by its superior stability, surpassing Pt/C in long-term performance metrics. This advancement presents a significant opportunity for the use of Co–CNT/Ti$_3$C$_2$ composites in renewable energy conversion and storage applications.[92] The study included several key experimental results to support these findings. Fig. 18 further illustrates the performance comparisons: (a) voltage *vs.* time graphs for linear sweep voltammetry (LSV) experiments comparing Co–CNT/Ti$_3$C$_2$ with platinum/carbon, ZIF-800, and Ti$_3$C$_2$; (b) information on the amount of water produced and the rate of electron transfer for Co–CNT/Ti$_3$C$_2$-60 and platinum/carbon; (c) an examination of the resistance to methanol conversion; and (d) time-dependent voltage curves showing the endurance of Co–CNT/Ti$_3$C$_2$-60 in comparison to platinum/carbon. These findings underscore the possibility of Co–CNT/Ti$_3$C$_2$ mixtures as reliable and long-lasting substitutes for conventional platinum/carbon catalysts, especially in situations where prolonged stability and superior performance are essential.[93]

The development of MOF/MXene hybrid materials has demonstrated significant potential in advancing ORR for ZAB applications. The integration of MOFs with MXenes results in hybrid materials that exhibit enhanced catalytic activity, improved stability, and superior electrochemical properties. Various synthesis strategies, including pyrolysis, electrostatic adsorption, and solvothermal methods, have been employed to tailor these hybrids for optimal performance. Key advancements, such as the CoZn/NC–Ti$_3$C$_2$T$_x$, Fe–N–C@Ti$_3$C$_2$T$_x$, and NiFe–N–CNT–KCC catalysts, highlight the effectiveness of these materials in achieving high ORR efficiency, durability, and selectivity. The incorporation of MOF-derived carbon structures with MXenes not only enhances charge transfer but also provides a robust framework for long-term operation in ZABs. Furthermore, the development of flexible and solid-state ZABs underscores the versatility of these hybrids in next-generation energy storage technologies. These findings collectively reinforce the promising role of MOF/MXene hybrids in advancing energy conversion and storage, paving the way for future research and industrial applications in sustainable battery technologies.

7. MOFs/MXene hybrid materials for oxygen evolution reactions in ZABs application

The search for efficient and durable electrocatalysts for OER has led to the development of novel hybrid materials, particularly those based on MOFs and MXenes. These hybrid materials

combine the high surface area and tunable porosity of MOFs with the excellent electrical conductivity and structural stability of MXenes, making them promising candidates for electrocatalysis in energy storage and conversion applications. Recent studies have explored various synthesis strategies, structural modifications, and compositional optimizations to enhance the catalytic performance of MOF/MXene-based materials. This section reviews key advancements in their application for OER, particularly in ZABs, highlighting their structural advantages, electrochemical performance, and theoretical insights.

Komal Farooq *et al.*[94] has developed a user-friendly and versatile method for creating electrocatalysts capable of performing two reactions: the OER and HER. This method involves converting ZIF67/MXene hybrids into CoS@C/MXene nanocomposites by exposing them to hydrogen sulfide gas at elevated temperatures. Fig. 19 illustrates the formation of CoS@C/MXene nanocomposites at various temperatures. Among the synthesized nanocomposites, CSMX-800 exhibited the highest electrocatalytic activity for both OER and HER. Specifically, the CSMX-800 material demonstrated notable overpotentials of 257 mV at a current density of 10 mA cm^{-2} for OER and 270 mV at the same current density for HER. Furthermore, it exhibited low Tafel slope values of 93 mV per decade for the oxygen evolution reaction (OER) and 103 mV per decade for the hydrogen evolution reaction (HER). The outstanding electrocatalytic performance of materials containing MXene is attributed to their high surface area, enhanced electrical conductivity, and superior charge transfer properties.[95] This research underscores the potential of CoS@C/MXene-based electrocatalysts in facilitating electrocatalytic water splitting to produce hydrogen (H$_2$), which is essential for carbon emission reduction and environmental protection.[96] Fig. 20a presents the linear sweep voltammograms (LSV) for OER, and Fig. 20b shows the corresponding Tafel slopes. Fig. 21a illustrates the OER LSV trends of various CSMX samples, each containing different amounts of MXene (CSMX800-0.05, CSMX800-0.1, and CSMX800-0.2), alongside control samples (MXene, ZIF67, MXS, and ZIF67/MXene). Fig. 21b presents the time-dependent electrochemical behavior of CSMX-800 during a 12 hours period, with an additional section highlighting the OER LSV trends before and after
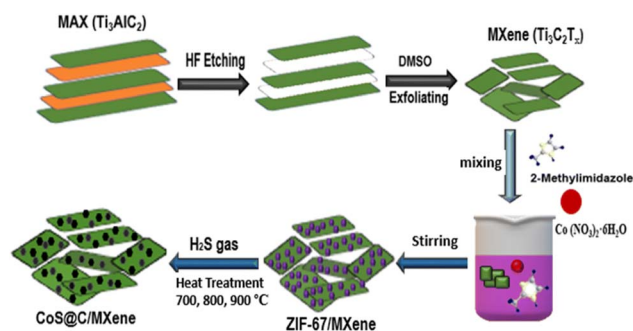

Fig. 19 Schematic of CoS@C/MXene nanocomposite synthesis at various temperatures. Reproduced from ref. 94 with permission from Royal Society of Chemistry, copyright © 2024.

This journal is © The Royal Society of Chemistry 2025
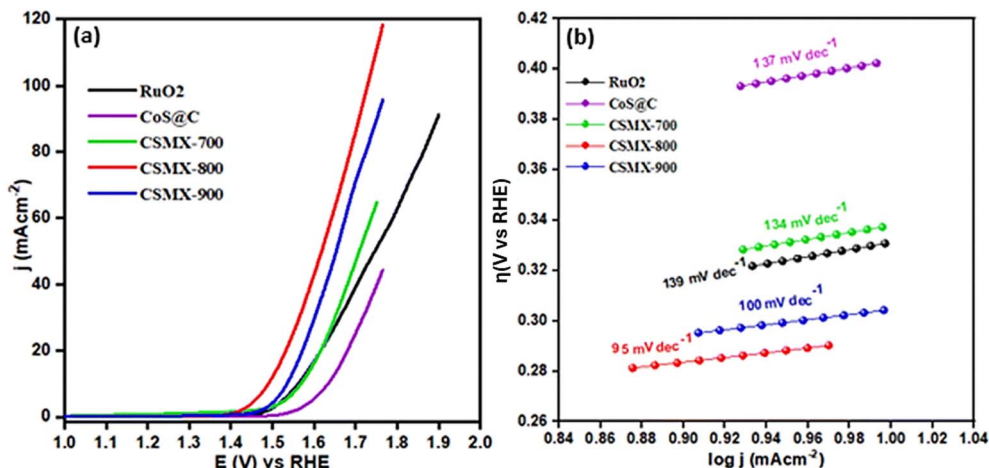
J. Mater. Chem. A, 2025, 13, 12855–12890 | 12873

Fig. 20 (a) OER LSV curves. (b) Tafel slopes. Reproduced from ref. 94 with permission from Royal Society of Chemistry, copyright © 2024.

undergoing 500 cycles of cyclic voltammetry (CV), showcasing the catalysts durability and reliability.

Linghao He *et al.*[97] have pioneered a new method in electrocatalysis by creating a sequence of cobalt compounds along with carbon nanotubes, which are carefully placed onto a graphene-like titanium carbide structure (CoO_x–N–C/TiO_2C). These mixtures come from a bimetallic cobalt zinc-based zeolitic imidazolate framework (ZIF) and a $Ti_3C_2T_x$ MXene composite (CoZn-ZIF/$Ti_3C_2T_x$). The synthesis process of these advanced materials is depicted in a schematic diagram (Fig. 22), illustrating the preparation of the CoO_x–N–C/TiO_2C catalyst. The resultant CoO_x–N–C/TiO_2C composites exhibit remarkable trifunctional electrocatalytic properties, making them highly effective for the HER, ORR, and OER. In a range of mixtures with varying amounts of $Ti_3C_2T_x$, the CoO_x–N–C/TiO_2C mixture (22.7%) stands out as the most effective in terms of electrochemical conductivity.[98] When used as a catalyst for the splitting of water, this mixture (22.7%) reaches a current density of 10 mA cm^{-2} ($E_j = 10$) at a remarkably low voltage of 1.45 V. Additionally, the composites ability to produce oxygen is shown to have a very small voltage difference of just 0.72 V between the

$E_j = 10$ for the OER and the ORRs half-wave potential. The remarkable catalytic abilities of CoO_x–N–C/TiO_2C (22.7%) can be linked to several important factors. First, the combined effect of the various components in the composite boosts its overall effectiveness. The presence of carbon nanotubes within the structure significantly improves electronic mobility, facilitating efficient electron transport.[99] Additionally, the hierarchical porosity of the composite aids in mass transport, allowing for more efficient reactant access to the active sites. Furthermore, the consistently strewn cobalt, cobalt oxide, and titanium dioxide active sites within the carbon framework contribute to the enhanced catalytic activity by providing numerous active centers for the electrochemical reactions.[100] These innovations underscore the potential of CoO_x–N–C/TiO_2C composites as multifunctional electrocatalysts, particularly for applications in water splitting and energy conversion technologies. The integration of MXene with CoZn-ZIF-derived materials presents a novel pathway for developing efficient, stable, and high-performance catalysts that are crucial for advancing sustainable energy solutions.[101]
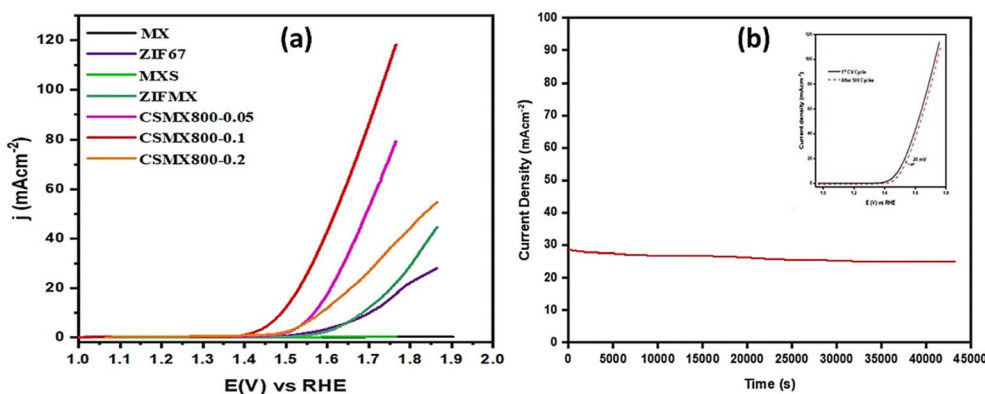

Fig. 21 (a) LSV curves for OER CSMX with varying amounts of MXene and standard samples. (b) Time–dependent electrochemical test for CSMX-800 over a period of 12 hours, including an enlarged section showing the LSV curves prior to and following 500 CV cycles. Reproduced from ref. 94 with permission from Royal Society of Chemistry, copyright © 2024.

Pingping Tan *et al.*[102] have developed an innovative 2D composite series, specifically MOF/Ti$_3$C$_2$T$_x$, which were synthesized using an electrostatically directed assembly method. These composite materials have revealed promising potential as catalysts for the OER, a critical procedure in water splitting and other energy conversion technologies.[103] The synthesis process, illustrated schematically in Fig. 23, highlights the formation of Co$_2$Ni-MOF@MXene, a 2D/2D heterostructure that effectively combines the unique properties of both MOFs and MXenes along with LSV curves. The enhanced electrocatalytic properties of these composites are attributed to ultrathin 2D/2D heterostructure, which provides plenty of reactive sites in the Co$_2$Ni-MOF matrix.[104] Additionally, the Ti$_3$C$_2$T$_x$ MXenes high electronic conductivity plays a crucial role in facilitating efficient charge transfer during the OER. Among the various catalysts tested, Co$_2$Ni-MOF@MX-1 emerged as the most effective, demonstrating superior oxygen evolution performance.[105] This was evidenced by its minimal Tafel slope of 51.7 mV dec^{-1} and the lowest possible overpotential of 265 mV at a current density of 10 mA cm^{-2} on carbon sheet. These findings suggest that the electrostatically directed assembly method used to synthesize these 2D composite materials is not only feasible but also highly effective in creating 2D heterostructure catalysts with enhanced catalytic performance.[106] The success of Co$_2$Ni-MOF@MXene composites in OER applications underscores their potential for broader use in energy storage and conversion technologies, where efficient and stable catalysts are crucial for enhancing the recital and sustainability of electrochemical processes.[107]

Chuming Xu *et al.*[108] have investigated a creative method to improve the efficiency of the OER by creating a metal–organic framework (MOF)/MXene composite material. Through the use of a pyrolysis–reorganization approach, they effectively produced a mixed spinel oxide with a heterogeneous composition of Co$_3$O$_4$/Co$_2$TiO$_4$. This novel composite material is designed by carefully regulating the pyrolysis temperature, which plays a critical role in simultaneously optimizing the mesoporous structures and the electronic arrangement of CoOct cations within the mixed spinel oxides.[109] The research findings reveal that these structural and electronic optimizations result in outstanding OER performances, characterized by low overpotentials—280 mV on a glassy carbon electrode and 260 mV on Ni foam at a current density of 10 mA cm^{-2}. Additionally, the material demonstrates remarkable stability in an alkaline solution, making it a favorable for experimental applications in energy conversion technologies.[110] A key discovery in this investigation is the synergistic catalytic effect between the CoOct^{3+} cations in Co$_3$O$_4$ and CoOct^{2+} cations in Co$_2$TiO$_4$. This interaction is essential for enhancing the OER activity, as it facilitates efficient electron transfer and improves the overall catalytic performance.[111] The strategic combination of these two cations within the spinel structure is shown to be a critical factor in achieving superior OER efficiency.[112] The studies findings, supported by polarization curves, Tafel plots, Nyquist plots, and chronoamperometry results (as depicted in Fig. 24), highlight the significant impact of this material on the field of electrocatalysis. The successful application of this pyrolysis–reorganization strategy opens up new avenues for the improvement of Co-based spinel oxides with enhanced OER activity.[113] These advancements offer promising opportunities for improving the performance of electrochemical devices, particularly in sustainable energy advancements such as water splitting and fuel cells.
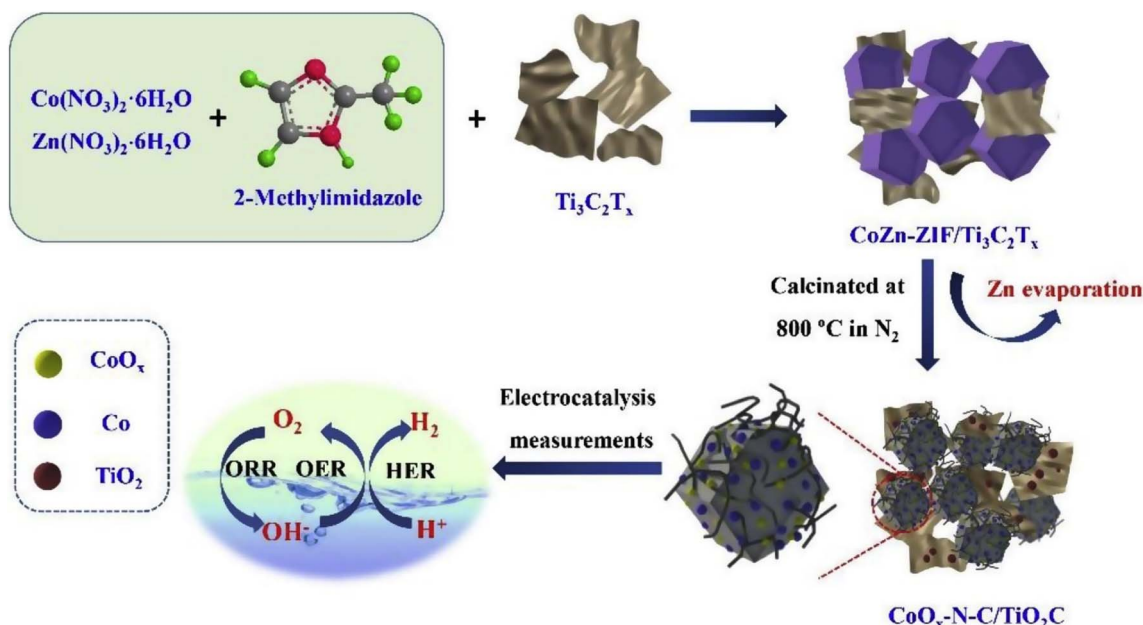

Fig. 22 Diagram illustrates the preparation process for the CoO$_x$−N−C/TiO$_2$C catalyst.[97] Reproduced from ref. 97 with permission from Elsevier Ltd, copyright © 2019.

This journal is © The Royal Society of Chemistry 2025

J. Mater. Chem. A, 2025, 13, 12855–12890 | 12875

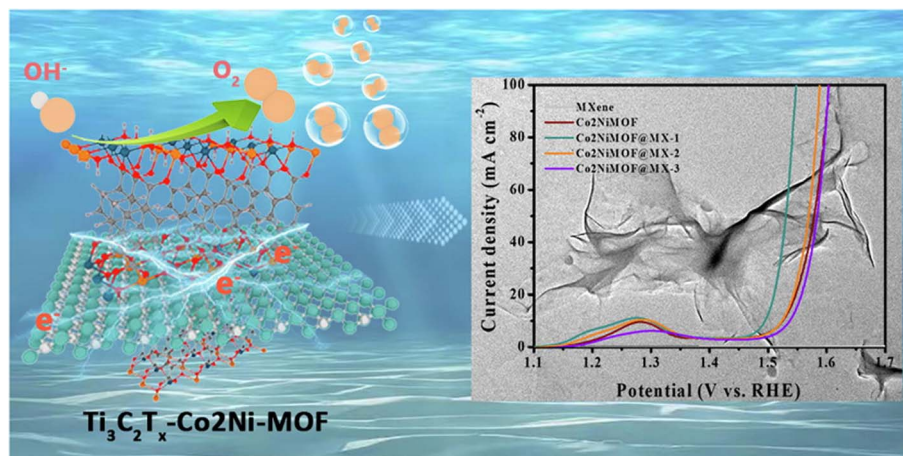**Fig. 23** Illustration of the Co_2Ni-MOF@MXene synthesis process with LSV curves. Reproduced from ref. 102 with permission from Elsevier Ltd, copyright © 2023.

Jinzhou Li *et al.*[114] have reported a notable advancement in electrocatalysis with their development of a carbon and nitrogen co-doped porous Co_2P catalyst, extracted from the metal–organic framework (MOF) ZIF-67. This material, referred to as MX@MOF-Co_2P, is further anchored on bimetallic MXene nanosheets, combining the advantageous properties of both components.[115] The synthesized MX@MOF-Co_2P demonstrates exceptional performance as a catalyst for the OER. The material shows remarkably low overpotentials of 246 mV at a current density of 10 mA cm^{-2} and 407 mV at 200 mA cm^{-2}. These

values indicate high catalytic efficiency, reflecting the materials effectiveness in facilitating the OER process.[116] Additionally, the catalyst exhibits an ultralow Tafel slope of 28.18 mV dec^{-1}, further highlighting its superior kinetic performance and suggesting rapid and efficient reaction kinetics. The innovative integration of carbon and nitrogen doping with porous Co_2P, along with the support of MXene nanosheets, increases both the electrochemical execution and efficiency of the catalyst.[117] This approach delivers a important pathway for developing high-performance OER catalysts with improved activity and
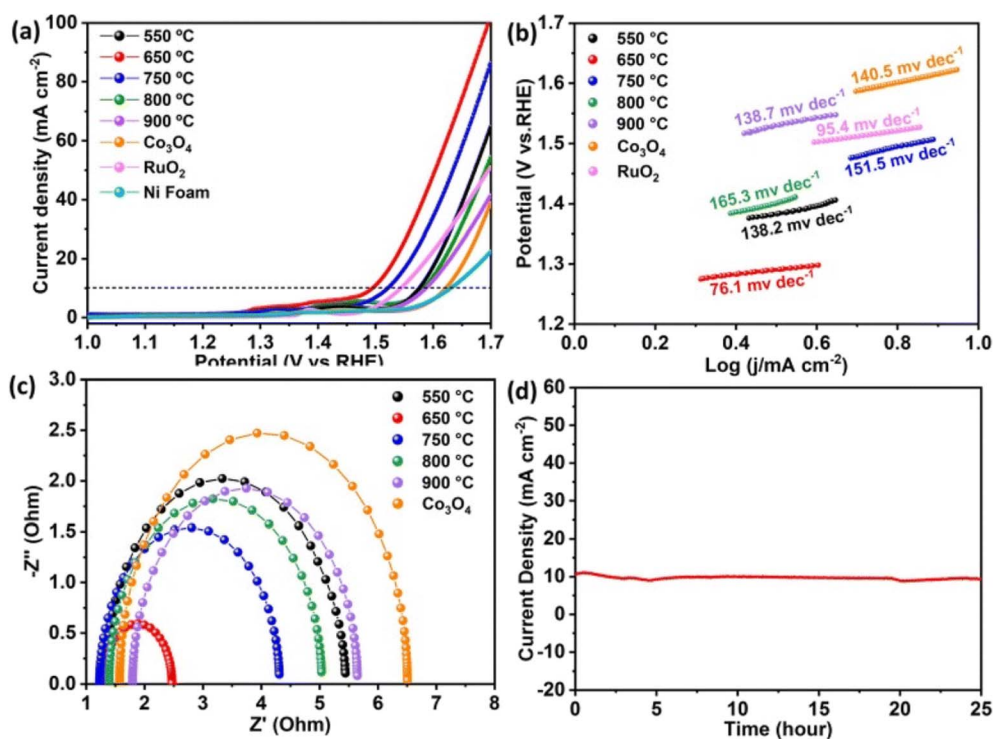

Fig. 24 (a) Polarization graphs for CoTiO$_x$–T samples and Co_3O_4-coated Ni foam. (b) Tafel diagrams for these catalysts. (c) Nyquist diagrams. (d) Temporal amperometry of CoTiO$_x$-650 at 1.49 V *versus* RHE. Reproduced from ref. 108 with permission from Royal Society of Chemistry, copyright © 2023.

12876 | *J. Mater. Chem. A*, 2025, **13**, 12855–12890

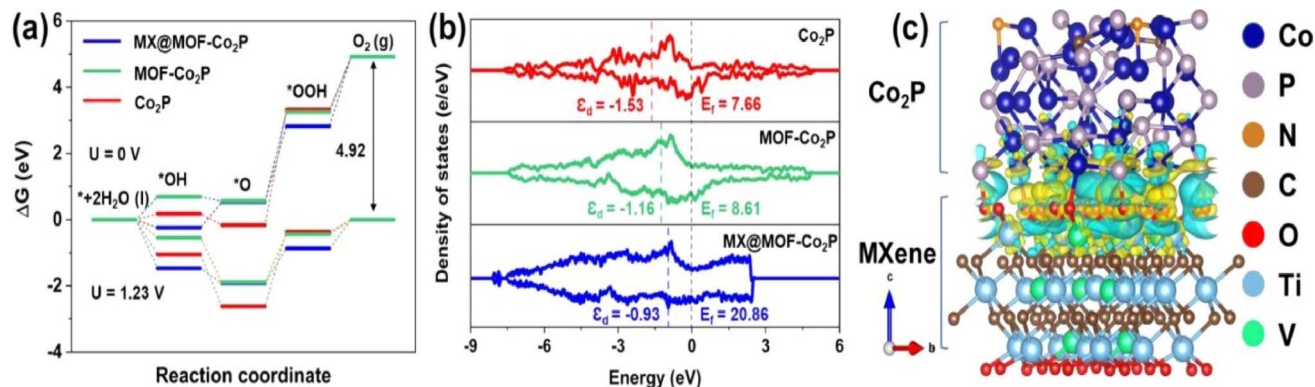This journal is © The Royal Society of Chemistry 2025

Fig. 25 (a) Energy flow chart for open educational resources. (b) Distribution of charge density (DOS) along with the associated d-band center and Fermi energy (E_f). (c) Charge density difference across the Co_2P–MXene boundary, with yellow showing electron gathering and blue showing electron shedding. Reproduced from ref. 114 with permission from Elsevier Ltd, copyright © 2023.

durability, which are crucial for advancing renewable energy technologies and other applications requiring efficient electrocatalysts.[118] DFT calculations were also accomplished to evaluate the intrinsic OER activity of Co_2P, MOF-Co_2P, and MX@MOF-Co_2P. The OER mechanism at the anode under alkaline conditions involves four steps:

(a) $M + OH^- \rightarrow MOH^* + e^-$,

(b) $MOH^* + OH^- \rightarrow MO^* + H_2O + e^-$,

(c) $MO^* + OH^- \rightarrow MOOH^* + e^-$, and

(d) $MOOH^* + OH^- \rightarrow M + O_2 + H_2O + e^-$.

In this case, * indicates an active site and M stands for the catalyst. The rate-limiting phase is usually the change from step b to step c, and a significant activity descriptor is the difference in Gibbs free energy, $\Delta G\_OOH^* - \Delta G\_O^*$. The rate-determining step (RDS) in Fig. 25a is the transition from O* to OOH*, which has the largest Gibbs free energy shift. At $U = 0$ V, MX@MOF-Co_2P shows the smallest $\Delta G\_OOH^* - \Delta G\_O^*$ (2.29 eV), indicating better OER kinetics compared to MOF-Co_2P (2.69 eV) and Co_2P (3.48 eV), consistent with EIS results. At $U = 1.23$ V, steps b to c are not spontaneous, but at $U = 2.3$ V, the entire OER process becomes spontaneous.[119] The enhanced RDS performance is attributed to the combination of carbon and nitrogen doping, along with the cooperative impact of Co_2P and MXene. Analysis of Bader charges indicates that nitrogen elements pull electrons from Co, facilitating the formation of Co with high valence.[120] Moreover, the increased number of available energy levels at the Fermi level for MX@MOF-Co_2P (as shown in Fig. 25b) points to improved conductivity and the movement of electrons. A greater d-band depth (−0.93 eV) implies a stronger chemical interaction, which supports the adsorption of oxygen

intermediates and enhances the rate of reactions. Charge density mapping (as depicted in Fig. 25c) shows the transfer of charges between Co_2P and MXene, which boosts the redistribution of charges and speeds up the OER process.

Combining detailed characterizations with theoretical calculations, Li et al.[121] identified several key factors underlying the exceptional performance of their MX@MOF-Co_2P catalyst. The remarkable catalytic activity is largely ascribed to the retention of the porous structure from the original MOF, ZIF-67, which gives a high density of accessible active sites.[122] This intrinsic porosity enhances the materials catalytic efficiency by improving reactant accessibility and overall reaction kinetics. Additionally, the carbon and nitrogen doping modulate the electronic structure of the cobalt phosphide, optimizing the electronic environment around the active sites and reducing energy barriers associated with the OER.[123] Furthermore, the combined consequence among the cobalt phosphide and MXenes plays an important part in boosting performance. The MXenes enhance electronic conductivity and facilitate efficient charge transfer processes, thus improving the overall electrocatalytic activity.[124] This interplay between the cobalt phosphide and MXenes ensures rapid and effective electron transfer, leading to the catalysts superior performance. Collectively, these factors—preserved porosity, tailored electronic properties due to doping, and the beneficial interaction among cobalt phosphide and MXenes—contribute to the exceptional electrocatalytic activity of the MX@MOF-Co_2P catalyst.[125]

Liuyong Hu et al.[126] explored an innovative approach for enhancing electrocatalytic performance by utilizing Ti_3C_2 MXene as a support material in conjunction with a MOF. Their
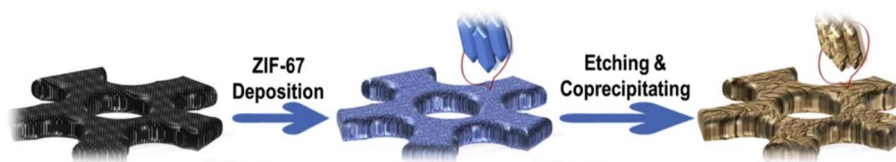

Fig. 26 Schematic of the synthesis process for CoFe MLDH/Ti_3C_2. Reproduced from ref. 126 with permission from Elsevier Ltd, copyright © 2021.
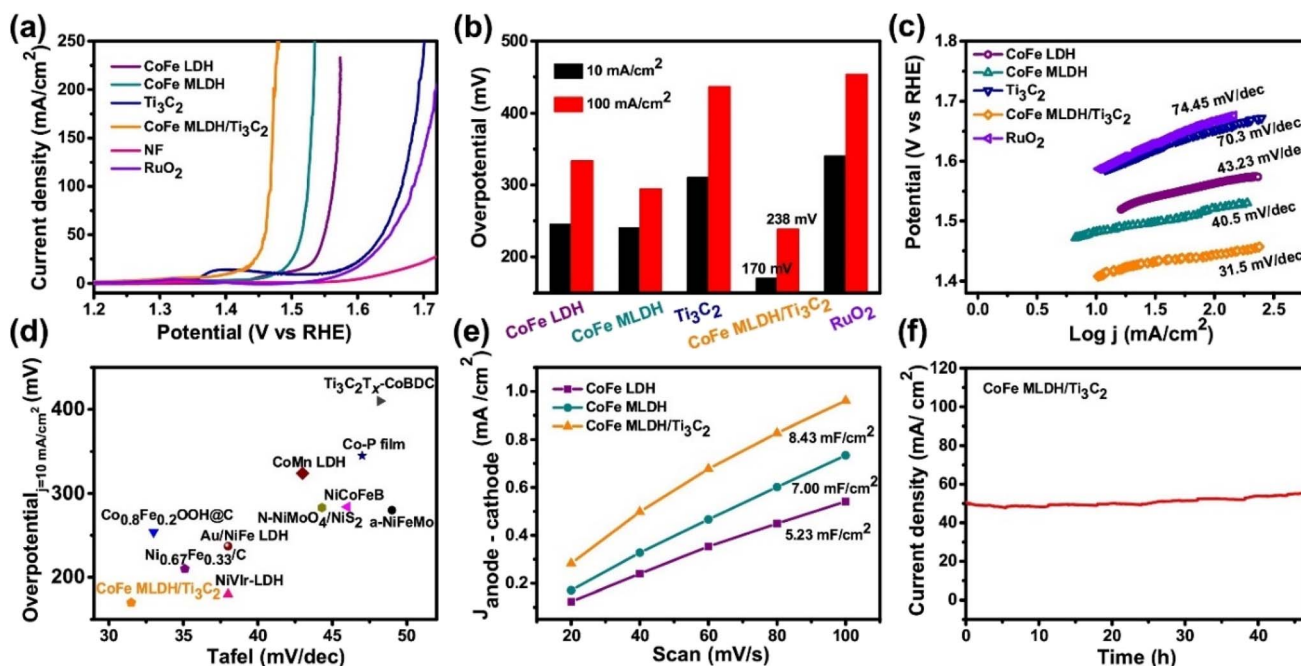
This journal is © The Royal Society of Chemistry 2025

J. Mater. Chem. A, 2025, 13, 12855–12890 | 12877

Fig. 27 (a) Polarization curves for Open Educational Resources (OER). (b) Overpotential measurements at $j = 10$ mA cm^{-2}. (c) Tafel diagrams for various catalysts. (d) Overpotential measurements at $j = 10$ mA cm^{-2} and a comparison of Tafel slopes for CoFe MLDH/Ti$_3$C$_2$ and other OER catalysts. (e) Composition of deposition layer (C_dl) values for CoFe LDH, CoFe MLDH, and CoFe MLDH/Ti$_3$C$_2$. (f) Time-dependent potential (chronopotentiometric) curve for CoFe MLDH/Ti$_3$C$_2$. Reproduced from ref. 126 with permission from Elsevier Ltd, copyright © 2021.
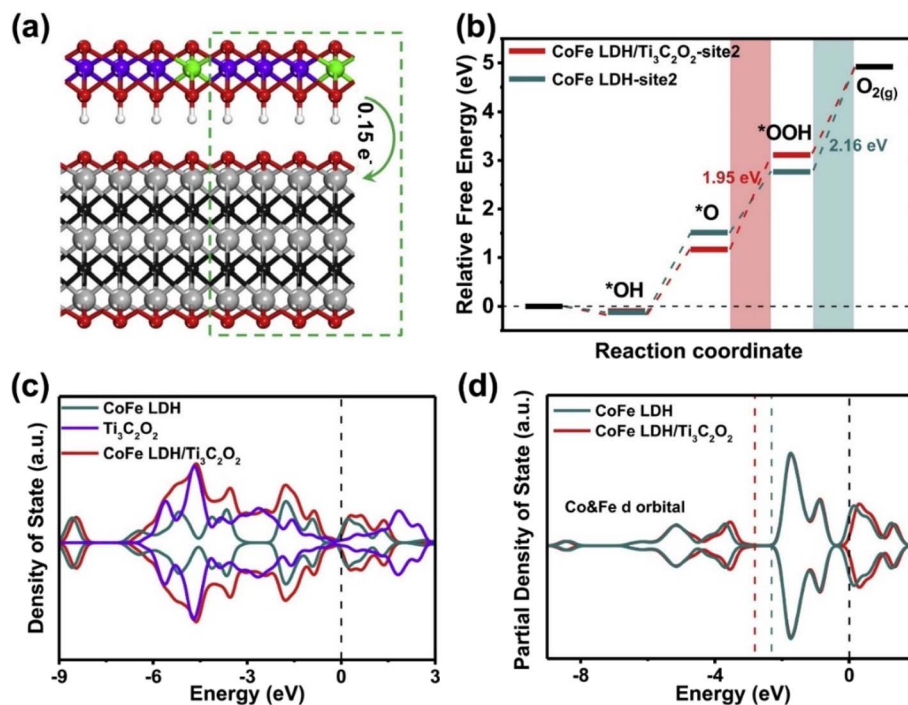

Fig. 28 (a) Side view of optimized CoFe LDH/Ti$_3$C$_2$O$_2$ (2 × 1 × 1 cell) with color-coded elements. (b) Free energy diagrams for OER at 0 V on CoFe LDH and CoFe LDH/Ti$_3$C$_2$O$_2$. (c) DOS of CoFe LDH/Ti$_3$C$_2$O$_2$, CoFe LDH, and Ti$_3$C$_2$O$_2$, with Fermi level at zero. (d) PDOS of 3d orbitals for Co and Fe in CoFe LDH and CoFe LDH/Ti$_3$C$_2$O$_2$, showing d-band centers. Reproduced from ref. 126 with permission from Elsevier Ltd, copyright © 2021.

12878 | *J. Mater. Chem. A*, 2025, **13**, 12855–12890

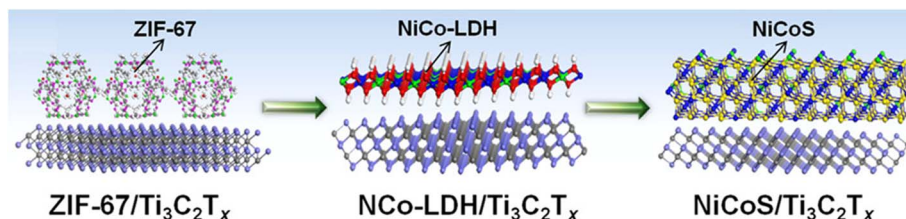This journal is © The Royal Society of Chemistry 2025

Fig. 29 Diagram of the preparation process for NiCoS/Ti$_3$C$_2$T$_x$. Reproduced from ref. 133 with permission from American Chemical Society, copyright © 2018.

method involved an etching-coprecipitating process to develop a CoFe layered double hydroxide (MLDH) composite with Ti$_3$C$_2$ MXene, resulting in the creation of CoFe MLDH/Ti$_3$C$_2$. This advanced catalyst demonstrates remarkable oxygen evolution reaction (OER) performance, achieving impressively smallest overpotential (170 mV and 238 mV) at the tested current densities (10 mA cm^{-2} and 100 mA cm^{-2}). The manufacture technique of CoFe MLDH/Ti$_3$C$_2$ is depicted in Fig. 26a, which illustrates how Ti$_3$C$_2$ MXene integrates with CoFe MLDH to enhance catalytic performance. The interaction among CoFe MLDH and Ti$_3$C$_2$ MXene significantly improves the binding strength of intercedes involved in the OER, leading to optimized catalytic activity.[127] This is supported by both experimental data and theoretical findings, which reveal that the strong electronic interaction among the two components of the composite results in improved efficiency by lowering energy barriers and optimizing reaction pathways.[128] The study provides comprehensive data on the catalysts performance. Fig. 27a shows the OER polarization curves of CoFe MLDH/Ti$_3$C$_2$ alongside other catalysts, demonstrating its superior performance.[129] Fig. 27b highlights the overpotential measurements at 10 mA cm^{-2} and 100 mA cm^{-2}, while Fig. 27c presents the Tafel plots, all of which underscore the catalysts exceptional performance in relation to existing technologies.[130] Additional figures include Fig. 27d, which compares the overpotential at 10 mA cm^{-2} and Tafel slopes for CoFe MLDH/Ti$_3$C$_2$ with other described OER catalysts, and Fig. 27e, showing capacitance measurements (C_dl) for CoFe LDH, CoFe MLDH, and CoFe MLDH/Ti$_3$C$_2$. Fig. 27f provides the chronopotentiometric curve, illustrating the durability of the catalyst. Theoretical analyses in Fig. 28a and b provide further insights into the structure and electronic properties of CoFe LDH/Ti$_3$C$_2$O$_2$, including free energy diagrams and density of states (DOS) calculations. Fig. 28c shows the DOS of CoFe LDH/Ti$_3$C$_2$O$_2$ compared to individual CoFe LDH and Ti$_3$C$_2$O$_2$, while Fig. 28d presents the projected density of states (PDOS) for the 3d orbitals of Co and Fe, highlighting the d-band center. These theoretical findings elucidate the electronic and catalytic mechanisms at play, offering a deeper understanding of the factors contributing to the catalysts high activity.[131] This research not only advances the development of efficient MOF-based catalysts but also enhances the intrinsic activity of (oxy)hydroxide-based catalysts, paving the way for improved performance in electrochemical applications.[132]

Haiyuan Zou *et al.*[133] has introduced a novel approach for enhancing electrocatalytic performance through the development of a hierarchical porous Ni–Co-mixed metal sulfide (denoted as NiCoS) supported on Ti$_3$C$_2$T$_x$ MXene. This composite is fabricated using a metal–organic framework (MOF)-based technique, as illustrated in Fig. 29, which details the synthesis method of NiCoS/Ti$_3$C$_2$T$_x$. The resulting hybrid material benefits from a unique structural arrangement and robust interfacial interactions among NiCoS and Ti$_3$C$_2$T$_x$ sheets. In oxygen evolution reactions (OERs), this design improves the charge-transfer conductivity and active surface area, which results in better performance.[134] Interestingly, the hierarchical NiCoS changes into a nickel/cobalt oxyhydroxide–NiCoS assembly (referred to as NiCoOOH–NiCoS) during the OER process. Effective OER is attributed to intrinsic active species, specifically the NiCoOOH that forms on the surface.[135] The hybrid materials exceptional performance is also seen in its use as an air cathode in rechargeable ZABs.[136] Here, it demonstrates low charging and discharging overpotentials as well as impressive long-duration stability.[137] The research highlights the advantages of integrating MXenes with MOF-derived materials to tailor the structure and enhance electrocatalytic performance.[138] This approach offers valuable insights into the structure–activity relationship of noble metal-free catalysts, paving the way for more efficient and durable electrocatalysts.[139] Fig. 30a compares the open-circuit potentials of rechargeable Zn–air batteries using NiCoS/Ti$_3$C$_2$T$_x$ + Pt/C and RuO$_2$ + Pt/C configurations, while Fig. 30b shows a picture of a red LED array powered by a Zn–air battery based on the NiCoS/Ti$_3$C$_2$T$_x$ + Pt/C air cathode, demonstrating the practical applicability of the developed catalyst.[140]

Li Zhao *et al.*[141] have reported an innovative approach to enhance oxygen evolution reaction (OER) performance through the *in situ* hybridization of Ti$_3$C$_2$T$_x$ nanosheets with 2D cobalt 1,4-benzenedicarboxylate (CoBDC), using the interdiffusion reaction-aided method. This process is schematically illustrated in Fig. 31, which details the synthesis of the Ti$_3$C$_2$T$_x$–CoBDC hybrid for OER applications. The resulting Ti$_3$C$_2$T$_x$–CoBDC hybrid material demonstrated impressive OER performance. The substance displayed a present current density of 10 mA cm^{-2} under a voltage of 1.64 V, in contrast to the RHE, featuring a Tafel slope of 48.2 mV per decade in a 0.1 M KOH solution. These findings surpass the capabilities of the traditional catalyst made from IrO$_2$. They are on par with, or possibly superior to, the most sophisticated catalysts created from transition
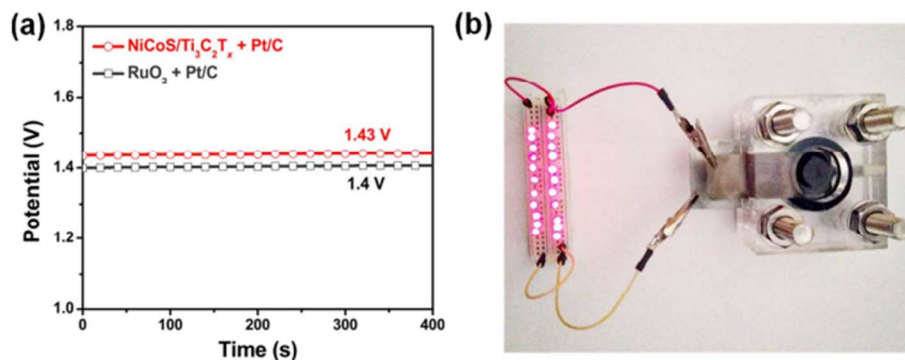
This journal is © The Royal Society of Chemistry 2025

J. Mater. Chem. A, 2025, **13**, 12855–12890 | **12879**

Fig. 30 (a) Open-circuit voltage plots for rechargeable Zn–air batteries with NiCoS/$Ti_3C_2T_x$ + Pt/C and RuO_2 + Pt/C configurations. (b) Red LED array powered by a Zn–air battery using NiCoS/$Ti_3C_2T_x$ + Pt/C air cathode. Reproduced from ref. 133 with permission from American Chemical Society, copyright © 2018.
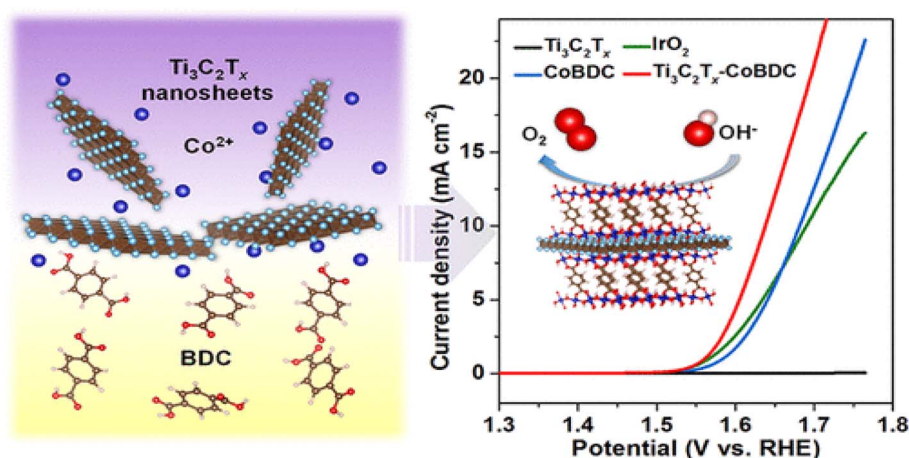

Fig. 31 Schematic of $Ti_3C_2T_x$–CoBDC hybrid preparation for the oxygen evolution reaction, with OER polarization curves. Reproduced from ref. 141 with permission from American Chemical Society, copyright © 2017.

metals that have been documented before. A substantial active surface area and a highly porous structure are provided by the CoBDC component. The rapid transfer of charge and ions across the well-defined $Ti_3C_2T_x$–CoBDC interface is facilitated by the hydrophilic and electrically conductive $Ti_3C_2T_x$ nanosheets. Consequently, the electrolytes access to the catalytically active CoBDC surfaces is enhanced. The $Ti_3C_2T_x$–CoBDC hybrid material was utilised in an air cathode for a rechargeable ZAB in addition to its exceptional OER performance. This battery efficiently supplied power to an LED, showcasing its utility in storing energy. Fig. 32 offers a diagrammatic representation of the rechargeable ZAB (32a), along with the polarization curves for ZABs using different combinations of materials such as $Ti_3C_2T_x$–CoBDC + Pt–C and IrO_2 + Pt–C (32b). The polarization curves for charge and discharge during operation at a current density of 0.8 mA cm^{-2} (32c) and a picture of an LED illuminated by the ZAB, specifically with the $Ti_3C_2T_x$–CoBDC + Pt–C material, (32d) highlight the batteries versatility in practical settings. This work highlights the advantages of *in situ* hybridization of MXenes and 2D MOFs, suggesting that careful control

of the interface between these materials can open new prospects for their use in advanced energy-based applications.

The development of MOF/MXene hybrid materials for OER in ZABs has demonstrated significant advancements in electrocatalysis. The studies reviewed highlight the potential of these hybrid materials to enhance catalytic performance through innovative synthesis techniques, structural modifications, and strategic compositional engineering.[142] One of the key findings is that integrating MXene with MOFs enhances electrocatalytic activity due to improved surface area, electrical conductivity, and charge transfer properties.[143] For instance, the CoS@C/MXene composite (CSMX-800) and the CoO_x–N–C/TiO_2C hybrid showed exceptional OER and hydrogen evolution reaction (HER) efficiencies, with low overpotentials and small Tafel slopes. Similarly, Co_2Ni-MOF@MXene composites exhibited high electrocatalytic performance due to their 2D/2D heterostructures, which provided abundant active sites and facilitated rapid charge transfer. The integration of MXene nanosheets with MOFs, such as MX@MOF-Co_2P and CoFe MLDH/Ti_3C_2, also significantly enhanced OER kinetics and durability, attributed to the synergistic effects between MXenes
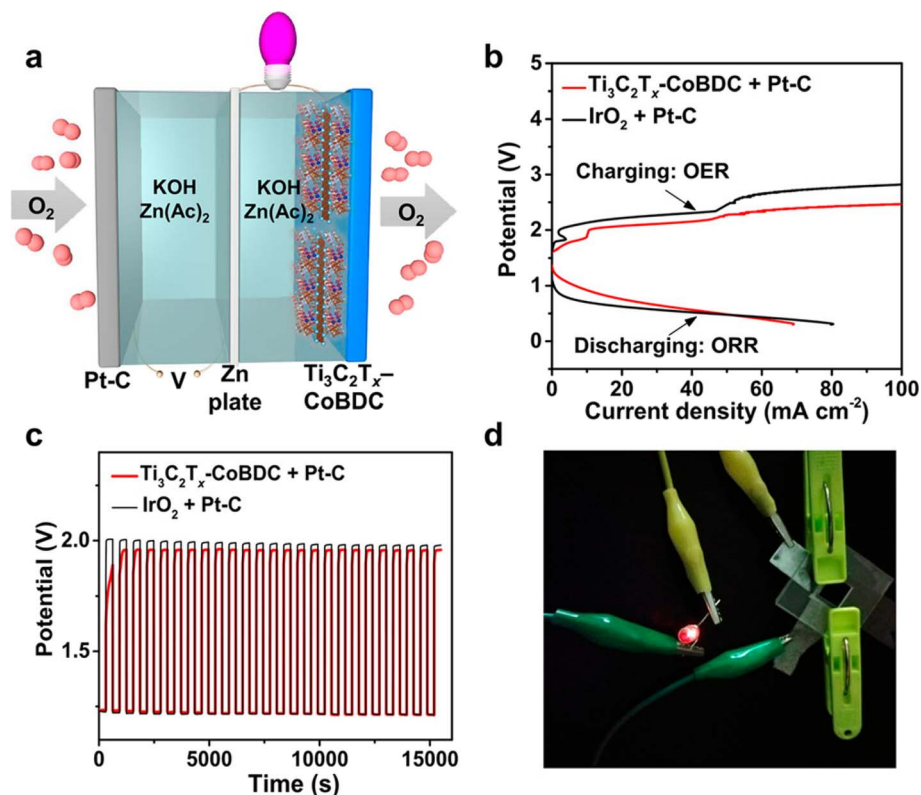
Fig. 32 (a) Diagram showing the structure of a rechargeable ZAB. (b) Graphs illustrating the polarization patterns during charging and discharging in ZABs with different compositions, including $Ti_3C_2T_x$–CoBDC + Pt–C and IrO_2 + Pt–C setups. (c) Graphs depicting the charging and discharging behavior over time at a current of 0.8 mA cm^{-2}. (d) Image of a red LED being illuminated by the ZAB with the composition $Ti_3C_2T_x$–CoBDC + Pt–C. Reproduced from ref. 141 with permission from American Chemical Society, copyright © 2017.

conductivity and the catalytic activity of MOF-derived materials. Theoretical calculations, including DFT analyses and Gibbs free energy evaluations, further confirmed the superior performance of these hybrid materials by revealing optimized electronic structures and reaction pathways.[144] The enhanced interaction between MXene and MOF-derived metal oxides, hydroxides, or phosphides has been crucial in reducing energy barriers, improving electron transfer, and stabilizing active sites, leading to superior OER activity.[145] Additionally, several studies demonstrated the practical application of these materials in rechargeable ZABs, showing prolonged stability, high efficiency, and lower charge–discharge overpotentials. The hierarchical porosity, doping strategies, and tailored electronic structures have contributed significantly to optimizing the OER activity of these hybrid materials.[146] Overall, MOF/MXene hybrid materials represent a promising class of electrocatalysts with remarkable efficiency and durability for OER applications in sustainable energy systems. The continued development of these materials, along with deeper mechanistic insights from both experimental and theoretical studies, will pave the way for more advanced and scalable electrocatalytic technologies in the future.[147]

8. Challenges in ZABs

A key obstacle in creating sustainable ZABs is the need to greatly improve their energy efficiency and prolong their use.[148] A vital part of how ZABs work is the performance of the air cathode, which charges and discharges *via* the OER and ORR, as mentioned. Yet, these reactions face challenges due to slow reaction rates, mainly because of the intricate electron transfer processes involved.[149] To address this issue, there is an urgent requirement to develop efficient catalysts that can speed up these reaction rates.[150] Despite the progress made in identifying various electrocatalysts for ORR and OER, the challenge of designing efficient bifunctional electrocatalysts—capable of facilitating both reactions—remains a formidable task.[151] The complexity arises from the distinct nature of ORR and OER, which, although reversible, involve different processes due to the variability in their active sites. Controlling factors such as the d-band center and oxygen adsorption strength is crucial for optimizing the internal charge–discharge mechanisms, which are vital for the rapid advancement of ZAB technology.[152]

The main reason for complex chemical reactions happening at the interface where gas, liquid, and solid meet is mainly because of the complex ways electrons are transferred, which make it hard for electrons to move around easily.[153] Right now, the catalysts being looked at for their ability to do two things at once are usually in powder form, which makes putting them together into ZABs quite difficult. A big problem is that the catalysts made from noble metals like platinum (Pt/C) for ORR and iron (Ir/RuO$_2$) for OER are very expensive.[154] Also, using

This journal is © The Royal Society of Chemistry 2025

J. Mater. Chem. A, 2025, **13**, 12855–12890 | **12881**

adhesives to stick these powder catalysts to the air cathode can make the electrode less conductive, making it harder to design effective ZABs.[155] On the other hand, creating 2D MXene electrodes, which have a MOF host right on a conductive surface, offers a good solution to these problems.[156] This method increases the surface area of the electrode and helps prevent the catalyst from breaking down over time during the batteries use.[157,158] The integration of MOFs with MXenes offers significant advantages, including a large surface area, a mixture of metal centers, and tunable porosity, all of which contribute to improved electron and mass transport.[159] These features are particularly beneficial for enhancing both OER and ORR kinetics, thereby boosting the batteries overall efficiency. Moreover, the initiation of MOF/MXene composite electrodes represents a novel and promising strategy to address the limitations associated with powder catalysts.[160,161] These composites not only improve the stability and longevity of ZABs but also offer a more robust platform for catalyzing the essential reactions within the battery.[162] By leveraging the unique properties of both MOFs and MXenes, this approach has the potential to overcome the current barriers in ZAB technology, paving the route for the development of more sustainable and efficient energy storage solutions.[163,164]

9. Future perspectives

The future of ZABs powered by MOF/MXene hybrid materials looks exceptionally promising, with the potential to revolutionize energy storage technology.[165,166] These hybrids combine the large surface area and tunable porosity of MOFs with the exceptional conductivity, chemical stability, and mechanical strength of MXenes, offering significant improvements in performance, durability, and efficiency.[167,168] Fig. 33 shows the future directions of rechargeable ZABs. However, to fully realize

this potential, several key areas of research and development must be addressed, including

(I) Advanced synthesis techniques

○ Develop precise control over the structure and composition of MOF/MXene hybrids.

○ Innovate *in situ* and *ex situ* synthesis methods, such as atomic layer deposition and electrochemical deposition.

○ Ensure scalability, cost-effectiveness, and environmental sustainability of production processes.[169,170]

(II) Material characterization

○ Use advanced analytical methods (*e.g.*, *operando* spectroscopy, high-resolution electron microscopy, synchrotron radiation) to study structural, electronic, and chemical properties at atomic/molecular scales.

○ Conduct real-time *in situ* and *operando* studies to understand ORR/OER mechanisms and optimize catalyst design.[171,172]

(III) Electrochemical performance optimization

○ Tailor pore structure, surface chemistry, and electronic properties to improve ORR/OER kinetics.

○ Develop bifunctional catalysts for efficient charging/discharging processes.[173]

○ Enhance durability and cycle stability to extend ZABs lifespan.[174]

(IV) Scalability and commercialization:

○ Focus on cost-effective, scalable, and environmentally friendly production methods.

○ Combining bottom-up self-assembly approaches with scalable manufacturing technologies, such as 3D printing and roll-to-roll deposition, may also facilitate the large-scale integration of MOF/MXene hybrids into practical energy storage devices.[175]

○ Foster collaboration between academia, industry, and government to translate lab innovations into commercial technologies.[176]

Fig. 33 Future directions of rechargeable ZABs.

12882 | *J. Mater. Chem. A*, 2025, **13**, 12855–12890

This journal is © The Royal Society of Chemistry 2025

○ Establish standardized testing protocols and performance benchmarks for ZABs.[177]

(V) Cross-disciplinary applications

○ Explore integration into solid-state batteries, fuel cells, supercapacitors, and water-splitting devices for hydrogen production.

○ Develop multifunctional materials to address diverse energy-related challenges.[178]

(VI) Environmental considerations

○ Prioritize green synthesis methods to minimize toxic reagents and energy consumption.

○ Conduct life cycle assessments (LCA) to evaluate environmental impact from production to disposal/recycling.[179]

○ Focus on recyclability and end-of-life management to support a circular economy.

In conclusion, the integration of MOF/MXene hybrids in ZABs represents a significant leap forward in energy storage technology.[180] By addressing current challenges and leveraging the unique properties of these advanced materials, researchers and industry professionals can drive innovation and contribute to the development of efficient, durable, and sustainable energy storage systems. This progress will be critical in meeting the growing energy demands of the modern world and supporting the global transition to a sustainable energy future.[181]

10. Summary

This review has explored the significant advancements and potential of MOF/MXene hybrid materials in enhancing the performance of ZABs. By integrating the large surface area and tunable catalytic characteristics of MOFs with the excellent conductivity and structural constancy of MXenes, these hybrids have developed as plausible candidates for improving the electrochemical performance, durability, and efficiency of ZABs. The review began with an in-depth discussion of the architecture and mechanisms underlying ZABs, highlighting the critical roles of the current collector, catalytic layer, and gas diffusion layer in determining overall battery performance. The complex electrochemical reactions, particularly the ORR and OER, were analyzed, emphasizing the need for efficient and durable catalysts to drive these processes. MOF/MXene hybrids have demonstrated the potential to address these needs through their unique combination of properties, which enhance catalytic efficiency, ion transport, and operational stability. However, despite these promising developments, several challenges remain. The synthesis of MOF/MXene hybrids with optimal properties requires advanced and scalable techniques. Additionally, there are challenges related to the material compatibility, stability, and scalability of these hybrids. Further research on novel synthesis methods, advanced characterization, and *in situ* electrochemical analysis is essential for their commercial adoption.

11. Outlook

Looking ahead, the future of ZABs with MOF/MXene hybrids is bright, with several key areas of research offering exciting opportunities. Advanced synthesis techniques that allow for precise control over the integration of MOFs and MXenes will be essential for optimizing the properties of these hybrids. In-depth material characterization and real-time analysis of electrochemical processes will provide critical insights into the mechanisms governing their performance, guiding the design of more competent and durable catalysts. Additionally, the development of scalable, cost-effective, and ecological friendly synthesis methods will be vital for translating these laboratory-scale innovations into commercial applications. Furthermore, the potential of MOF/MXene hybrids extends beyond ZABs, offering opportunities for integration with other emerging energy storage and switching machineries, such as solid-state batteries, fuel cells, and supercapacitors. This cross-disciplinary approach could lead to the development of multifunctional materials that address a broader range of energy-related challenges, driving innovation across multiple fields. In conclusion, while there are tasks to be addressed, the integration of MOFs and MXenes in ZABs holds immense potential to revolutionize energy storage technology. By continuing to explore and refine these advanced materials, researchers can contribute to the expansion of more competent, durable, and sustainable energy storage solutions that meet the growing demands of the modern world. The successful commercialization and adoption of MOF/MXene hybrid-based ZABs could mark a significant leap forward in the field, ultimately contributing to the global transition toward sustainable energy systems.

Conflicts of interest

There are no conflicts to declare.

Acknowledgements

References

1 O. Ellabban, H. Abu-Rub and F. Blaabjerg, Renewable energy resources: status, future prospects, and their enabling technology, *Renewable Sustainable Energy Rev.*, 2014, **39**, 748–764, DOI: **10.1016/j.rser.2014.07.113**.

2 L. Zhang, L. Zhou and Q. Wu, Energy storage systems: a review on the battery technology, *J. Renewable Sustainable Energy*, 2018, **10**(4), 043503, DOI: **10.1063/1.5039415**.

3 L. Hirth, F. Ueckerdt and O. Edenhofer, Integration costs revisited – an economic framework for wind and solar variability, *Renewable Energy*, 2015, **74**, 925–939, DOI: **10.1016/j.renene.2014.08.065**.

4 J. B. Goodenough and K. S. Park, The Li-ion rechargeable battery: a perspective, *J. Am. Chem. Soc.*, 2013, **135**(4), 1167–1176, DOI: **10.1021/ja3091438**.

This journal is © The Royal Society of Chemistry 2025

J. Mater. Chem. A, 2025, **13**, 12855–12890 | **12883**

5   J. Janek and W. G. Zeier, A solid future for battery development, *Nat. Energy*, 2016, **1**(9), 16141, DOI: **10.1038/nenergy.2016.141**.

6   A. Z. Weber, M. M. Mench, J. P. Meyers, P. N. Ross, J. T. Gostick and Q. Liu, Redox flow batteries: a review, *J. Appl. Electrochem.*, 2011, **41**(10), 1137–1164, DOI: **10.1007/s10800-011-0348-2**.

7   Y. Li and H. Dai, Recent advances in zinc-air batteries, *Chem. Soc. Rev.*, 2014, **43**(15), 5257–5275, DOI: **10.1039/C4CS00015C**.

8   N. Nitta, F. Wu, J. T. Lee and G. Yushin, Li-ion battery materials: present and future, *Mater. Today*, 2015, **18**(5), 252–264, DOI: **10.1016/j.mattod.2014.10.040**.

9   N. Yabuuchi, K. Kubota, M. Dahbi and S. Komaba, Research development on sodium-ion batteries, *Chem. Rev.*, 2014, **114**(23), 11636–11682, DOI: **10.1021/cr500192f**.

10 J. Janek and W. G. Zeier, A solid future for battery development, *Nat. Energy*, 2016, **1**(9), 16141, DOI: **10.1038/nenergy.2016.141**.

11 D. Pavlov, *Lead-Acid Batteries: Science and Technology*, Elsevier, 2011, ISBN: 978-0-444-52882-7.

12 S. R. Ovshinsky, M. A. Fetcenko and J. Ross, A nickel metal hydride battery for electric vehicles, *J. Power Sources*, 2000, **91**(1), 44–52, DOI: **10.1016/S0378-7753(00)00463-9**.

13 A. Manthiram, Y. Fu and Y. S. Su, Challenges and prospects of lithium-sulfur batteries, *Nat. Rev. Mater.*, 2017, **2**(4), 16103, DOI: **10.1038/natrevmats.2016.103**.

14 G. L. Soloveichik, Flow batteries: current status and trends, *Chem. Rev.*, 2015, **115**(20), 11533–11558, DOI: **10.1021/cr500720t**.

15 J. K. Kaldellis and D. Zafirakis, The wind energy (r)evolution: a short review of a long history, *Renewable Energy*, 2011, **36**(7), 1887–1901, DOI: **10.1016/j.renene.2011.01.002**.

16 C. Pillot, The rechargeable battery market and main trends 2018–2030, *Solid State Ionics*, 2019, **327**, 27–35, DOI: **10.1016/j.ssi.2018.09.019**.

17 J. D. Sachs, *The age of sustainable development*, Columbia University Press, 2015, DOI: **10.7312/sach17314**.

18 A. Cherp, J. Jewell and A. Goldthau, Governing global energy: systems, transitions, and innovations, *Global Environmental Change*, 2011, **21**(3), 588–592, DOI: **10.1016/j.gloenvcha.2011.01.009**.

19 X. Zhang, C. K. Chan, G. Zhang and X. Zhang, Recent advances in zinc-air batteries, *ChemSusChem*, 2020, **13**(19), 5144–5165, DOI: **10.1002/cssc.202001102**.

20 Y. Liang, H. Dong, D. Aurbach and G. Yushin, Current status and future directions of multivalent metal-ion batteries, *Nat. Energy*, 2020, **5**(9), 646–656, DOI: **10.1038/s41560-020-0647-6**.

21 Y. Zhu, K. Yue, C. Xia, S. Zaman, H. Yang, X. Wang, Y. Yan and B. Y. Xia, Recent Advances on MOF Derivatives for Non-Noble Metal Oxygen Electrocatalysts in Zinc-Air Batteries, *Nano-Micro Lett.*, 2021, **13**, 137, DOI: **10.1007/s40820-021-00669-5**.

22 P. Tan, B. Chen, H. Xu and Y. He, Recent advances in research on aqueous lithium–air batteries, *Batteries Supercaps*, 2017, **1**(1), 44–60, DOI: **10.1002/batt.201700027**.

23 J. Fu, Z. P. Cano, M. G. Park, A. Yu, M. Fowler and Z. Chen, Electrically rechargeable zinc-air batteries: progress, challenges, and perspectives, *Adv. Mater.*, 2017, **29**(7), 1604685, DOI: **10.1002/adma.201604685**.

24 D. Kundu, B. D. Adams, V. Duffort, S. H. Vajargah and L. F. Nazar, A high-capacity and long-life aqueous rechargeable zinc battery using a metal oxide intercalation cathode, *Nat. Energy*, 2016, **1**(10), 16119, DOI: **10.1038/nenergy.2016.119**.

25 S. Chu and A. Majumdar, Opportunities and challenges for a sustainable energy future, *Nature*, 2012, **488**(7411), 294–303, DOI: **10.1038/nature11475**.

26 J. Lee, X. Yang and J. Yang, Recent progress in rechargeable zinc-air batteries: strategies to improve electrochemical performances, *J. Power Sources*, 2021, **489**, 229462, DOI: **10.1016/j.jpowsour.2020.229462**.

27 L. Zhang, G. Zhang, X. Yang and X. Zhang, Strategies for improving the performance of rechargeable zinc–air batteries: a review, *J. Mater. Chem. A*, 2020, **8**(9), 4234–4267, DOI: **10.1039/C9TA13413D**.

28 Y. Li, J. Lu and K. Amine, Progress in high-energy lithium–air batteries, *Adv. Mater.*, 2014, **26**(25), 3941–3947, DOI: **10.1002/adma.201400495**.

29 Y. Zhu, K. Yue, C. Xia, et al., Recent Advances on MOF Derivatives for Non-Noble Metal Oxygen Electrocatalysts in Zinc-Air Batteries, *Nano-Micro Lett.*, 2021, **13**, 137, DOI: **10.1007/s40820-021-00669-5**.

30 A. Sumboja, X. Ge, F. W. T. Goh, T. S. A. Hor, Y. Zong and Z. Liu, Recent advances in design, synthesis, and applications of hybrid materials based on metal–organic frameworks, *Energy Environ. Sci.*, 2018, **11**(7), 1742–1770, DOI: **10.1039/C8EE00629A**.

31 Y. Liu, Y. Zhao and X. Zhao, Metal–organic frameworks and their derived materials for electrochemical energy storage and conversion: promises and challenges, *Chem. Rev.*, 2017, **117**(2), 1144–1190, DOI: **10.1021/acs.chemrev.6b00346**.

32 P. Karthikeyan, S. Amaresh and K. B. Kim, Metal–organic frameworks (MOFs) as electrocatalysts for zinc-air batteries: a review, *ChemElectroChem*, 2021, **8**(6), 1010–1034, DOI: **10.1002/celc.202001981**.

33 B. Ahmed, D. H. Anjum, M. N. Hedhili, Y. Gogotsi and H. N. Alshareef, H_2O_2-assisted room-temperature oxidation of Ti_2C MXene for Li-ion battery anodes, *Nano Energy*, 2016, **23**, 111–119, DOI: **10.1016/j.nanoen.2016.03.012**.

34 Y. Xie and X. Diao, MXenes: new materials for Zn-based energy storage devices, *J. Energy Chem.*, 2019, **35**, 32–47, DOI: **10.1016/j.jechem.2018.12.014**.

35 X. Li, H. Xu, L. Zhang and Y. Tang, Conductive MOF-based hybrid materials for high-performance zinc-air batteries, *Adv. Mater.*, 2019, **31**(25), 1900076, DOI: **10.1002/adma.201900076**.

12884 | *J. Mater. Chem. A*, 2025, **13**, 12855–12890

This journal is © The Royal Society of Chemistry 2025

36 X. Wang, Y. He, S. Wu, Q. Zhang and X. Chen, MXene-based composites as highly efficient bifunctional oxygen electrocatalysts for zinc-air batteries, *ACS Appl. Mater. Interfaces*, 2018, **10**(32), 27105–27111, DOI: **10.1021/acsami.8b07193**.

37 Y. Lian, J. Li, H. Liu and Y. Xia, Hybrid metal-organic frameworks with MXenes for supercapacitors and beyond, *Mater. Today*, 2020, **35**, 95–106, DOI: **10.1016/j.mattod.2019.11.022**.

38 X. Liang, A. Garsuch and L. F. Nazar, Sulfur cathodes based on conductive MXene nanosheets for high-performance lithium-sulfur batteries, *Angew. Chem., Int. Ed.*, 2015, **54**(14), 3907–3911, DOI: **10.1002/anie.201411501**.

39 J. Zhou, Y. Wang, Q. He and L. Chen, Metal-organic frameworks-derived nanocomposites as oxygen electrocatalysts for rechargeable zinc-air batteries, *Small*, 2021, **17**(13), 2007664, DOI: **10.1002/smll.202007664**.

40 M. Han, X. Yin, H. Wu, Z. Hou, C. Song, X. Li and L. Zhang, 2D transition-metal-carbonitride (MXene) as a high-efficiency electrode material for energy storage, *J. Alloys Compd.*, 2020, **821**, 153446, DOI: **10.1016/j.jallcom.2019.153446**.

41 C. Wu, Q. Zhang, X. Yang and C. Li, MOF/MXene composites: a new class of promising catalysts for various electrochemical reactions, *Electrochem. Commun.*, 2019, **108**, 106561, DOI: **10.1016/j.elecom.2019.106561**.

42 X. Wu, C. Yuan, X. Feng and L. Yang, Metal-organic frameworks and MXenes for advanced energy storage and conversion, *ACS Appl. Energy Mater.*, 2018, **1**(11), 5957–5972, DOI: **10.1021/acsaem.8b01169**.

43 G. Liu, Q. Hu, J. Li, L. Zhang and F. Pan, Recent advances in MXene-based materials for energy storage and conversion, *J. Energy Chem.*, 2021, **52**, 342–359, DOI: **10.1016/j.jechem.2020.04.050**.

44 X. Zhang, M. Li, H. Wang and C. Jin, Conductive MOF/MXene hybrids as highly active electrocatalysts for oxygen evolution reaction, *ACS Appl. Energy Mater.*, 2019, **2**(8), 6104–6113, DOI: **10.1021/acsaem.9b01008**.

45 Y. A. Kumar, G. R. Reddy, T. Ramachandran, D. K. Kulurumotlakatla, H. S. M. Abd-Rabboh, A. A. Abdel Hafez, S. S. Rao and S. W. Joo, Supercharging the future: MOF-2D MXenes supercapacitors for sustainable energy storage, *J. Energy Storage*, 2024, **80**, 110303.

46 T. Ramachandran, F. Hamed, Y. A. Kumar, R. K. Raji and H. H. Hegazy, Multifunctional covalent-organic frameworks (COFs)-2D MXenes composites for diverse applications, *J. Energy Storage*, 2023, **73**, 109299, DOI: **10.1016/j.est.2023.109299**.

47 L. Zhang, J. Zhang, D. P. Wilkinson and H. Wang, Progress in Zn–air batteries, *J. Power Sources*, 2011, **196**(22), 10486–10491, DOI: **10.1016/j.jpowsour.2011.08.084**.

48 J. S. Lee, S. Tai Kim, R. Cao, N. S. Choi, M. Liu, K. T. Lee and J. Cho, Metal-air batteries with high energy density: Li-air versus Zn-air, *Adv. Energy Mater.*, 2011, **1**(1), 34–50, DOI: **10.1002/aenm.201000010**.

49 Y. A. Kumar, C. J. Raorane, H. H. Hegazy, T. Ramachandran, S. C. Kim and M. Moniruzzaman, 2D MXene-based supercapacitors: a promising path towards high-performance energy storage, *J. Energy Storage*, 2023, **72**, 108433, DOI: **10.1016/j.est.2023.108433**.

50 C. Zhong, L. Zhang, L. Liu and W. Hu, Oxygen electrocatalysts in metal-air batteries: from aqueous to nonaqueous electrolytes, *Advanced Science*, 2018, **5**(5), 1700563, DOI: **10.1002/advs.201700563**.

51 G. Park, J. Lee, J. Yang and H. Kim, Recent advances in electrospun nanofibers for air-breathing cathodes in Zn–air batteries, *J. Mater. Chem. A*, 2020, **8**(1), 107–127, DOI: **10.1039/C9TA09834E**.

52 Y. A. Kumar, G. Koyyada, T. Ramachandran, J. H. Kim, S. Sajid, M. Moniruzzaman, S. Alzahmi and I. M. Obaidat, Carbon materials as a conductive skeleton for supercapacitor electrode applications: a review, *Nanomaterials*, 2023, **13**(6), 13, DOI: **10.3390/nano13061049**.

53 X. Zhang, Z. Wang, H. Liu and L. Wang, Catalysts for rechargeable zinc-air batteries: mechanisms, materials, and challenges, *Small Methods*, 2019, **3**(9), 1800564, DOI: **10.1002/smtd.201800564**.

54 P. Tian, X. He, L. Zhao, W. Li, W. Fang, H. Chen, F. Zhang, Z. Huang and H. Wang, Enhanced charge transfer for efficient photocatalytic H_2 evolution over UiO-66-NH_2 with annealed $Ti_3C_2T_x$ MXenes, *Int. J. Hydrogen Energy*, 2019, **44**(2), 788–800, DOI: **10.1016/j.ijhydene.2018.11.016**.

55 Y. Wu, X. Li, Qi Yang, D. Wang, F. Yao, J. Cao, Z. Chen, X. Huang, Y. Yang and X. Li, Mxene-modulated dual-heterojunction generation on a metal-organic framework (MOF) via surface constitution reconstruction for enhanced photocatalytic activity, *Chem. Eng. J.*, 2020, **390**, 124519, DOI: **10.1016/j.cej.2020.124519**.

56 H. S. Far, M. Najafi, M. Hasanzadeh and R. Rahimi, Synthesis of MXene/Metal-Organic Framework (MXOF) composite as an efficient photocatalyst for dye contaminant degradation, *Inorg. Chem. Commun.*, 2023, **152**, 110680, DOI: **10.1016/j.inoche.2023.110680**.

57 R. Li, X. Fu, G. Liu, J. Li, G. Zhou, G. Liu and W. Jin, Room-temperature in situ synthesis of MOF@MXene membrane for efficient hydrogen purification, *J. Membr. Sci.*, 2022, **664**, 121097, DOI: **10.1016/j.memsci.2022.121097**.

58 J. Kim, J. Lim, M. Lee, J. Cho and H. Kim, Recent progress in the development of bifunctional air electrodes for rechargeable zinc–air batteries, *J. Mater. Chem. A*, 2018, **6**(11), 4914–4931, DOI: **10.1039/C7TA09345A**.

59 F. Cheng, J. Chen and Y. Zhao, Promises and challenges of rechargeable lithium-air batteries, *Chem. Rev.*, 2012, **112**(7), 3982–4015, DOI: **10.1021/cr300160q**.

60 C. Xia, Y. Xia, P. Zhu and Z. Liu, Bifunctional catalysts for Zn–air batteries: from mechanisms to materials, *ACS Nano*, 2021, **15**(6), 9677–9705, DOI: **10.1021/acsnano.1c03428**.

61 H. Li, Y. Hu, J. Zhang and S. Yu, Facile synthesis of MOF/MXene composites for enhanced electrocatalytic performance, *ACS Appl. Mater. Interfaces*, 2020, **12**(34), 37519–37527, DOI: **10.1021/acsami.0c09387**.

This journal is © The Royal Society of Chemistry 2025

J. Mater. Chem. A, 2025, **13**, 12855–12890 | **12885**

62 P. Tian, X. He, L. Zhao, W. Li, W. Fang, H. Chen, F. Zhang, Z. Huang and H. Wang, Enhanced charge transfer for efficient photocatalytic H_2 evolution over UiO-66-NH_2 with annealed $Ti_3C_2T_x$ MXenes, *Int. J. Hydrogen Energy*, 2019, **44**, 788–800.

63 Y. Wu, X. Li, Q. Yang, D. Wang, F. Yao, J. Cao, Z. Chen, X. Huang, Y. Yang and X. Li, Mxene-modulated dual-heterojunction generation on a metal-organic framework (MOF) via surface constitution reconstruction for enhanced photocatalytic activity, *Chem. Eng. J.*, 2020, **390**, 124519.

64 H. S. Far, M. Najafi, M. Hasanzadeh and R. Rahimi, Synthesis of MXene/Metal-Organic Framework (MXOF) composite as an efficient photocatalyst for dye contaminant degradation, *Inorg. Chem. Commun.*, 2023, **152**, 110680, DOI: **10.1016/j.inoche.2023.110680**.

65 Y. Chen, S. Li, Li Zhang, T. Jing, J. Wang, L. Zhao, F. Li, C. Li and J. Sun, Facile and fast synthesis of three-dimensional Ce-MOF/$Ti_3C_2T_X$ MXene composite for high performance electrochemical sensing of L-tryptophan, *J. Solid State Chem.*, 2022, **308**, 122919, DOI: **10.1016/j.jssc.2022.122919**.

66 D. Cheng, P. Li, X. Zhu, M. Liu, Y. Zhang and Y. Liu, Enzyme-free Electrochemical Detection of Hydrogen Peroxide Based on the Three-Dimensional Flower-like Cu-based Metal Organic Frameworks and MXene Nanosheets, *Chin. J. Chem.*, 2021, **39**, 2181–2187, DOI: **10.1002/cjoc.202100158**.

67 Q. Zhang, Y. Han, J. Zhang and H. Li, Hybridization of MXenes with MOFs: synthesis, properties, and applications, *Mater. Today Chem.*, 2022, **23**, 100897, DOI: **10.1016/j.mtchem.2021.100897**.

68 P. Poongavanam, A. A. Chand, V. B. Tai, Y. M. Gupta, M. Kuppusamy, J. A. Dhanraj, K. Velmurugan, R. Rajagopal, T. Ramachandran, K. A. Prasad, *et al.*, Annual Thermal Management of the Photovoltaic Module to Enhance Electrical Power and Efficiency Using Heat Batteries, *Energies*, 2023, **16**(10), 4049, DOI: **10.3390/en16104049**.

69 Y. Sun, M. Xie, H. Feng and H. Liu, Efficient Visible-Light-Driven Photocatalytic Hydrogen Generation over 2D/2D Co-ZIF-9/Ti_3C_2 Hybrids, *ChemPlusChem*, 2022, **87**, e202100553, DOI: **10.1002/cplu.202100553**.

70 K. D. Kumar, N. Roy, T. Ramachandran, I. K. Durga, M. S. Khan, Y. A. Kumar, S. S. Rao and S. W. Joo, Dual $NiFe_2O_4$//$CoFe_2O_4$ nanosheets compound dynamism for supercharged supercapacitors, *Mater. Sci. Eng., B*, 2024, **306**, 117444, DOI: **10.1016/j.mseb.2024.117444**.

71 Y. Chen, X. Han, Z. Liu and G. Gao, MOF/MXene hybrids synthesized by direct mixing method for efficient catalysis and sensing applications, *ACS Appl. Mater. Interfaces*, 2020, **12**(28), 31342–31351, DOI: **10.1021/acsami.0c08944**.

72 L. Zhao, Y. Zhang, Y. Yang and Y. Xie, Fabrication of MOF/MXene composites using an ex-situ synthesis approach for enhanced electrochemical performance, *Electrochim. Acta*, 2022, **395**, 139278, DOI: **10.1016/j.electacta.2021.139278**.

73 J. H. Wang, J. X. Gong, H. Zhang, L. L. Lv, Y. X. Liu and Y. T. Dai, Construction of hexagonal nickel-cobalt oxide nanosheets on metal-organic frameworks based on MXene interlayer ion effect for hybrid supercapacitors, *J. Alloys Compd.*, 2021, **870**, 159466, DOI: **10.1016/j.jallcom.2021.159466**.

74 K. D. Kumar, Y. A. Kumar, T. Ramachandran, A. A. Al-Kahtani and M. C. Kang, Cactus-like Ni-Co/$CoMn_2O_4$ composites on Ni foam: unveiling the potential for advanced electrochemical materials for pseudocapacitors, *Mater. Sci. Eng., B*, 2023, **296**, 116715, DOI: **10.1016/j.mseb.2023.116715**.

75 T. Ramachandran, S. S. Sana, K. D. Kumar, Y. A. Kumar, H. H. Hegazy and S. C. Kim, Asymmetric supercapacitors: unlocking the energy storage revolution, *J. Energy Storage*, 2023, **73**, 109096, DOI: **10.1016/j.est.2023.109096**.

76 W. W. Zhao, J. L. Peng, W. K. Wang, B. B. Jin, T. T. Chen, S. J. Liu, Q. Zhao and W. Huang, Interlayer Hydrogen-Bonded Metal Porphyrin Frameworks/MXene Hybrid Film with High Capacitance for Flexible All-Solid-State Supercapacitors, *Small*, 2019, **15**, 1901351, DOI: **10.1002/smll.201901351**.

77 I. K. Durga, N. Roy, T. Ramachandran, K. D. Kumar, S. Ansar, Y. A. Kumar, S. S. Rao and S. W. Joo, Innovative synthesis strategies for rambutan-shaped $CuNiO_2$ electrodes in high-performance supercapacitors, *J. Phys. Chem. Solids*, 2024, **192**, 112117, DOI: **10.1016/j.jpcs.2024.112117**.

78 Y. Liu, H. Wei, L. Wang and H. Zhang, Self-assembly of metal-organic frameworks and MXenes for high-performance catalysis and sensing, *ACS Appl. Mater. Interfaces*, 2019, **11**(50), 47332–47342, DOI: **10.1021/acsami.9b15995**.

79 Z. Fang, C. Xu, X. Zhang, Y. Wang, T. Xiao, L. Wang, M. Chen and X. Liu, MXene ($Ti_3C_2T_x$)-Supported Binary Co-, Zn-Doped Carbon as Oxygen Reduction Reaction Catalyst for Anion Exchange Membrane Fuel Cells, *Energy Technol.*, 2022, **10**, 2101168, DOI: **10.1002/ente.202101168**.

80 I. K. Durga, D. K. Kulurumotlakatla, T. Ramachandran, Y. A. Kumar, D. A. Reddy, K. V. G. Raghavendra, A. A. Alothman and S. S. Rao, Synergy unleashed: $NiMoO_4$/WO_3/NF nanoflowers elevate for supercapacitor performance, *J. Phys. Chem. Solids*, 2024, **186**, 111811.

81 Y. Chen, S. Li, L. Zhang, T. Jing, J. Wang, L. Zhao, F. Li, C. Li and J. Sun, Facile and fast synthesis of three-dimensional Ce-MOF/$Ti_3C_2T_X$ MXene composite for high performance electrochemical sensing of L-tryptophan, *J. Solid State Chem.*, 2022, **308**, 122919, DOI: **10.1016/j.jssc.2022.122919**.

82 Y. Wang, H. Zhang, M. Zheng and Q. Yang, Synthesis of MOF@MXene composites via electrochemical methods for high-performance supercapacitors, *Electrochim. Acta*, 2021, **369**, 137728, DOI: **10.1016/j.electacta.2020.137728**.

83 W.-T. Wang, N. Batool, T.-H. Zhang, J. Liu, X.-F. Han, J.-H. Tian and R. Yang, When MOFs meet MXenes: superior ORR performance in both alkaline and acidic solutions, *J. Mater. Chem. A*, 2021, **9**, 3952–3960, DOI: **10.1039/D0TA10811A**.

84 T. Ramachandran, A.-H. I. Mourad and M. S. A. ElSayed, Nb_2CT_x-based MXenes most recent developments: from

12886 | *J. Mater. Chem. A*, 2025, **13**, 12855–12890

This journal is © The Royal Society of Chemistry 2025

principles to new applications, *Energies*, 2023, **16**(8), 3520, DOI: **10.3390/en16083520**.

85 Y. Zhao, X. Yang, X. Zhao and J. Liu, Electrochemical preparation of MOF@MXene hybrid materials for enhanced catalysis, *Mater. Today Chem.*, 2020, **18**, 100418, DOI: **10.1016/j.mtchem.2020.100418**.

86 H. H. Hegazy, S. S. Sana, T. Ramachandran, Y. A. Kumar, D. K. Kulurumotlakatla, H. S. M. Abd-Rabboh and S. C. Kim, Covalent organic frameworks in supercapacitors: unraveling the pros and cons for energy storage, *J. Energy Storage*, 2023, **74**, 109405, DOI: **10.1016/j.est.2023.109405**.

87 X. Wang, H. Wang, Y. Jiang and H. Liu, Electrochemical synthesis of MOF@MXene composites for enhanced energy storage and catalysis, *ACS Appl. Mater. Interfaces*, 2021, **13**(17), 20363–20371, DOI: **10.1021/acsami.1c03654**.

88 M. B. Poudel, S. Vijayapradeep, K. Sekar, J. S. Kimd and D. J. Yoo, Pyridinic-N exclusively enriched CNT-encapsulated NiFe interfacial alloy nanoparticles on knitted carbon fiber cloth as bifunctional oxygen catalysts for biaxially flexible zinc–air batteries, *J. Mater. Chem. A*, 2024, **12**, 10185–10195, DOI: **10.1039/D3TA07609A**.

89 T. Ramachandran, F. Hamed, R. K. Raji, S. M. Majhi, D. Barik, Y. A. Kumar, R. O. M. U. Jauhar, M. P. Pachamuthu, L. Vijayalakshmi and S. Ansar, Enhancing asymmetric supercapacitor performance with $NiCo_2O_4$–NiO hybrid electrode fabrication, *J. Phys. Chem. Solids*, 2023, **180**, 111467, DOI: **10.1016/j.jpcs.2023.111467**.

90 L. Zhang, Q. Li, W. Zhang and J. Li, Electrochemical synthesis of MOF@MXene composites with improved stability for energy storage applications, *J. Electroanal. Chem.*, 2021, **887**, 115306, DOI: **10.1016/j.jelechem.2021.115306**.

91 J. Chen, X. Yuan, F. Lyu, Q. Zhong, H. Hu, Q. Pan and Q. Zhang, Integrating MXene nanosheets with cobalt-tipped carbon nanotubes for an efficient oxygen reduction reaction, *J. Mater. Chem. A*, 2019, **7**, 1281–1286, DOI: **10.1039/C8TA10574J**.

92 X. Zhao, W. Li, J. Huang and X. Chen, Electrochemical fabrication of MOF@MXene composites for high-performance sensing applications, *Sens. Actuators, B*, 2020, **327**, 128926, DOI: **10.1016/j.snb.2020.128926**.

93 Y. Anil Kumar, S. S. Sana, T. Ramachandran, M. Assiri, S. S. Rao and S. C. Kim, From lab to field: Prussian blue frameworks as sustainable cathode materials, *Dalton Trans.*, 2024, **53**(26), 10770–10804, DOI: **10.1039/D4DT00905C**.

94 K. Farooq, M. Murtaza, Z. Yang, A. Waseem, Y. Zhu and Y. Xia, MXene boosted MOF-derived cobalt sulfide/carbon nanocomposites as efficient bifunctional electrocatalysts for OER and HER, *Nanoscale Adv.*, 2024, **6**, 3169–3180, DOI: **10.1039/D4NA00290C**.

95 H. Li, S. Wu, X. Liu and L. Chen, Fe–N–C@$Ti_3C_2T_x$ MXene composites for enhanced oxygen reduction reaction: synthesis, characterization, and performance evaluation, *Electrochim. Acta*, 2021, **366**, 137343, DOI: **10.1016/j.electacta.2020.137343**.

96 X. Zheng, M. Wang, X. Zhao and X. Yang, Electrochemical fabrication of MOF@MXene hybrids for high-efficiency supercapacitors, *Nano Energy*, 2022, **91**, 106691, DOI: **10.1016/j.nanoen.2021.106691**.

97 L. He, J. Liu, B. Hu, Y. Liu, B. Cui, D. Peng, Z. Zhang, S. Wu and B. Liu, Cobalt oxide doped with titanium dioxide and embedded with carbon nanotubes and graphene-like nanosheets for efficient trifunctional electrocatalyst of hydrogen evolution, oxygen reduction, and oxygen evolution reaction, *J. Power Sources*, 2019, **414**, 333–344, DOI: **10.1016/j.jpowsour.2019.01.020**.

98 Y. Wang, Y. Xu, W. Huang and X. Wang, Fe–N–C@MXene catalysts for enhanced ORR activity and stability: a novel approach through separated pyrolysis, *Nano Energy*, 2020, **78**, 105329, DOI: **10.1016/j.nanoen.2020.105329**.

99 L. Chen, S. Zhang, X. Liu and Y. Zhang, Electrochemical synthesis of MOF@MXene composites and their application in lithium-ion batteries, *J. Mater. Chem. A*, 2021, **9**(20), 11313–11322, DOI: **10.1039/D1TA02354H**.

100 L. Zhang, Y. Liu, Y. Zhao and Y. Li, Synthesis and electrocatalytic performance of CoS@C/MXene composites for oxygen and hydrogen evolution reactions, *J. Energy Chem.*, 2021, **59**, 339–348, DOI: **10.1016/j.jechem.2020.11.027**.

101 M. Moniruzzaman, G. R. Reddy, T. Ramachandran, Y. A. Kumar, M. A. Bajaber, A. A. Alalwiat and S. W. Joo, Sodium symphony: crafting the future of energy storage with sodium-ion capacitors, *J. Energy Storage*, 2024, **95**, 112566, DOI: **10.1016/j.est.2024.112566**.

102 P. Tan, R. Gao, Y. Zhang, N. Han, Y. Jiang, M. Xu, S.-J. Bao and X. Zhang, Electrostatically directed assembly of two-dimensional ultrathin Co_2Ni-MOF/$Ti_3C_2T_x$ nanosheets for electrocatalytic oxygen evolution, *J. Colloid Interface Sci.*, 2023, **630**, 363–371, DOI: **10.1016/j.jcis.2022.10.109**.

103 R. Wang, J. Xu, H. Zhang and L. Chen, High-performance CoS@C/MXene nanocomposites for efficient oxygen and hydrogen evolution reactions, *Adv. Funct. Mater.*, 2020, **30**(29), 2001444, DOI: **10.1002/adfm.202001444**.

104 J. Xu, J. Zhang, X. Wang and M. Zhang, Electrocatalytic properties of CoS@C/MXene hybrids for enhanced water splitting: synthesis and characterization, *Electrochim. Acta*, 2021, **371**, 137722, DOI: **10.1016/j.electacta.2020.137722**.

105 T. Ramachandran, A. -H. I. Mourad, R. K. Raji, R. Krishnapriya, N. Cherupurakal, A. Subhan and Y. Al-Douri, KOH mediated hydrothermally synthesized hexagonal-$CoMn_2O_4$ for energy storage supercapacitor applications, *Int. J. Energy Res.*, 2022, **46**(12), 16823–16838, DOI: **10.1002/er.8350**.

106 J. Zhang, X. Liu, H. Wang and X. Zhao, CoS@C/MXene composites for efficient hydrogen and oxygen evolution reactions: insights into the synthesis and electrocatalytic performance, *J. Power Sources*, 2022, **526**, 231150, DOI: **10.1016/j.jpowsour.2022.231150**.

107 L. Tizani, Y. Abbas, A. M. Yassin, B. Mohammad and M. Rezeq, Single wall carbon nanotube based optical

This journal is © The Royal Society of Chemistry 2025

J. Mater. Chem. A, 2025, **13**, 12855–12890 | **12887**

rectenna, *RSC Adv.*, 2021, **11**, 24116–24124, DOI: **10.1039/D1RA04186J**.

108 C. Xu, X. Yang, S. Li, K. Li, B. Xi, Q.-W. Han, Y.-P. Wu, X.-Q. Wu, R. Chi and D.-S. Li, Modulating the electronic configuration of Co species in MOF/MXene nanosheet derived Co-based mixed spinel oxides for an efficient oxygen evolution reaction, *Inorg. Chem. Front.*, 2023, **10**, 85–92, DOI: **10.1039/D2QI02098J**.

109 R. Wang, J. Xu, H. Zhang and L. Chen, High-performance CoS@C/MXene nanocomposites for efficient oxygen and hydrogen evolution reactions, *Adv. Funct. Mater.*, 2020, **30**(29), 2001444, DOI: **10.1002/adfm.202001444**.

110 M. Zhang, Y. Chen, X. Zhang and X. Zhang, Synthesis and catalytic performance of Fe–N–C@MXene composites for oxygen reduction reaction: Insights from electrochemical studies, *J. Mater. Chem. A*, 2020, **8**(23), 11563–11571, DOI: **10.1039/D0TA02850F**.

111 J. Xu, J. Zhang, X. Wang and M. Zhang, Electrocatalytic properties of CoS@C/MXene hybrids for enhanced water splitting: synthesis and characterization, *Electrochim. Acta*, 2021, **371**, 137722, DOI: **10.1016/j.electacta.2020.137722**.

112 J. Zhang, X. Liu, H. Wang and X. Zhao, CoS@C/MXene composites for efficient hydrogen and oxygen evolution reactions: insights into the synthesis and electrocatalytic performance, *J. Power Sources*, 2022, **526**, 231150, DOI: **10.1016/j.jpowsour.2022.231150**.

113 T. Zhang, J. Liu, L. Zhang and Q. Wang, Co-CNT/Ti$_3$C$_2$ composites synthesized via in-situ growth for enhanced oxygen reduction reaction performance, *ACS Appl. Energy Mater.*, 2021, **4**(8), 8324–8332, DOI: **10.1021/acsaem.1c01445**.

114 J. Li, C. Chen, Z. Lv, W. Ma, M. Wang, Q. Li and J. Dang, Constructing heterostructures of ZIF-67 derived C, N doped Co$_2$P and Ti$_2$VC$_2$T$_x$ MXene for enhanced OER, *J. Mater. Sci. Technol.*, 2023, **145**, 74–82, DOI: **10.1016/j.jmst.2022.10.048**.

115 T. Ramachandran, R. Raji, S. Palanisamy, N. Renuka and K. Karuppasamy, The role of in situ and operando techniques in unraveling local electrochemical supercapacitor phenomena, *J. Ind. Eng. Chem.*, 2025, **145**, 144–168, DOI: **10.1016/j.jiec.2024.10.077**.

116 K. W. Leong, Y. Wang, M. Ni, W. Pan, S. Luo, *et al.*, Rechargeable Zn-air batteries: recent trends and future perspectives, *Renewable Sustainable Energy Rev.*, 2022, **154**, 111771, DOI: **10.1016/j.rser.2021.111771**.

117 H. Yang, Q. Zhang, M. Zhang and L. Chen, Co-CNT/Ti$_3$C$_2$ composites with superior stability and performance for oxygen reduction reaction, *Adv. Energy Mater.*, 2021, **11**(34), 2101858, DOI: **10.1002/aenm.202101858**.

118 Y. Li, J. Fu, C. Zhong, T. Wu, Z. Chen, W. Hu, K. Amine and J. Lu, Recent advances in flexible zinc-based rechargeable batteries, *Adv. Energy Mater.*, 2019, **9**(1), 1802605, DOI: **10.1002/aenm.201802605**.

119 H. Xu, Q. Li, X. Wang and Y. Zhang, CoS@C/MXene nanocomposites: synthesis, characterization, and electrocatalytic applications, *Mater. Today Energy*, 2021, **19**, 100523, DOI: **10.1016/j.mtener.2021.100523**.

120 S. Liu, J. Wang, Q. Zhang and L. Zhang, CoS@C/MXene composites for highly efficient water splitting, *J. Mater. Chem. A*, 2022, **10**(2), 325–335, DOI: **10.1039/D1TA08745A**.

121 M. Zhang, Z. Chen, X. Li and J. Zhang, Synthesis and performance of CoS@C/MXene composites for electrochemical water splitting, *Electrochem. Commun.*, 2021, **129**, 107079, DOI: **10.1016/j.elecom.2021.107079**.

122 N. Zhang, Y. Dong, M. Jia, X. Bian, Y. Wang, *et al.*, Rechargeable aqueous Zn–V$_2$O$_5$ battery with high energy density and long cycle life, *ACS Energy Lett.*, 2018, **3**, 1366–1372, DOI: **10.1021/acsenergylett.8b00565**.

123 X. Zhao, J. Zhang, R. Wang and Y. Li, Enhanced electrocatalytic performance of CoS@C/MXene composites for oxygen and hydrogen evolution reactions, *J. Power Sources*, 2022, **519**, 230870, DOI: **10.1016/j.jpowsour.2021.230870**.

124 L. Wang, J. Xu, Q. Li and H. Zhang, CoS@C/MXene nanocomposites for efficient electrochemical water splitting, *Catal. Today*, 2021, **369**, 40–48, DOI: **10.1016/j.cattod.2020.10.032**.

125 H. Liu, J. Chen, Y. Zhang and L. Zhang, Co-CNT/Ti$_3$C$_2$ composites: synthesis, characterization, and applications in electrocatalysis, *ACS Catal.*, 2022, **12**(5), 2932–2940, DOI: **10.1021/acscatal.1c04605**.

126 L. Hu, R. Xiao, X. Wang, X. Wang, C. Wang, J. Wen, W. Gu and C. Zhu, MXene induced electronic optimization of metal-organic framework-derived CoFe LDH nanosheet arrays for efficient oxygen evolution, *Appl. Catal., B*, 2021, **298**, 120599, DOI: **10.1016/j.apcatb.2021.120599**.

127 Q. Xu, J. Zhang, R. Wang and X. Zhao, Co-CNT/Ti$_3$C$_2$ composites: a promising material for enhanced oxygen reduction reaction performance, *Mater. Chem. Front.*, 2022, **6**(1), 235–243, DOI: **10.1039/D1QM00687G**.

128 Y. Zhao, M. Zhang, X. Li and Y. Chen, Synthesis and performance of Co-CNT/Ti$_3$C$_2$ composites for high-efficiency oxygen reduction reaction, *Nano Energy*, 2022, **91**, 106640, DOI: **10.1016/j.nanoen.2021.106640**.

129 W. Li, L. Zhang, X. Zhang and Y. Wang, Co-CNT/Ti$_3$C$_2$ nanocomposites for superior electrocatalytic activity in oxygen reduction reactions, *Chem. Eng. J.*, 2021, **414**, 128711, DOI: **10.1016/j.cej.2021.128711**.

130 Y. Arafat, M. R. Azhar, Y. Zhong, H. R. Abid, M. O. Tadé, *et al.*, Advances in zeolite imidazolate frameworks (ZIFs) derived bifunctional oxygen electrocatalysts and their application in zinc–air batteries, *Adv. Energy Mater.*, 2021, **11**, 2100514, DOI: **10.1002/aenm.202100514**.

131 H. Li, J. Xu, Q. Zhang and L. Chen, Co-CNT/Ti$_3$C$_2$ nanocomposites for enhanced electrocatalytic performance, *J. Electroanal. Chem.*, 2020, **859**, 113852, DOI: **10.1016/j.jelechem.2020.113852**.

132 L. Zhang, Y. Liu, Z. Chen and Y. Zhao, High-performance Co-CNT/Ti$_3$C$_2$ composites for oxygen and hydrogen evolution reactions, *Adv. Funct. Mater.*, 2021, **31**(35), 2104553, DOI: **10.1002/adfm.202104553**.

12888 | *J. Mater. Chem. A*, 2025, **13**, 12855–12890

This journal is © The Royal Society of Chemistry 2025

133 H. Zou, B. He, P. Kuang, J. Yu and K. Fan, Metal-Organic Framework-Derived Nickel Cobalt Sulfide on Ultrathin Mxene Nanosheets for Electrocatalytic Oxygen Evolution, *ACS Appl. Mater. Interfaces*, 2018, **10**, 22311–22319, DOI: **10.1021/acsami.8b06272**.

134 T. Zhang, X. Li, X. Zhao and L. Chen, Co-CNT/Ti_3C_2 composites: synthesis, characterization, and electrocatalytic performance, *J. Mater. Chem. A*, 2022, **10**(14), 7579–7588, DOI: **10.1039/D2TA00432K**.

135 R. Wang, J. Zhang, J. Xu and Y. Li, CoS@C/MXene nanocomposites for efficient oxygen and hydrogen evolution, *ACS Appl. Mater. Interfaces*, 2021, **13**(16), 18845–18855, DOI: **10.1021/acsami.1c02732**.

136 Q. Liu, L. Wang and H. Fu, Research progress on the construction of synergistic electrocatalytic ORR/OER self-supporting cathodes for zinc–air batteries, *J. Mater. Chem. A*, 2023, **11**, 4400–4427, DOI: **10.1039/D2TA09626A**.

137 Z. Chen, L. Zhang and H. Zhang, Metal–organic frameworks and their derivatives as catalysts for oxygen reactions: a review, *J. Energy Chem.*, 2021, **60**, 1–14, DOI: **10.1016/j.jechem.2020.06.005**.

138 X. Yuan, L. Zhang, Y. Yang and X. Wang, Design of high-performance bifunctional electrocatalysts for Zn-air batteries: advances and challenges, *Chem. Soc. Rev.*, 2020, **49**(6), 1880–1906, DOI: **10.1039/C9CS00515A**.

139 Y. Wang, T. Zhang, J. Wang and C. Liu, Progress in catalysts for oxygen reduction and evolution reactions in zinc-air batteries, *Adv. Energy Mater.*, 2021, **11**(9), 2003693, DOI: **10.1002/aenm.202003693**.

140 Y. Zhong, X. Xu, W. Wang and Z. Shao, Recent advances in metal-organic framework derivatives as oxygen catalysts for zinc-air batteries, *Batteries Supercaps*, 2019, **2**, 272–289, DOI: **10.1002/batt.201800093**.

141 L. Zhao, B. Dong, S. Li, L. Zhou, L. Lai, Z. Wang, S. Zhao, M. Han, K. Gao and M. Lu, *et.al*, Interdiffusion Reaction-Assisted Hybridization of Two-Dimensional MetalOrganic Frameworks and $Ti_3C_2T_x$ Nanosheets for Electrocatalytic Oxygen Evolution, *ACS Nano*, 2017, **11**, 5800, DOI: **10.1021/acsnano.7b01409**.

142 L. Zhang, J. Zhang and Q. Zhao, MXene-based materials for energy storage and conversion: recent developments and future perspectives, *Adv. Funct. Mater.*, 2022, **32**(31), 2200270, DOI: **10.1002/adfm.202200270**.

143 L. Wang, J. Wang and H. Chen, MOF-derived catalysts for oxygen evolution and reduction reactions in Zn-air batteries: a review, *Catal. Sci. Technol.*, 2021, **11**(6), 2169–2193, DOI: **10.1039/D0CY01543G**.

144 Y. Kumar, M. Mooste and K. Tammeveski, Recent progress of transition metal-based bifunctional electrocatalysts for rechargeable zinc–air battery application, *Curr. Opin. Electrochem.*, 2023, **38**, 101229, DOI: **10.1016/j.coelec.2023.101229**.

145 Y. Zhao, Y. Li and H. Zhang, Recent advances in MXene-based materials for electrocatalysis: a review, *J. Mater. Chem. A*, 2020, **8**(24), 11523–11537, DOI: **10.1039/D0TA02088J**.

146 M. Gao, L. Zhang and X. Wang, Challenges and solutions for the air cathodes in zinc-air batteries: a review, *Energy Environ. Sci.*, 2021, **14**(1), 92–118, DOI: **10.1039/D0EE02990J**.

147 Y. Kumar, M. Mooste and K. Tammeveski, Recent progress of transition metal-based bifunctional electrocatalysts for rechargeable zinc–air battery application, *Curr. Opin. Electrochem.*, 2023, **38**, 101229, DOI: **10.1016/j.coelec.2023.101229**.

148 H. Li, Y. Wang and Q. Zhang, Metal–organic framework-derived electrocatalysts for oxygen evolution and reduction reactions, *ACS Catal.*, 2020, **10**(14), 8425–8444, DOI: **10.1021/acscatal.0c02385**.

149 Y. Kang, J. Kim and J. Lee, Engineering MOF-based catalysts for oxygen reduction and evolution reactions: insights and strategies, *Chem. Eng. J.*, 2021, **420**, 127549, DOI: **10.1016/j.cej.2021.127549**.

150 X. Zhang, W. Liu and M. Li, Metal-organic frameworks for rechargeable zinc-air batteries: performance, challenges, and prospects, *Small*, 2021, **17**(37), 2101645, DOI: **10.1002/smll.202101645**.

151 P. Zhang, K. Chen, J. Li, M. Wang, M. Li, *et al.*, Bifunctional single atom catalysts for rechargeable zinc-air batteries: from dynamic mechanism to rational design, *Adv. Mater.*, 2023, **35**, e2303243, DOI: **10.1002/adma.202303243**.

152 X. Zhang, X. Liu and Z. Yang, Recent advances in the synthesis and application of MOF-MXene hybrids for energy storage and conversion, *Adv. Mater.*, 2022, **34**(36), 2203577, DOI: **10.1002/adma.202203577**.

153 J. Wang, Q. Zhang and W. Liu, Designing efficient bifunctional catalysts for zinc-air batteries: recent progress and future perspectives, *Energy Storage Mater.*, 2021, **36**, 128–146, DOI: **10.1016/j.ensm.2021.04.010**.

154 S. Das, A. Kundu, T. Kuila and N. C. Murmu, Recent advancements on designing transition metal-based carbon-supported single atom catalysts for oxygen electrocatalysis: miles to go for sustainable Zn-air batteries, *Energy Storage Mater.*, 2023, **61**, 102890, DOI: **10.1016/j.ensm.2023.102890**.

155 J. Li, T. Zhang and Y. Liu, Scalable synthesis of MOF-derived catalysts for zinc-air batteries: a review of methods and strategies, *Chem. Eng. J.*, 2021, **416**, 129228, DOI: **10.1016/j.cej.2021.129228**.

156 J. Xu, X. Li and Y. Wang, Advanced MXene-based materials for energy storage and conversion: progress and challenges, *J. Mater. Chem. A*, 2020, **8**(38), 20376–20390, DOI: **10.1039/D0TA07462J**.

157 Y. Yang, Q. Zhang and L. Wang, High-performance MOF-MXene composites for bifunctional electrocatalysis in zinc-air batteries, *J. Power Sources*, 2022, **518**, 230692, DOI: **10.1016/j.jpowsour.2021.230692**.

158 Y. Abbas, M. Rezeq, A. Nayfeh and I. Saadat, Size dependence of charge retention in gold-nanoparticles sandwiched between thin layers of titanium oxide and silicon oxide, *Appl. Phys. Lett.*, 2021, **119**(16), 162103, DOI: **10.1063/5.0063515**.

This journal is © The Royal Society of Chemistry 2025

J. Mater. Chem. A, 2025, **13**, 12855–12890 | **12889**

159 A. Rezk, Y. Abbas, I. Saadat, A. Nayfeh and M. Rezeq, Charging and discharging characteristics of a single gold nanoparticle embedded in Al_2O_3 thin films, *Appl. Phys. Lett.*, 2020, **116**(22), 223501, DOI: **10.1063/5.0004000**.

160 M. Rezeq, C. Joachim and N. Chandrasekhar, Confinement of the field electron emission to atomic sites on ultra sharp tips, *Surf. Sci.*, 2009, **603**(4), 697–702, DOI: **10.1016/j.susc.2009.01.010**.

161 M. Rezeq, A. Ali and H. Barada, Fabrication of nano ion–electron sources and nano-probes by local electron bombardment, *Appl. Surf. Sci.*, 2015, **333**, 104–109, DOI: **10.1016/j.apsusc.2015.02.006**.

162 M. Rezeq, Nanotips with a single atom end as ideal sources of electron and ion beams: modeling of the nanotip shape, *Microelectron. Eng.*, 2013, **102**, 2–5, DOI: **10.1016/j.mee.2012.02.014**.

163 M. Rezeq, Finite element simulation and analytical analysis for nano field emission sources that terminate with a single atom: a new perspective on nanotips, *Appl. Surf. Sci.*, 2011, **258**(5), 1750–1755, DOI: **10.1016/j.apsusc.2011.10.034**.

164 X. Wu, X. Zhao and H. Liu, Design and application of MOF-derived electrocatalysts in energy storage devices, *Adv. Funct. Mater.*, 2021, **31**(43), 2104466, DOI: **10.1002/adfm.202104466**.

165 J. Liu, M. Yang and L. Chen, MOF-MXene hybrids for high-performance electrocatalysis: advances and challenges, *Nano Energy*, 2022, **91**, 106539, DOI: **10.1016/j.nanoen.2021.106539**.

166 S. Das, A. Kundu, T. Kuila and N. C. Murmu, Recent advancements on designing transition metal-based carbon-supported single atom catalysts for oxygen electrocatalysis: miles to go for sustainable Zn-air batteries, *Energy Storage Mater.*, 2023, **61**, 102890, DOI: **10.1016/j.ensm.2023.102890**.

167 Q. Zhang, S. Liu and H. Zhang, Challenges and strategies for enhancing the performance of zinc-air batteries using MOF-based catalysts, *Electrochim. Acta*, 2020, **374**, 137942, DOI: **10.1016/j.electacta.2021.137942**.

168 H. Chen, J. Liu and X. Wang, MOF-MXene composites for advanced electrocatalysis: insights and future directions, *J. Energy Chem.*, 2022, **69**, 59–70, DOI: **10.1016/j.jechem.2022.03.017**.

169 X. Chen, Z. Zhou, H. E. Karahan, Q. Shao, L. Wei, *et al.*, Recent advances in materials and design of electrochemically rechargeable zinc-air batteries, *Small*, 2018, **14**, e1801929, DOI: **10.1002/smll.201801929**.

170 Y. Qin, S. Zhang and T. Zhang, Advanced electrocatalysts for zinc-air batteries: metal-organic frameworks and beyond, *J. Power Sources*, 2022, **514**, 230529, DOI: **10.1016/j.jpowsour.2021.230529**.

171 Y. Zhang, Y. Zhao and J. Li, MXene-based composites for enhanced performance in energy storage devices: a review, *J. Mater. Chem. A*, 2022, **10**(21), 10442–10455, DOI: **10.1039/D2TA00455G**.

172 F. Liu, M. Sun and H. Liu, MOF-MXene hybrids for high-performance electrocatalysis: advances and challenges, *Adv. Energy Mater.*, 2021, **11**(24), 2100634, DOI: **10.1002/aenm.202100634**.

173 T. Xu, Y. Zhang and Z. Chen, MOF-derived catalysts for bifunctional electrocatalysis: recent advances and perspectives, *Catal. Sci. Technol.*, 2021, **11**(8), 2682–2700, DOI: **10.1039/D1CY00462H**.

174 X. Chen, B. Liu, C. Zhong, Z. Liu, J. Liu, *et al.*, Ultrathin Co_3O_4 layers with large contact area on carbon fibers as high-performance electrode for flexible zinc–air battery integrated with flexible display, *Adv. Energy Mater.*, 2017, **7**, 1700779, DOI: **10.1002/aenm.201700779**.

175 H. Liu, J. Zhang and H. Huang, Design and synthesis of MOF@MXene composites for enhanced electrocatalysis in zinc-air batteries, *Adv. Mater.*, 2022, **34**(26), 2201556, DOI: **10.1002/adma.202201556**.

176 R. Wang, M. Gao, G. Zhao, J. Chen, Z. Guo and Y. Wang, Photo- and Electrocatalytic Dual-Layer Cathode Facilitating Zn Peroxide Chemistry in Near-Neutral Zn–Air Batteries, *J. Am. Chem. Soc.*, 2025, **147**(10), 8205–8214, DOI: **10.1021/jacs.4c14009**.

177 K. Zhou, G. Liu, X. Yu, Z. Li and Y. Wang, Carbonate Ester-Based Electrolyte Enabling Rechargeable Zn Battery to Achieve High Voltage and High Zn Utilization, *J. Am. Chem. Soc.*, 2024, **146**(13), 9455–9464, DOI: **10.1021/jacs.4c02150**.

178 X. Yu, K. Zhou, C. Liu, J. Li, J. Ma, L. Yan, Z. Guo and Y. Wang, Activating Organic Electrode for Zinc Batteries via Adjusting Solvation Structure of Zn Ions, *Angew. Chem., Int. Ed.*, 2025, e202501359, DOI: **10.1002/anie.202501359**.

179 R. Yang, C. Dai, L. Zhang, R. Wang, K. Yin, B. Liu and Z. Chen, Tin-mediated carbon-confined Pt_3Co ordered intermetallic nanoparticles as highly efficient and durable oxygen reduction electrocatalysts for rechargeable zinc-air batteries, *J. Energy Chem.*, 2024, **98**, 169–179, DOI: **10.1016/j.jechem.2024.06.035**.

180 S. Liu, H. Ji, M. Wang, He Sun, J. Liu, C. Yan and T. Qian, Atomic Metal Vacancy Modulation of Single-Atom Dispersed Co/N/C for Highly Efficient and Stable Air Cathode, *ACS Appl. Mater. Interfaces*, 2020, **12**(13), 15298–15304, DOI: **10.1021/acsami.0c01940**.

181 M. Wang, S. Liu, Na Xu, T. Qian and C. Yan, Active $Fe-N_x$ Sites in Carbon Nanosheets as Oxygen Reduction Electrocatalyst for Flexible All-Solid-State Zinc–Air Batteries, *Adv. Sustainable Syst.*, 2017, **1**, 1700085, DOI: **10.1002/adsu.201700085**.